SANDIA REPORT

SAND95–1938 • UC–814
Unlimited Release
Printed October 1996

Yucca Mountain Site Characterization Project

Summary of Ground Motion Prediction Results for Nevada Test Site Underground Nuclear Explosions Related to the Yucca Mountain Project

Marianne C. Walck

Prepared by
Sandia National Laboratories
Albuquerque, New Mexico 87185 and Livermore, California 94550
for the United States Department of Energy
under Contract DE-AC04-94AL85000

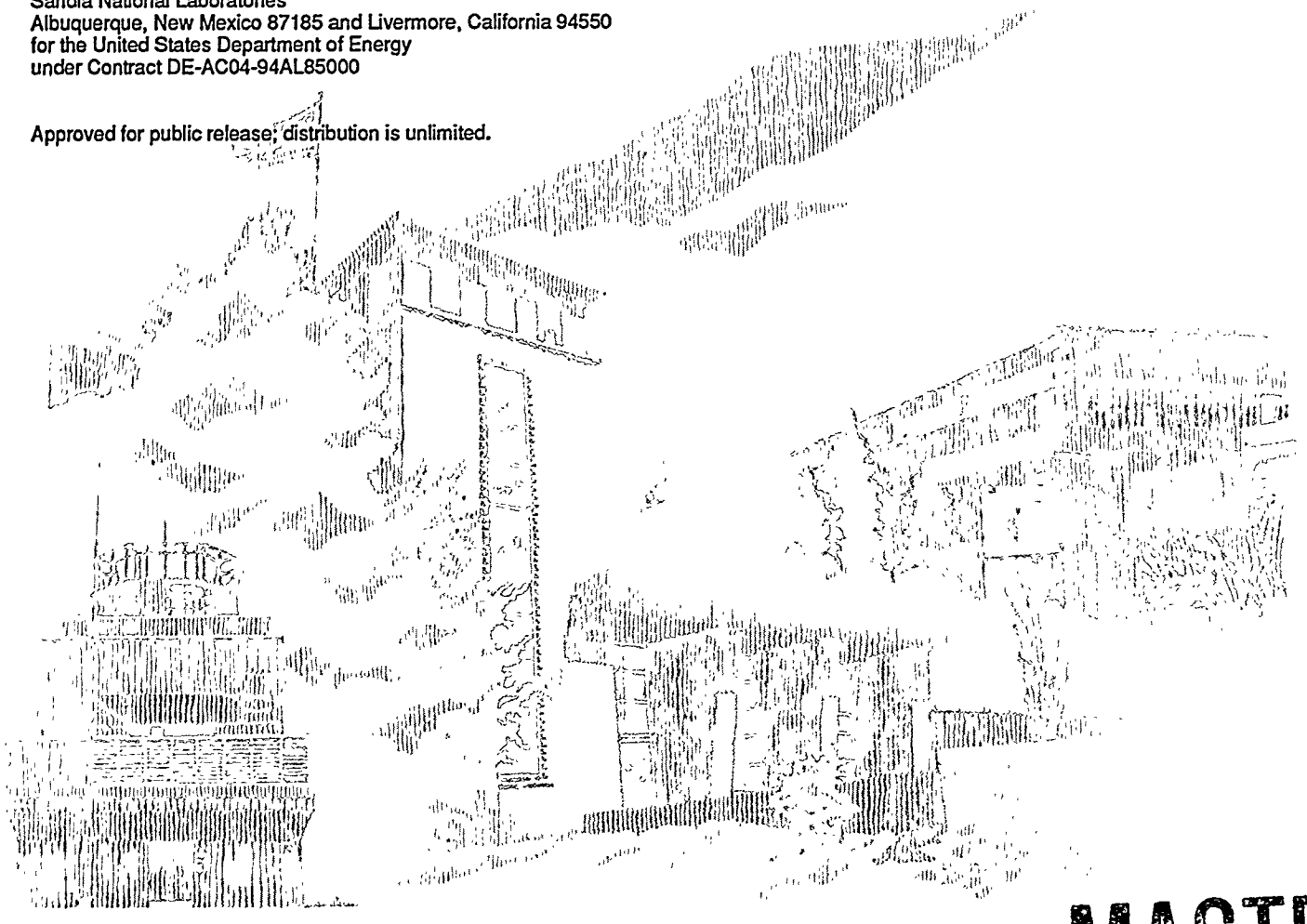

"Prepared by Yucca Mountain Site Characterization Project (YMSCP) participants as part of the Civilian Radioactive Waste Management Program (CRWM). The YMSCP is managed by the Yucca Mountain Project Office of the U.S. Department of Energy, DOE Field Office, Nevada (DOE/NV). YMSCP work is sponsored by the Office of Geologic Repositories (OGR) of the DOE Office of Civilian Radioactive Waste Management (OCRWM)."

Issued by Sandia National Laboratories, operated for the United States Department of Energy by Sandia Corporation.

Available to DOE and DOE contractors from
Office of Scientific and Technical Information
PO Box 62
Oak Ridge, TN 37831

Prices available from (615) 576-8401, FTS 626-8401

Available to the public from
National Technical Information Service
US Department of Commerce
5285 Port Royal Rd
Springfield, VA 22161

NTIS price codes
Printed copy: A05
Microfiche copy: A01

SAND95-1938
Unlimited Release
Printed October 1996

Distribution
Category UC-814

Summary of Ground Motion Prediction Results for Nevada Test Site Underground Nuclear Explosions related to the Yucca Mountain Project

Marianne C. Walck
Geophysics Department
Sandia National Laboratories
Albuquerque, NM 87185

ABSTRACT

This report summarizes available data on ground motions from underground nuclear explosions recorded on and near the Nevada Test Site, with emphasis on the ground motions recorded at stations on Yucca Mountain, the site of a potential high-level radioactive waste repository. Sandia National Laboratories, through the Weapons Test Seismic Investigations project, collected and analyzed ground motion data from NTS explosions over a 14-year period, from 1977 through 1990. By combining these data with available data from earlier, larger explosions, prediction equations for several ground motion parameters have been developed for the Test Site area for underground nuclear explosion sources. Also presented are available analyses of the relationship between surface and downhole motions and spectra and relevant crustal velocity structure information for Yucca Mountain derived from the explosion data. The data and associated analyses demonstrate that ground motions at Yucca Mountain from nuclear tests have been at levels lower than would be expected from moderate to large earthquakes in the region; thus nuclear explosions, while located relatively close, would not control seismic design criteria for the potential repository.

This work was supported by the United States Department of Energy under Contract DE-AC04-94AL85000 and was prepared under the Yucca Mountain Site Characterization Project WBS number 1.2.3.2.8.3.3. The planning document that guided this work activity was Work Agreement #0119, revision 01. The data analysis specifically conducted for this report was conducted under a fully qualified QA program. Earlier data analyses, the results of which are compiled in this report, may not have been conducted under a fully qualified QA program. All of the underground nuclear explosion ground motion data are unqualified due to their occurring prior to the existence of a fully qualified QA program. Some of the ground motion data do have associated TDIF numbers; these are: Contact (200226 DTN:SNF08000000001.00), Amarillo (200227 DTN:SNF08000000002.000), Alamo (200228 DTN:SNF08000000003.000), Dalhart (200229 DTN:SNF08000000004.000), Kearsarg (200230 DTN:SNF08000000005.000), Comstock (200233 DTN:SNF08000000008.000), Barnwell (200234 DTN:SNF08000000009.000), Delamar (200236 DTN:SNF08000000010.000), Kernville (200237 DTN:SNF08000000011.000), Lockney (200238 DTN:SNF08000000012.000), Hardin (200239 DTN:SNF08000000013.000), and Tahoka (200240 DTN:SNF08000000014.000).

This report supports work defined in the Site Characterization Plan section 8.3.1.17.3.3.2 and is discussed in Study Plan SP-8.3.1.17.3.3, Revision 0.

Most of the results presented in this report have been published previously. New results did not require the use of Scientific and Engineering Software as defined in Sandia National Laboratories Quality Assurance Implementing Procedure 19-1 and thus the software was not subject to software quality assurance requirements.

DISCLAIMER

Table of Contents

List of Tables

List of Figures

Introduction

An important element of the site characterization effort for the potential high-level radioactive waste repository at Yucca Mountain, Nevada, is the documentation and quantification of seismic risk at the site. Yucca Mountain is located in the southern Great Basin province, an extensional region that has spatially varying levels of present-day seismicity (e.g., Gomberg, 1991). While historical seismicity rates at Yucca Mountain itself have been extremely low (Gomberg, 1991; Brune et al., 1992), there are a number of geologically-observed faults in the immediate vicinity that have documented Quaternary movement and thus must be regarded as potential sources of fault displacement and vibratory ground motion (Pezzopane et al., 1994). In addition to the natural seismicity at the site, potential exists for ground motions occurring from man-made sources such as explosions. The largest recent source of man-made motion has been underground nuclear explosions (UNEs) detonated at the adjacent Nevada Test Site (NTS). No UNEs have occurred since 1992, however, future nuclear testing is possible on the test site. Any future UNEs would likely adhere to the size limits imposed by the Threshold Test Ban Treaty of 1976, which limits UNEs to 150 kt; this corresponds to body wave magnitude of about 5.7 at NTS (Vortman, 1991). The ground motions at Yucca Mountain from events of this size located at either the Pahute Mesa or Yucca Flat testing areas of NTS at distances of 40-60 km would be relatively small (Vortman, 1986), but must be considered in the overall seismic hazard assessment for the Yucca Mountain repository.

Sandia National Laboratories has been monitoring ground motions from UNEs at NTS for many years. In 1977, the Weapons Test Seismic Investigations (WTSI) project was initiated, funded jointly by the weapons and nuclear waste programs, to monitor ground motions from explosions in the context of placement of a nuclear waste repository somewhere in the vicinity of the test site. Data were initially collected at stations located around the NTS, and efforts were later focused at Yucca Mountain in response to program priorities. By 1990, the WTSI program had established 29 total monitoring sites for the Yucca Mountain Project (YMP), and had monitored 80 UNEs for a total of more than 800 three-component digital acceleration records. Many of the recording locations had both surface and downhole instrumentation. Table 1 lists the 29 WTSI stations, their locations, dates of operation, and other station information. In Figure 1, the station locations are shown superimposed on a map of the NTS.

During the duration of the WTSI project, relevant data analyses were performed in parallel with the data collection activities. Early efforts included Vortman's (1980) report on ground motion prediction; he proposed a prediction equation of the form

$$a = KW^{n}R^{-m}, \qquad (1)$$

where K, n, and m are empirically derived, W is yield in kilotons, R is range in km, and a is the ground motion parameter of interest, such as peak acceleration, velocity, or displacement. An equation of this form is a straight line in motion vs distance log-log space, unlike typical ground motion prediction equations for earthquakes (e.g., Trifunac, 1976; Boore et al., 1978, and many others) which typically are non-linear (rolling over to predict smaller ground motions) at close range. Although Vortman (1980) does not show any actual data plotted on equations of

Table 1: Station Locations for Weapons Test Seismic Investigations

Station Number	Description	Hole if app.	Depth m	Medium	Dates of Operation	Coordinates Nevada Grid m, N	m, E
1	Area 16	N/A	N/A	Eleana Shale	8/77 - 11/77	256189	193475
2	Syncline Ridge	N/A	N/A	Limestone	8/77 - 6/78	257023	196977
3	Piledriver	Ue-15.01	417	Granite	9/77 - 5/83	274670	206355
4	Area 6	Ue-6b	130	Alluvium	4/77 - 5/78	246888	206792
5	Skull Mountain	N/A	N/A	Tuff	10/77 - 10/83[1]	226193	198303
6	ETS-2	N/A	N/A	Alluvium	10/77 - 1990	231064	184252
7	Calico Hills	N/A	N/A	Eleana Shale	10/77 - 1990	234151	185518
8	Yacht Hole	Ue-1L	679,570[2]	Alluvium	3/78 - 8/78	255118	199340
9	Rainier Mesa	U-12g. 08 CH no. 1	432	Tuff	12/77 - 4/84	268887	193020
10	Well J-11	J-11	356[3], 343	Alluvium	3/78 - 1990	225798	186486
10'	200	J-11'	61	Alluvium	3/78 - 7/81	225826	186486
11	Area 4	Ue-4aa	346	Alluvium	3/78 - 4/84	260344	203239
12 (30)	Yucca Mountain	USW - GU3	352	Tuff	3/83 - 1990	229420	170232
13	Area 18	Ue-18r	762	Tuff	6/78 - 4/84	264597	172121

Table 1: Station Locations for Weapons Test Seismic Investigations, continued.

Station Number	Description	Hole if app.	Depth m	Medium	Dates of Operation	Coordinates Nevada Grid m, N	m, E
14	Yucca Mountain	N/A	N/A	Tuff	10/78 - 7/85	233834	172741
15	Dome Mountain	N/A	N/A	"Lava"	10/78 - 6/82	248047	176600
16	Forty-mile Canyon	N/A	N/A	Rhyolite	10/78 - 8/82	247506	178693
17	N. Timber Mtn.	N/A	N/A	Tuff	7/78 - 8/82	259172	171389
18	S. Timber Mtn.	N/A	N/A	Tuff	7/78 - 8/82	254204	170018
19	Mine Mountain	N/A	N/A	Limestone	2/79 - 9/80	248575	198715
20	Yucca Mountain	N/A	N/A	Tuff	7/80 - 4/82	235386	170861
21	Yucca Mountain	N/A	N/A	Tuff	7/80 - 8/85	232864	170350
22	Yucca Mountain	N/A	N/A	Tuff	7/80 - 8/85	235645	168888
23	Yucca Mountain	N/A	N/A	Tuff	7/80 - 8/85	236852	172250
24	Yucca Mountain	USW-G1	564	Alluvium	3/82 - 7/83	234842	170992
25	Yucca Mountain	USW-G1	358, 305[4]	Alluvium	8/83 - 1990	234848	170993
26	Yucca Mountain	N/A	N/A	Alluvium	4/84 - 1990	233233	174163

Table 1: Station Locations for Weapons Test Seismic Investigations, continued.

Station Number	Description	Hole if app.	Depth m	Medium	Dates of Operation	Coordinates Nevada Grid m, N	m, E
27	Yucca Mountain	N/A	N/A	Alluvium	5/84 - 8/84	232316	174008
28	Yucca Mountain	USW G-2	375, 358[4]	Tuff	6/84 - 1990	237386	170841
29	Yucca Mountain	UE-25-RF4	82	Alluvium	2/85 - 1990	232285	174365

Notes:
[1] Moved 5/81
[2] after 4/78
[3] before 12/78
[4] after 4/87

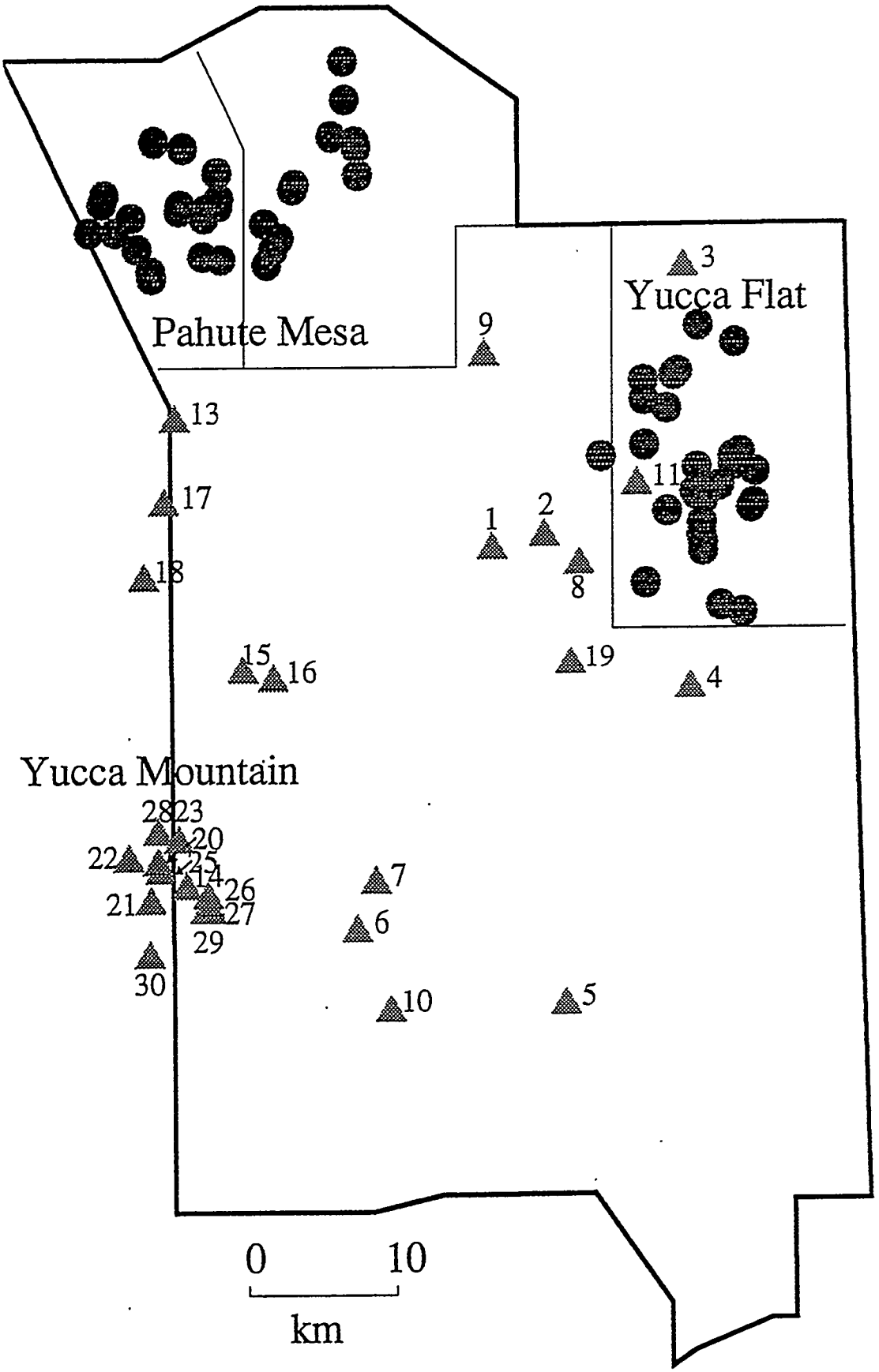

Figure 1: Map of the Nevada Test Site showing location of Weapons Test Seismic Investigations accelerometer stations (triangles) and events monitored from 1980 to 1990 (circles). Station numbers appear next to each station.

the form of equation (1), due to security considerations (the Department of Energy considers nuclear explosion yields to be classified information), other published nuclear explosion data as a function of distance also show a linear relationship in log-amplitude log-distance space closer than 1 km (Stump and Reinke, 1991). Thus it appears that the differences in source mechanisms between earthquakes and nuclear explosions result in a different behavior of peak ground motion at close distances.

Another set of reports early in the WTSI program (Vortman and Long, 1982a, 1982b; Long et al., 1983) examined the dependence of UNE ground motion amplitudes on the depth of the borehole receiver for a number of surface/downhole pairs located around the Test Site. The first two studies considered peak ground motions and response spectra ratios for Pahute Mesa and Yucca Flat tests, respectively. The authors did not establish a clear dependence of peak ground motion as a function of depth, but did note that the depth effect was clearly a function of the geology at the recording station. They attempted regressions of peak amplitude ratios but the coefficients of determination were very poor due to the large data scatter. Data from Yucca Flat tests showed a poorer correlation as a function of depth than did the Pahute Mesa data. The Long et al. (1983) study developed transfer functions between the surface and borehole instruments based on signal processing techniques. While these transfer functions were able to accurately reproduce waveforms at depth given the surface waveform, they were empirically derived and bear no relationship to physical parameters such as seismic velocity in the medium between the two receivers. Thus these transfer functions, which are specific both to the station and the source area, are of limited use. None of these studies included any data from stations on Yucca Mountain, which were not installed until the early 1980s.

Later studies have augmented data sets, including ground motions recorded at various sites around Yucca Mountain. Vortman (1986) developed sets of prediction equations for vector ground motions from Pahute Mesa. Long (1992) conducted a parallel study of the individual components of ground motion for the same data set. Phillips (1991a) looked at the surface and downhole ground motion levels for Pahute Mesa events recorded at Yucca Mountain, and later developed prediction equations (Phillips, 1991b) for Pahute Mesa UNE response spectra. The results from all of these studies will be compiled in later sections of this report.

In addition to the conventional ground motion analyses, Walck and Phillips (1990) and Durrani and Walck (1996) have examined other aspects of UNE body-wave propagation across the NTS to stations on Yucca Mountain. Walck and Phillips (1990) developed two-dimensional crustal velocity models for three paths from NTS testing areas to Yucca Mountain based on UNE travel times and relative amplitudes. This analysis demonstrated the existence of large lateral velocity variations in the NTS upper crust and showed that ground motion amplitudes recorded at Yucca Mountain are azimuthally dependent. Durrani and Walck (1996) performed a more sophisticated analysis of the surface and downhole waveforms than the early efforts summarized above. They used theoretical spectral ratios derived from velocity models based on the known local geology of Yucca Mountain to perform forward modeling of the medium between the surface and borehole instruments specifically at Yucca Mountain. They developed a two-dimensional model for the uppermost 350m of Yucca Mountain that can be used to predict ground motions at the repository depth for a specified surface motion.

This report compiles and summarizes the previously published results mentioned above. It also presents new results that help provide a more complete picture of the ground motions expected from UNEs at Yucca Mountain. None of the studies listed above considered Yucca Flat UNE data in ground motion prediction equations. In order to present a more complete picture of UNE ground motions at NTS, this report presents new results for peak vector and component motions from Yucca Flat events compared to the published equations of Vortman (1986) and Long (1992). We also summarize unpublished work of Phillips (personal communication, 1987) that evaluates the Vortman (1986) and Long (1992) equations specifically for Pahute Mesa events recorded at Yucca Mountain. This report will thus contain summary information for all known analyses of the WTSI data that could bear on the seismic hazard at the Yucca Mountain site.

Data Summary

Several of the previously published reports discuss in detail the data acquisition process used in the WTSI project to collect data relevant to the Yucca Mountain Project (e.g., Phillips, 1991a), so only a summary will be repeated here. Strong-ground motion accelerometers, generally Sundstrand AQ1100, 1200, 1300 or 1400 models were installed either at the ground surface or in a borehole. Installations included three components of instrumentation, oriented horizontally in the north-south, and east-west directions, and also vertically. Downhole instrumentation had unknown horizontal orientations; these directions were generally determined empirically from the known azimuths of approach for a number of events. The accelerometers did not record continually but were activated for specific periods of time corresponding to planned times for nuclear tests. Analog data were telemetered via radio to collection points around the NTS, including Control Point and a relay station in Jackass Flats. Typically, data were recorded for each component of motion in three different gains. Analysts reviewed the data streams and selected the most appropriate gain for retention in the data set. The data were digitized at a sample rate of 200 samples/sec at Sandia National Laboratories and preserved on ascii magnetic tapes; currently these data are also available on optical disk. Data processing included band-pass digital filtering based on observed signal-to-noise ratios; the data were integrated into velocity and displacement records. Horizontal components were rotated into radial and tangential components; both the original and rotated records are available in digital form. First-arrival travel times were picked and plots made of the waveforms. For some events, response spectra plots were generated and retained in paper notebooks.

Between 1977 and 1990, the WTSI project monitored a total of 80 nuclear tests; more than 800 three-component acceleration records were obtained. Most of the monitored tests were in either Pahute Mesa (34) or Yucca Flat (39), but data were also collected for a few Rainier Mesa events (7). WTSI station locations changed as a function of time, so not all locations recorded each event. Most events that were monitored, particularly later in the project, were of fairly large yield (greater than 80 kt, Phillips, 1991a), but quite a few smaller events also generated records that are in the data base. In general, only the larger yield events were used for ground motion prediction analyses (see, e.g., Vortman, 1986). Digital records of some pre-

1976, larger UNEs were also employed in selected studies to enhance the yield and distance range of recordings used in developing the prediction equations (Vortman, 1986).

As Table 1 demonstrates, several of the WTSI installations contained both borehole and surface instrumentation, with the borehole accelerometers at various depths due to constraints of hole depth, geology, or other factors. Vortman and Long (1982a, b) and Phillips (1991a, b) discuss the available borehole records in more detail.

While 12 WTSI stations were fielded at one time or another at Yucca Mountain, the station configuration changed over the years. When the monitoring program ended in 1990, there were five stations in the Yucca Mountain area: stations 25, 26, 28, 29, and 30 (formerly station 12). Of these, all but station 26 had borehole instrumentation as well as surface installations. Due to access restrictions to the site which severely limited maintenance, however, some of the deep borehole accelerometers failed prior to end of monitoring, and data were not obtained at depth for the last several UNEs .

Each data analysis, as documented in the cited reports, used a different subset of WTSI data. The reader is referred to the individual reports for details of data used.

Prediction Equations for Peak Vector Motions

Equations derived from Pahute Mesa UNE data

Vortman (1986) presented prediction equations in the form of equation 1 that are valid for peak vector acceleration, velocity, and displacement on the NTS from Pahute Mesa UNEs. The yield range is above 80 kt and the distance range is from near-zero to 70 km. He stated that these prediction equations supersede those presented in his earlier report (Vortman, 1980). Vector ground motion is defined as

$$a = (v^2 + h1^2 + h2^2)^{1/2} \qquad (2)$$

where a is the ground motion parameter, v is the zero-to-peak amplitude of the vertical component, and h1 and h2 are the horizontal components of ground motion. Vortman defined three different groups of data in his study: Group I included all available data and contained 469 records from 35 UNEs with a yield range of 80 to 1400 km. Seventeen of these events were detonated prior to the 1976 Threshold Test Ban Treaty and had yields of 155 kt or greater. Group II retained all of the source events but eliminated data from station locations determined to be anomalous; these included stations 3, 6, 9, 15, ETS-1 and ETS-2 (pre-1976 stations), and the "mobile" stations A, B, C, and D which were sited very close to station 6 on Jackass Flats, but which were moved slightly for each test (see Vortman, 1986). The mobile stations were placed to investigate a significant vertical acceleration anomaly observed at the ETS-2 site (also WTSI station 6) for certain Pahute Mesa UNEs (Environmental Research Corporation, 1974). The Group III data set was smaller still: data from the Yucca Mountain stations of the time as well as the anomalous stations were deleted. The additionally deleted

data were from stations 14, 20, 21, 22, 23, and 24 (see Table 1). In all cases, data from downhole instrumentation were not included in the regressions. Station geology was determined only to be "alluvium" or "rock" (Table 1). Alluvium at NTS is primarily unsaturated desert soil, often with shallow caliche layers present (e.g., Gibson et al, 1992); alluvium depths can vary from quite shallow (a few meters) to several hundred meters (e.g., station 10). The "rock" designation most often denotes tuff, but also includes granitoid rocks (station 3), other volcanics, and Paleozoic sedimentary rocks (e.g., stations 7, 19).

Table 2 presents the equations of Vortman (1986), by data group, separated into three site classifications: alluvium plus rock, rock only, and alluvium only. Standard errors on the ground motion parameter and range are included, as well as the number of data points used in the regressions. Ground motion units are g's for accelerations, cm/sec for velocity, and cm for displacement. Figures 2, 3, and 4 show the comparison between the acceleration equations for Groups I, II, and III for rock plus alluvium, rock only, and alluvium only sites, respectively. Figures 2 and 3 show that there are only small differences among the data groups for accelerations recorded on either rock plus alluvium or rock only stations. A substantial difference is seen between Groups I and II for the alluvium stations (Group III is identical to Group II for alluvium stations). The large vertical accelerations at stations 6, ETS-2 and the "mobile" stations A, B, C, and D pull the Group I alluvium equation up at larger distances.

Vortman (1986) also examines the then-available Yucca Mountain ground motion data, looking for acceleration anomalies similar to those observed at station 6 (Environmental Research Corporation, 1974; Vortman, 1986; Walck, 1988). No large anomalies are observed, although Vortman notes that peak vector acceleration values at those Yucca Mountain stations are often higher than predicted by the Group III equations.

Phillips (unpublished data, 1987) further compared Vortman's (1986) Group III prediction equations with a more comprehensive data set of Pahute Mesa events recorded at Yucca Mountain stations. He concluded that the data from Yucca Mountain were generally within the range of uncertainty of the published vector prediction equations. Figures 5, 6, and 7 show Phillips' results for vector acceleration, velocity, and displacement, respectively. For acceleration, only station 20 shows a mean value significantly outside the expected range, with the observed values being larger than those predicted from the equations. Variations are smaller for velocities, with stations 20 and 23 exhibiting larger than expected values, while several of the Yucca Mountain stations record peak vector displacements larger than predicted by the Vortman (1986) equations.

It should be noted that while station 25 is identified as being on "rock" in the earlier reports, it actually was sited on 18m of alluvium overlying tuff. In the Yucca Flat data analyses described in this report, station 25 is included in the alluvium category.

Table 2: Prediction Equations for Vector Ground Motions from Vortman (1986)

Group No.	Eqn. No.	Ground Motion Parameter	Constant	Yield exponent	Range exponent	σ gd. mot.	σ range	Number of data	Medium
I	T21	accel (g)	0.436	0.490	-1.624	2.063	1.562	415	A+R
I	T22	accel	0.435	0.502	-1.685	1.965	1.493	303	Rock
I	T23	accel.	0.198	0.276	-1.075	2.153	2.041	112	Alluv.
I	T24	vel(cm/s)	11.11	0.629	-1.522	1.732	1.435	421	A+R
I	T25	vel	12.13	0.621	-1.561	1.744	1.428	309	Rock
I	T26	vel.	12.33	0.566	-1.434	1.653	1.420	112	Alluv.
I	T27	disp(cm)	2.633	0.665	-1.556	1.789	1.453	418	A+R
I	T28	disp	2.884	0.656	-1.593	1.819	1.456	306	Rock
I	T29	disp.	2.882	0.606	-1.468	1.671	1.419	112	Alluv.
II	T210	accel.	0.549	0.466	-1.687	1.909	1.467	320	A+R
II	T211	accel.	0.581	0.456	-1.678	1.944	1.486	266	Rock
II	T212	accel.	0.0687	0.504	-1.233	1.694	1.533	54	Alluv.
II	T213	vel.	13.12	0.607	-1.549	1.582	1.345	326	A+R
II	T214	vel.	13.25	0.606	-1.547	1.579	1.343	272	Rock
II	T215	vel.	9.777	0.619	-1.494	1.617	1.379	54	Alluv.
II	T216	disp.	3.230	0.636	-1.581	1.712	1.405	323	A+R
II	T217	disp.	2.964	0.650	-1.584	1.677	1.386	269	Rock
II	T218	disp.	4.484	0.532	-1.503	1.888	1.526	54	Alluv.
III	T219	accel.	0.450	0.501	-1.709	1.897	1.454	285	A+R
III	T220	accel.	0.511	0.482	-1.717	1.941	1.471	231	Rock
III	T221	accel.	0.0687	0.504	-1.233	1.694	1.533	54	Alluv.
III	T222	vel.	11.14	0.638	-1.574	1.556	1.324	291	A+R
III	T223	vel.	12.04	0.628	-1.593	1.543	1.313	237	Rock
III	T224	vel.	9.777	0.619	-1.494	1.617	1.379	54	Alluv.
III	T225	disp.	2.732	0.667	-1.609	1.693	1.387	288	A+R
III	T226	disp.	2.683	0.675	-1.640	1.632	1.348	234	Rock
III	T227	disp.	4.484	0.532	-1.503	1.888	1.526	54	Alluv.

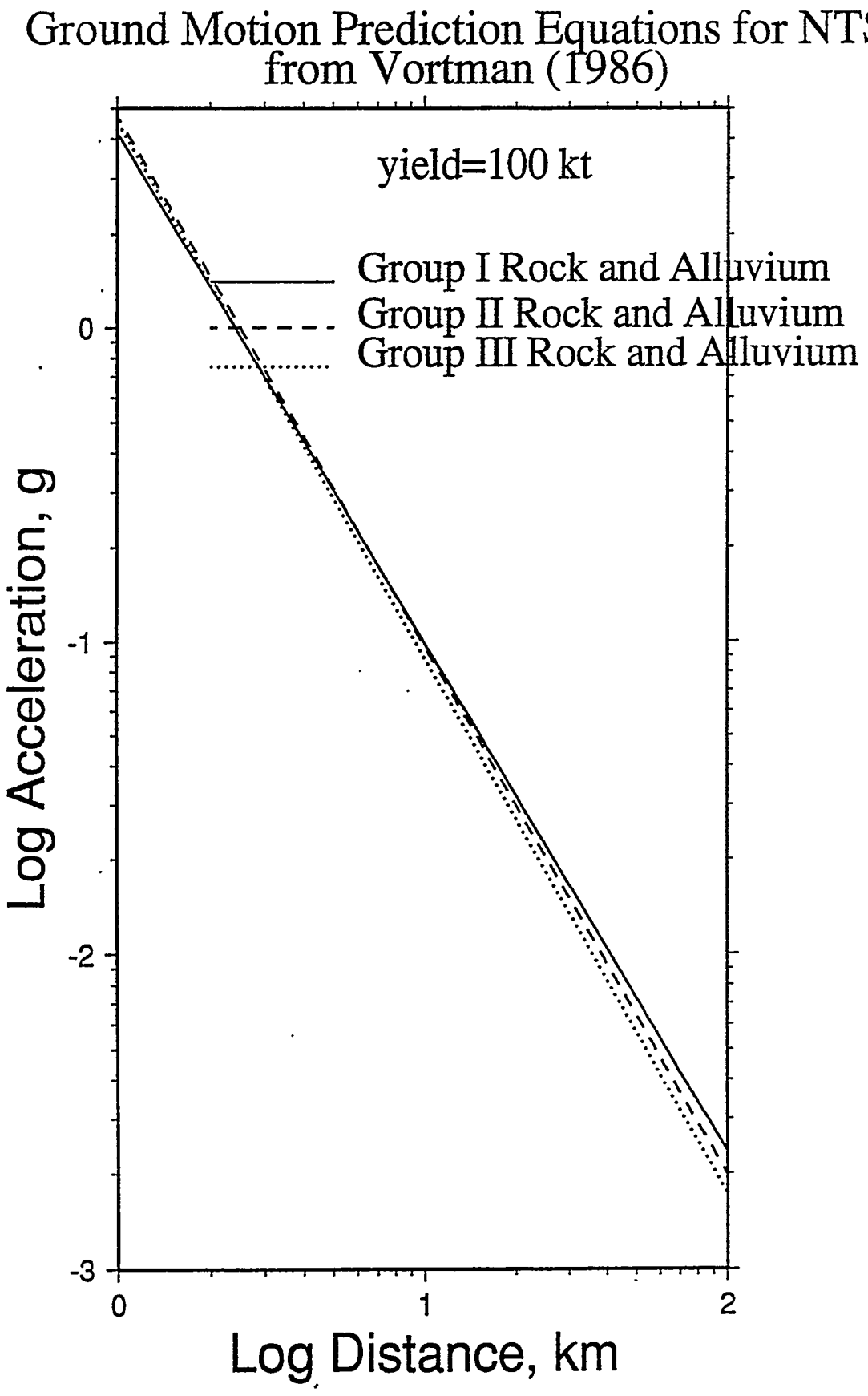

Figure 2: Log-log plot of amplitude vs distance for the Vortman (1986) peak acceleration equations, data groups I, II, and III, rock plus alluvium stations, yield = 100 kt

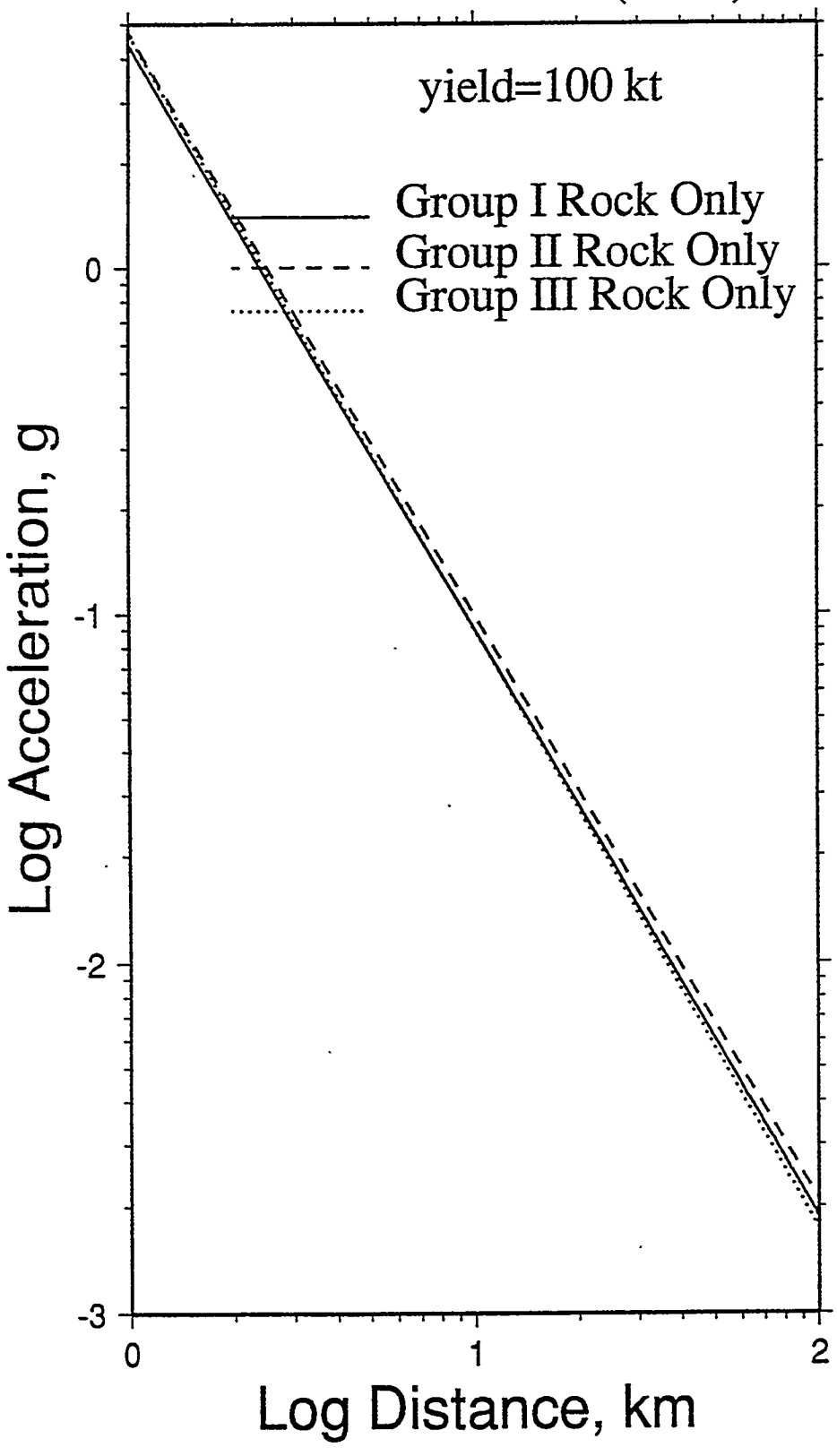

Figure 3: Log-log plot of amplitude vs distance for the Vortman (1986) peak acceleration equations, data groups I, II, and III, rock stations only, yield = 100 kt

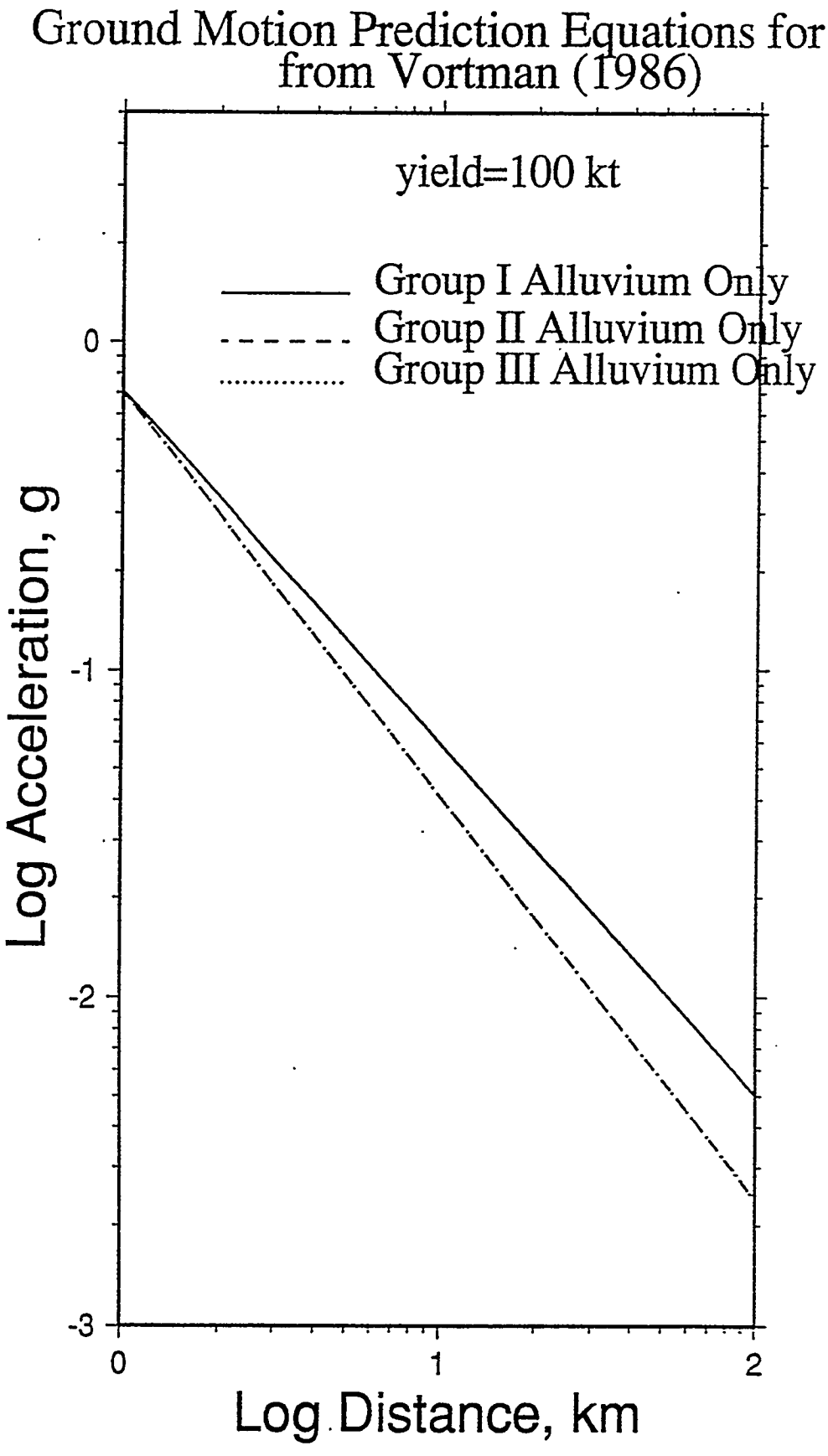

Figure 4: Log-log plot of amplitude vs distance for the Vortman (1986) peak acceleration equations, data groups I, II, and III, alluvium stations only, yield = 100kt.

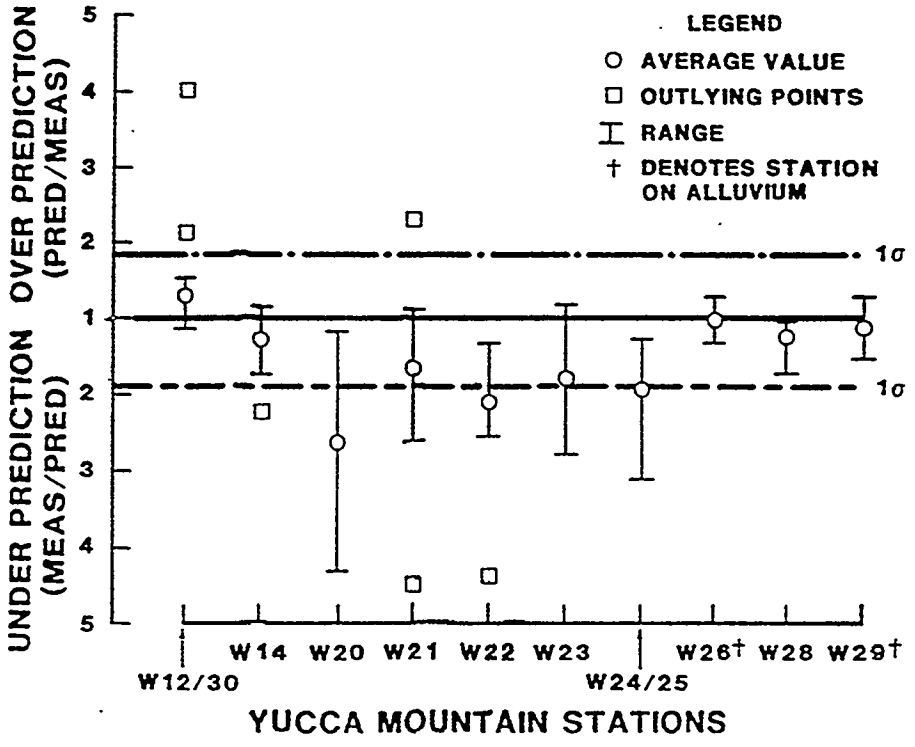

Figure 5: Comparison of ratio of measured-to-predicted vector acceleration for Yucca Mountain stations and the Vortman (1986) group III equations (unpublished data courtesy of J. S. Phillips)

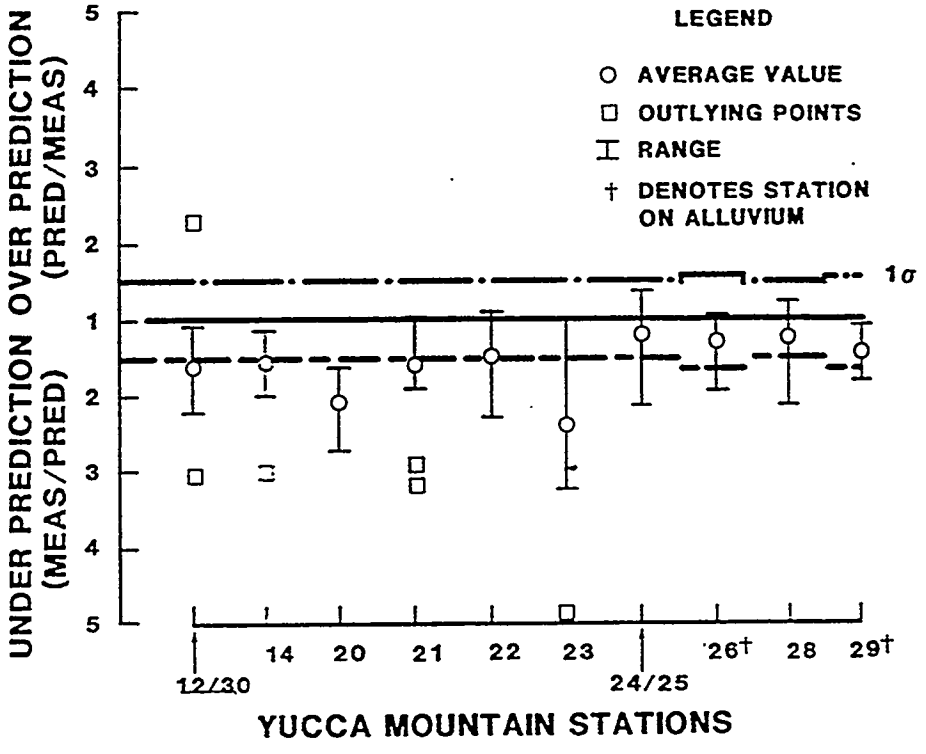

Figure 6: Comparison of ratio of measured-to-predicted vector velocity for Yucca Mountain stations and the Vortman (1986) group III equations (unpublished data courtesy of J. S. Phillips)

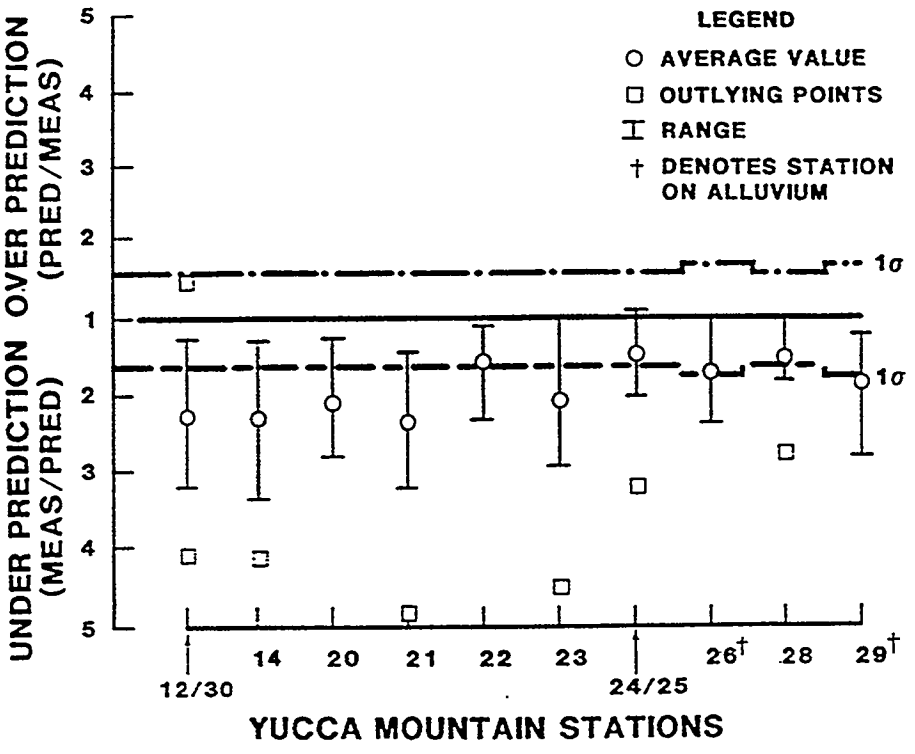

Figure 7: Comparison of ratio of measured-to-predicted vector displacement for Yucca Mountain stations and the Vortman (1986) group III equations (unpublished data courtesy of J. S. Phillips)

Table 3: Yucca Flat UNEs used in regression equation comparison

Name	Date	Number of WTSI stations
Dalhart	10/13/88	8
Tahoka	8/13/87	8
Hermosa	4/2/85	12
Cottage	3/23/85	12
Caprock	5/31/84	10
Mundo	5/1/84	10
Tortugas	3/3/84	11
Romano	12/16/83	12
Turquoise	4/14/83	2
Atrisco	8/5/82	16
Jornada	1/28/82	16
Baseball	1/15/81	17

Comparison of the Vortman (1986) prediction equations with Yucca Flat UNE data

The published data analyses of the WTSI UNE ground motion data have focused on Pahute Mesa sources. Vortman (1986) noted that a parallel study of peak vector ground motions should be conducted for Yucca Flat events, but none has been published to date. In this section, we present results of a simple comparison of the Yucca Flat peak vector ground motion data to the equations previously presented (Vortman, 1986; Table 2) that were derived from Pahute Mesa data alone.

The WTSI data base contains 12 events with yields of 70 kt to 150 kt that occurred in the Yucca Flat testing area (Table 3). While Vortman (1986) restricted his data to events with yields over 80kt, we extended our range down to 70 kt for better statistics. We can get a general feel for the appropriateness of Vortman's equations for the Yucca Flat data by plotting the observed Yucca Flat data superimposed on his prediction equations for a specified yield. Figure 8 shows the acceleration equation for Group I, alluvium plus rock (equation T21 in Table 2) for a specified yield of 100kt, with the standard deviation values displayed as dashed lines, and the Yucca Flat peak vector acceleration data for the yield range 70-150 kt. We expect some mismatch due to the range in explosion sizes, but note that in general, the Yucca Flat data fall within the ranges expected from the Pahute Mesa data analysis. Figures 9 and 10 show the analogous plots for velocity and displacement (equations T24 and T27 in Table 2). There are more data points in these plots that fall outside the expected range, but the agreement is generally still encouraging.

Figures 11-13 present the results of a more detailed analysis in which we calculated the ratio of the observed to predicted ground motion based on the above equations; in these plots, the yields of the individual explosions were incorporated. Figure 11 presents ratios of measured-to-predicted ground motion for acceleration at most of the WTSI stations for the Yucca Flat events relative to the appropriate Group I equation. Note that all of the stations have their mean ratios within one standard deviation of the prediction equation, except for station 3. This station is located in the Climax granite stock near Rainier Mesa, and has historically recorded much smaller ground motions than other NTS stations (see Vortman, 1986, for a discussion). A few events produced clearly anomalous points that are identified as outliers on the plots and not included in the statistics. As Figure 11 shows, the vector acceleration equation T21 of Vortman (1986) appears to be quite adequate for predicting motion from Yucca Flat events as well as Pahute Mesa events.

Figures 12 and 13 present the analogous results for peak vector velocity and displacement. Station 3 still demonstrates markedly smaller motions than expected. Station 9, also identified as "anomalous" by Vortman (1986), demonstrates higher-than-expected velocities and displacements. Several Yucca Mountain stations also have higher-than expected mean velocities and displacements, although the data scatter is large enough that there is generally overlap between the low end of those motions and the upper end of the prediction range. These results are quite comparable to those for the Pahute Mesa data of Phillips (unpublished; see Figures 6 and 7); in general the Yucca Mountain stations have larger vector displacements

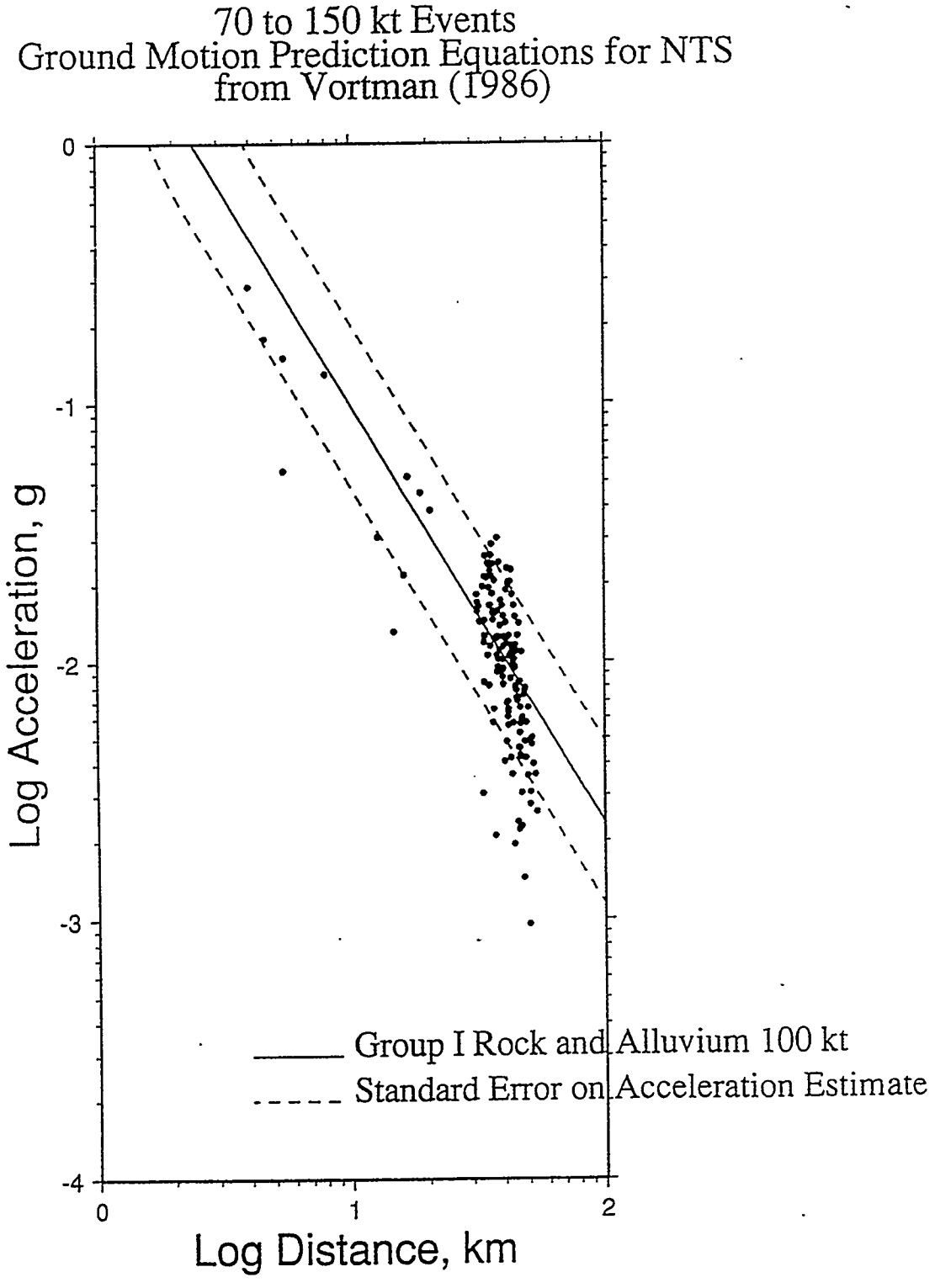

Figure 8: Yucca Flat peak vector acceleration data plotted as a function of distance, superimposed on Vortman's (1986) group I alluvium plus rock prediction equations for a yield of 100 kt. Standard deviations of the prediction equation are shown as dashed lines.

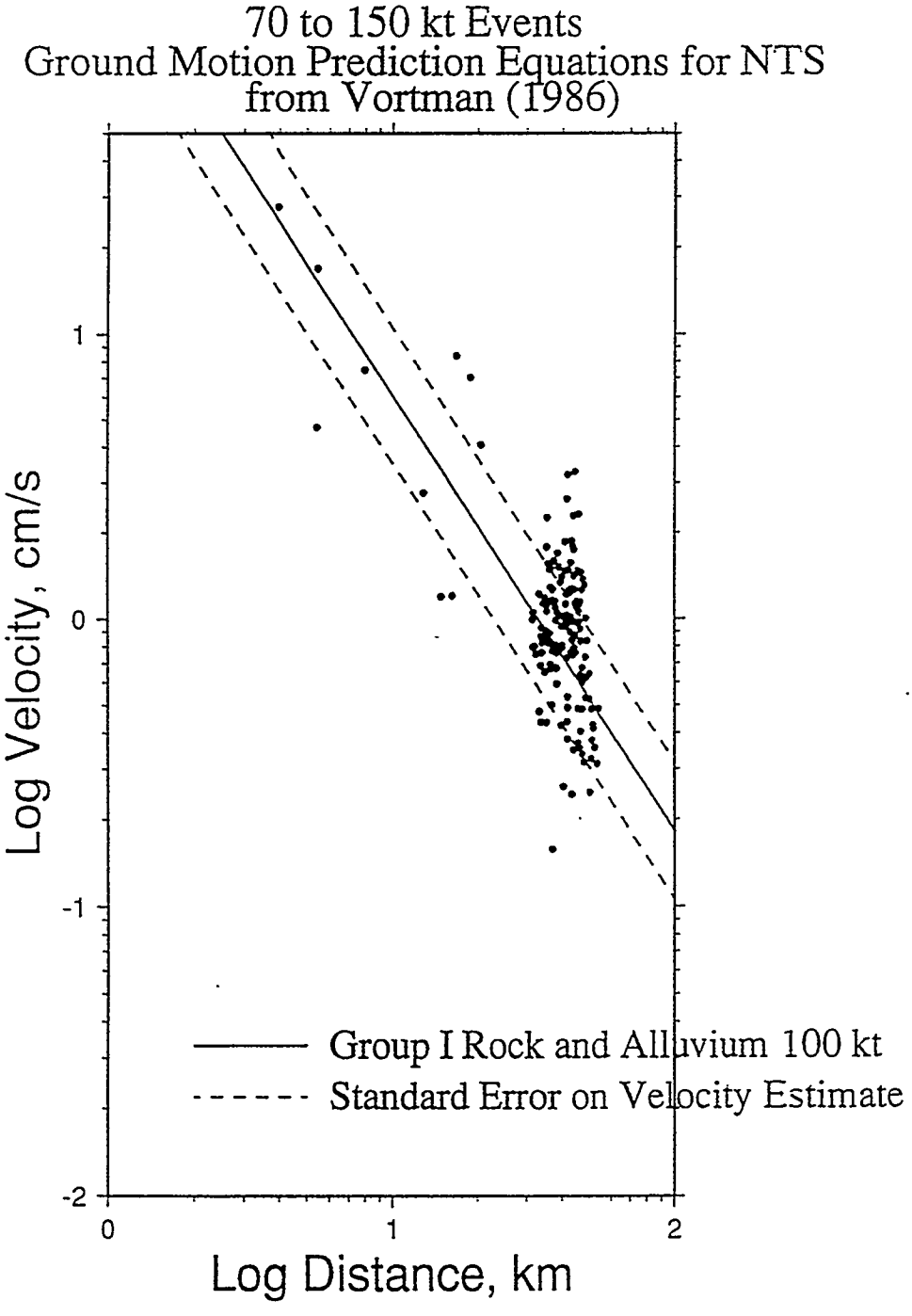

Figure 9: Same as figure 8 for peak vector velocity data.

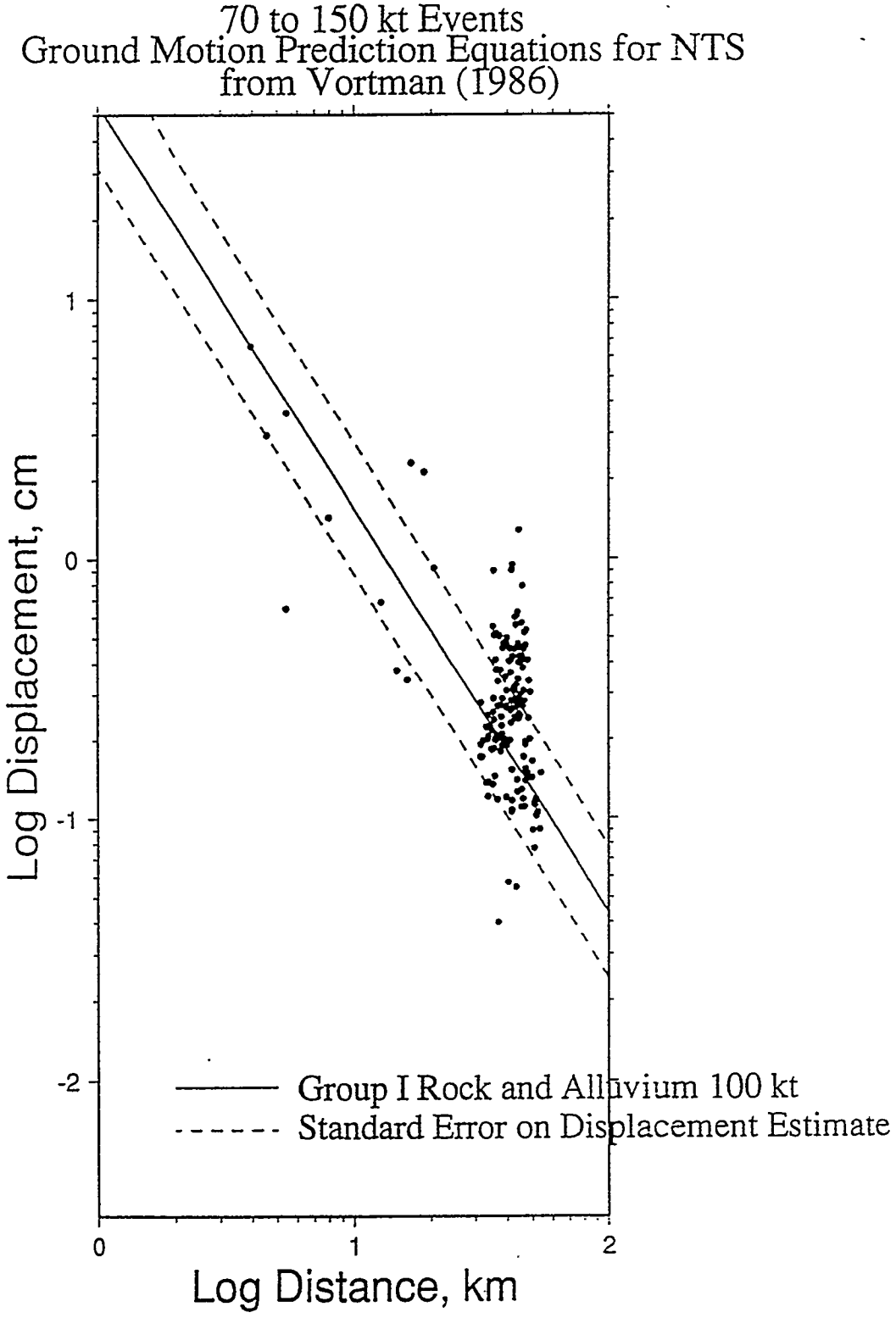

Figure 10: Same as figure 8 for peak vector displacement data.

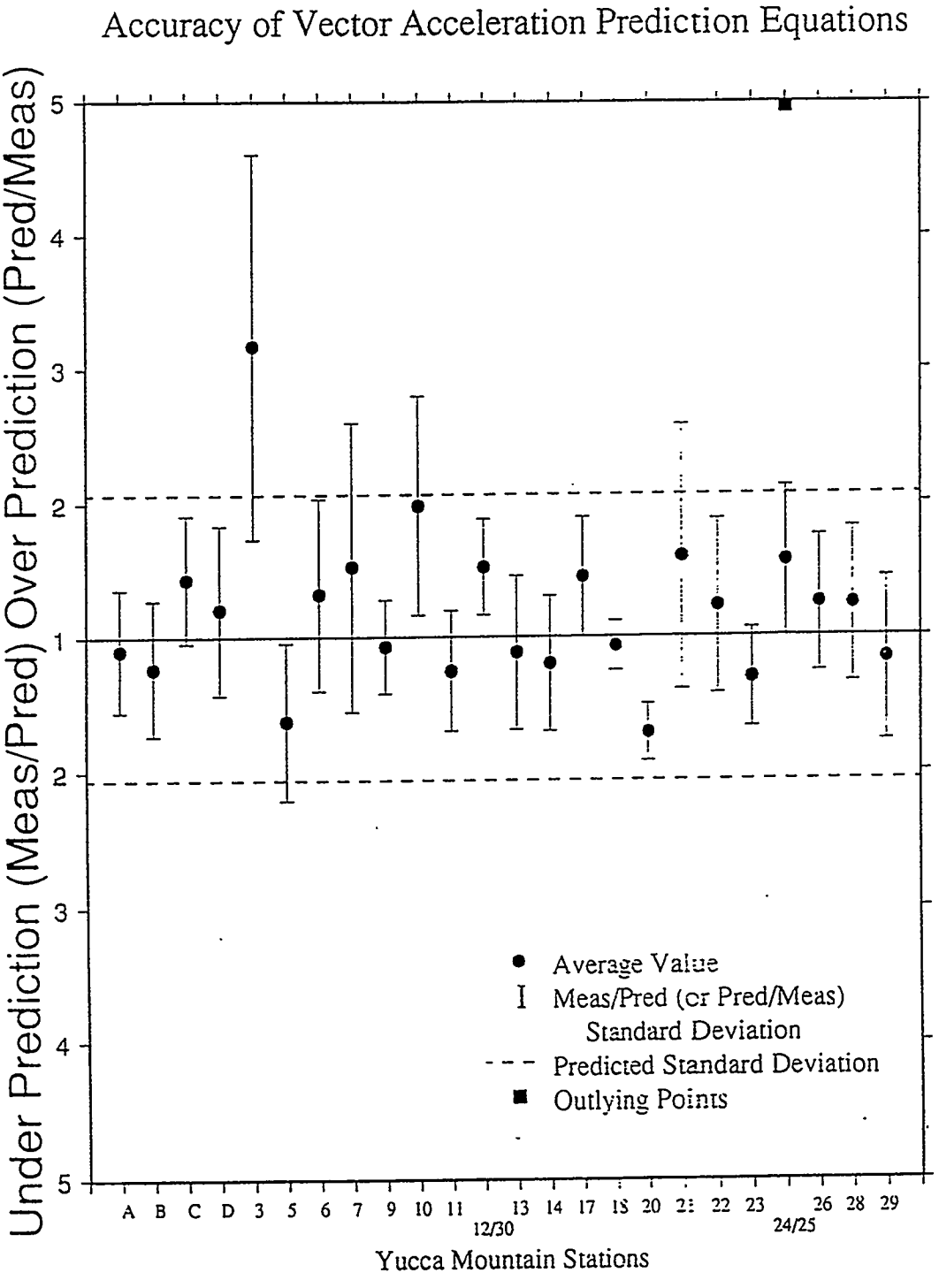

Figure 11: Comparison of ratio of measured-to-predicted vector acceleration for WTSI stations, Yucca Flat sources, and Vortman (1986) group I equations.

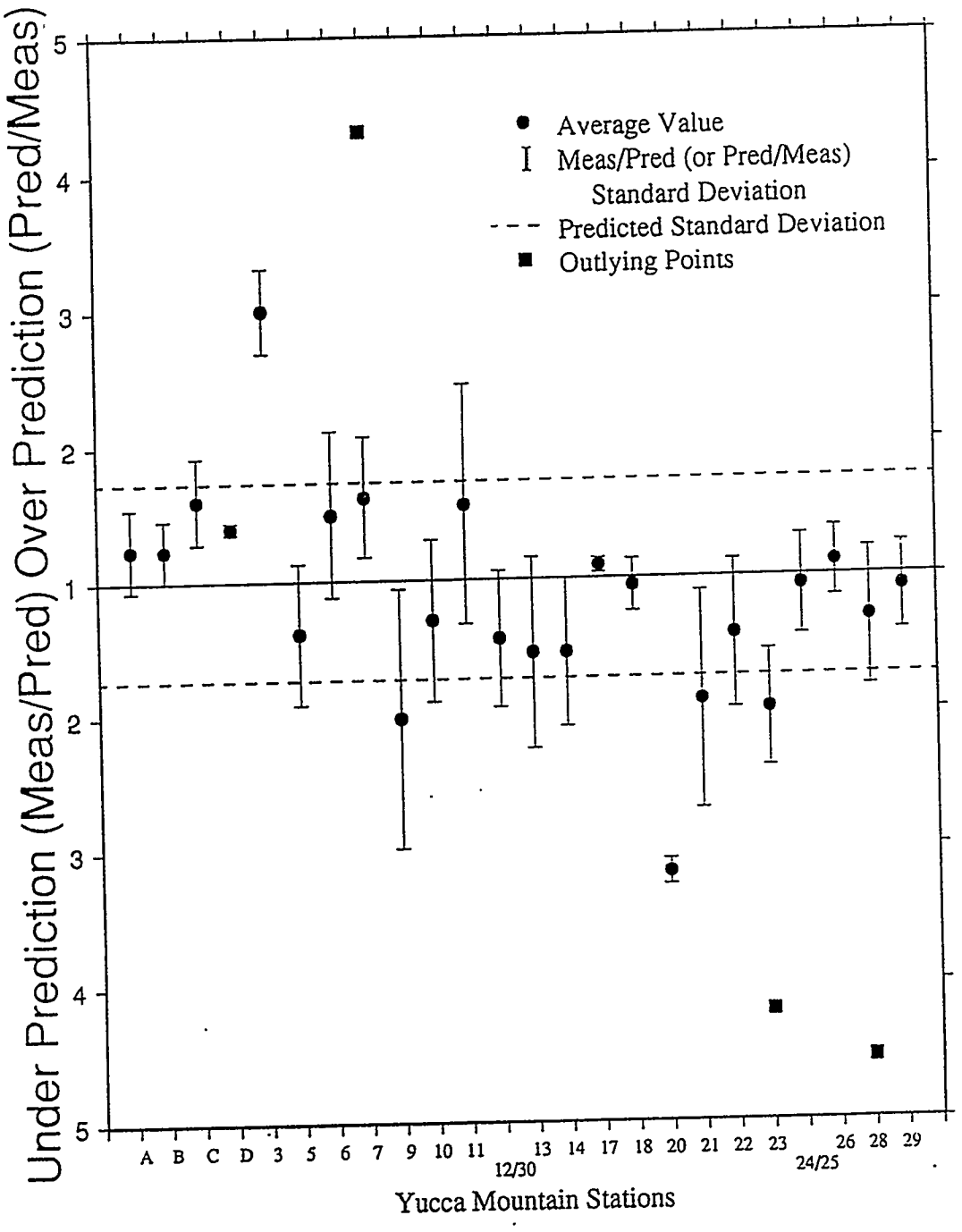

Figure 12: Same as figure 11 for vector velocity.

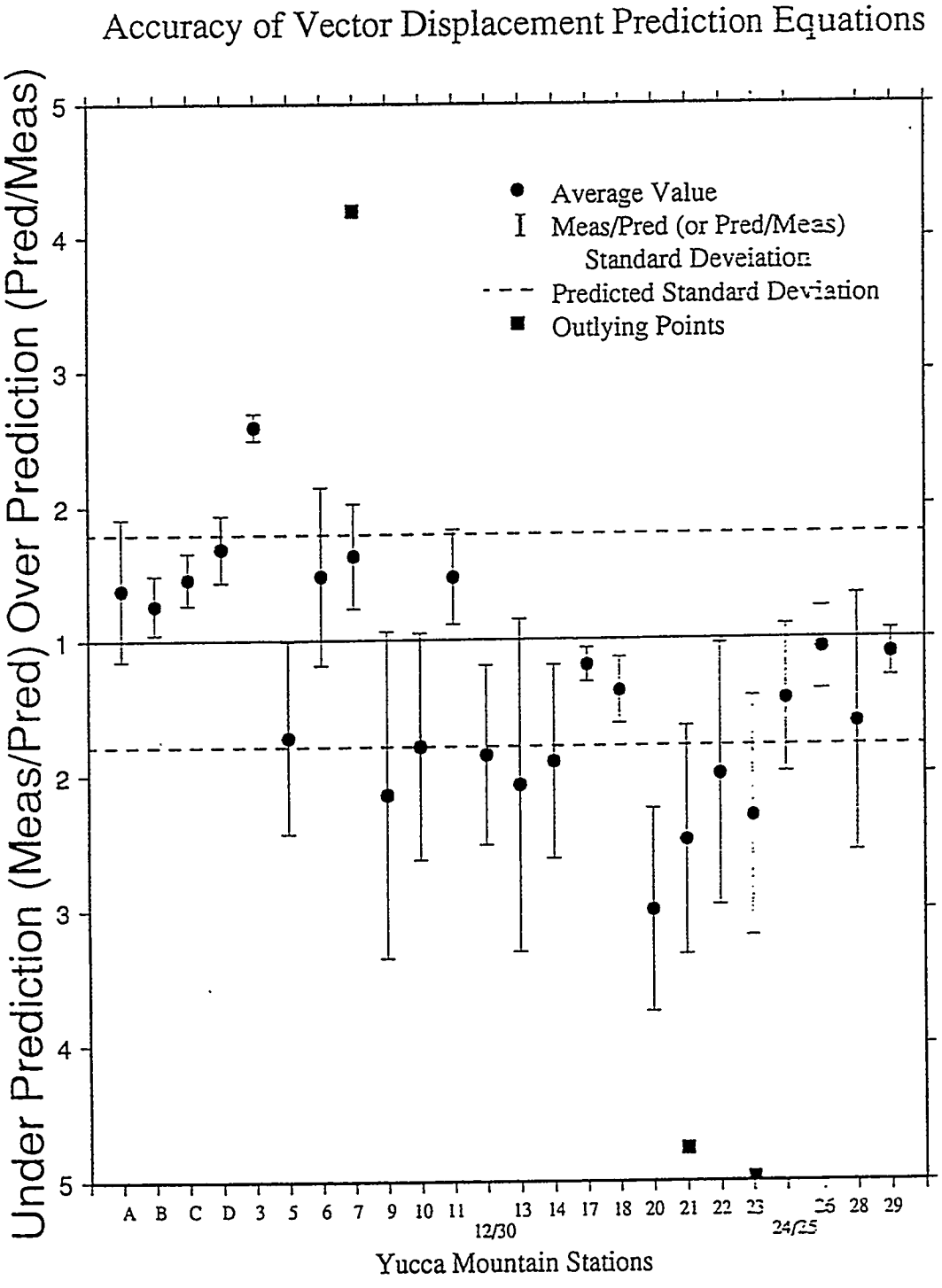

Figure 13: Same as figure 11 for vector displacement.

than the equations predict, but the velocity and acceleration data fits are reasonably good. The larger displacements could be due to the observed large surface waves which have been previously noted at Yucca Mountain stations from UNEs. The surface waves do not tend to be that large in the acceleration waveforms, but produce very large displacements and sometimes velocities. The reasons for the generation of such large surface waves at Yucca Mountain is currently not well determined.

In general, the prediction equations of Vortman (1986), developed solely from Pahute Mesa, fit the Yucca Flat data in an acceptable fashion. Velocity and displacement ground motion estimates for certain Yucca Mountain stations could be multiplied by a correction factor of approximately two for more accurate estimates. We are unable to assess the Vortman equations' accuracy at higher yield ranges with this data set. Ground motions expected from the 70-150kt yield range observed at Yucca Mountain (distances of 40-60 km) are quite small and are insignificant from a seismic hazard perspective.

Prediction Equations for Peak Component Motions

Prediction equations for the individual components of motion observed from Pahute Mesa data at WTSI stations were developed by Long (1992) in a fashion analogous to that of Vortman's 1986 study of vector motions. Long (1992) separated out radial and tangential motions instead of the more standard seismic hazard practices of examining either the larger of the two horizontal components, or an average of the two horizontal components (Boore et al., 1993). Generally, the radial ground motions observed from UNEs in the distance ranges considered here are larger than the tangential motions, however, the tangential motions are still of significant size.

Long (1992) used a data set very similar to that of Vortman (1986) in his analysis and used identical methods and computer codes to achieve his regression equations. Table 4 presents the prediction equation results for the individual components of ground motion. Figures 14 - 16 compare the vertical, radial, and tangential equations for each of the three defined site conditions (alluvium plus rock, rock only, and alluvium only) and the Group II acceleration data. We show Group II instead of Group I because of a tendency of large accelerations at certain anomalous stations in Group I that seem to skew the alluvium-only equation in that data set.

Phillips (unpublished, 1987) compared an expanded Pahute Mesa UNE data set to Long's component equations. Peak component accelerations were generally quite well predicted by the equations. Velocities and displacements recorded at Yucca Mountain stations tend to be larger than those predicted by the equations, however the scatter is quite large and the error bars on the measured and predicted ranges overlap. The greatest discrepancies in prediction are in the displacements, particularly for the vertical component. Phillips (unpublished) concluded that while the Yucca Mountain stations tend to record larger-than-average ground motions for NTS, that they lie within the expected range, and development of new equations is not warranted by the data.

Table 4: Prediction Equations for Component Ground Motions from Long (1992)

A. Vertical Motions (in g, cm/sec, and cm)

Group No.	Eqn. No.	Ground Motion Parameter	Constant	Yield exponent	Range exponent	σ gd. mot.	σ range	Number of data	Medium
I	T41	accel (g)	0.504	0.467	-1.702	2.223	1.599	474	A+R
I	T42	accel	0.417	0.510	-1.762	2.081	1.516	358	Rock
I	T43	accel.	0.080	0.104	-0.676	2.351	3.538	115	Alluv.
I	T44	vel(cm/s)	7.161	0.689	-1.603	1.831	1.459	484	A+R
I	T45	vel	6.784	0.707	-1.656	1.763	1.409	368	Rock
I	T46	vel.	3.810	0.476	-1.098	1.869	1.767	115	Alluv.
I	T47	disp(cm)	0.991	0.764	-1.590	1.836	1.465	481	A+R
I	T48	disp	1.163	0.747	-1.645	1.850	1.454	365	Rock
I	T49	disp.	0.274	0.680	-1.101	1.692	1.612	115	Alluv.
II	T410	accel.	0.508	0.477	-1.752	2.041	1.503	377	A+R
II	T411	accel.	0.573	0.459	-1.750	2.042	1.504	319	Rock
II	T412	accel.	0.023	0.492	-1.001	1.978	1.978	57	Alluv.
II	T413	vel.	8.554	0.668	-1.632	1.691	1.380	387	A+R
II	T414	vel.	9.675	0.649	-1.639	1.661	1.363	329	Rock
II	T415	vel.	2.060	0.692	-1.301	1.864	1.614	57	Alluv.
II	T416	disp.	1.331	0.722	-1.608	1.816	1.449	384	A+R
II	T417	disp.	1.584	0.698	-1.635	1.786	1.426	326	Rock
II	T418	disp.	0.393	0.689	-1.218	1.974	1.748	57	Alluv.
III	T419	accel.	0.409	0.516	-1.777	2.037	1.492	340	A+R
III	T420	accel.	0.487	0.491	-1.792	2.039	1.488	283	Rock
III	T421	accel.	0.023	0.492	-1.001	1.978	1.977	57	Alluv.
III	T422	vel.	7.171	0.701	-1.658	1.668	1.362	350	A+R
III	T423	vel.	8.390	0.679	-1.684	1.625	1.334	293	Rock
III	T424	vel.	2.060	0.692	-1.301	1.864	1.614	57	Alluv.
III	T425	disp.	1.069	0.763	-1.642	1.783	1.422	347	A+R
III	T426	disp.	1.319	0.737	-1.699	1.717	1.375	290	Rock

Table 4: Prediction Equations for Component Ground Motions from Long (1992), continued

Group No.	Eqn. No.	Ground Motion Parameter	Constant	Yield exponent	Range exponent	σ gd. mot.	σ range	Number of data	Medium
III	T427	disp.	0.393	0.689	-1.218	1.974	1.748	57	Alluv.
B. Radial motions									
I.	T428	accel.	0.161	0.432	-1.359	2.128	1.743	430	A+R
I.	T429	accel.	0.192	0.413	-1.406	2.150	1.724	313	Rock
I.	T430	accel.	0.022	0.349	-0.703	2.019	2.718	115	Alluv.
I.	T431	vel.	5.306	0.579	-1.319	1.920	1.640	443	A+R
I.	T432	vel.	6.090	0.560	-1.336	1.993	1.676	326	Rock
I.	T433	vel.	1.879	0.589	-1.058	1.712	1.662	115	Alluv.
I.	T434	disp.	1.059	0.704	-1.436	1.965	1.601	442	A+R
I.	T435	disp.	1.035	0.710	-1.445	2.020	1.627	325	Rock
I.	T436	disp.	0.708	0.648	-1.248	1.819	1.615	115	Alluv.
II.	T437	accel.	0.174	0.427	-1.383	2.116	1.719	330	A+R
II.	T438	accel.	0.251	0.369	-1.396	2.148	1.729	273	Rock
II.	T439	accel.	0.009	0.635	-0.944	1.844	1.912	57	Alluv.
II.	T440	vel.	6.046	0.559	-1.318	1.868	1.607	343	A+R
II.	T441	vel.	7.105	0.533	-1.321	1.863	1.602	286	Rock
II.	T442	vel.	1.726	0.668	-1.164	1.892	1.730	57	Alluv.
II.	T443	disp.	1.176	0.688	-1.437	1.957	1.596	342	A+R
II.	T444	disp.	1.068	0.704	-1.435	1.916	1.573	285	Rock
II.	T445	disp.	1.157	0.590	-1.289	2.188	1.837	57	Alluv.
III.	T446	accel.	0.154	0.449	-1.401	2.219	1.715	294	A+R
III.	T447	accel.	0.239	0.382	-1.425	2.175	1.725	237	Rock
III.	T448	accel.	0.009	0.635	-0.944	1.844	1.912	57	Alluv.
III.	T449	vel.	5.513	0.577	-1.337	1.887	1.608	307	A+R
III.	T450	vel.	6.861	0.544	-1.352	1.888	1.600	250	Rock

Table 4: Prediction Equations for Component Ground Motions from Long (1992), continued

Group No.	Eqn. No.	Ground Motion Parameter	Constant	Yield exponent	Range exponent	σ gd. mot.	σ range	Number of data	Medium
III.	T451	vel.	1.726	0.668	-1.164	1.892	1.730	57	Alluv.
III.	T452	disp.	1.060	0.709	-1.464	1.933	1.569	306	A+R
III.	T453	disp.	1.024	0.719	-1.486	1.872	1.525	249	Rock
III.	T454	disp.	1.157	0.590	-1.289	2.188	1.837	57	Alluv.
C. Tangential Motions									
I.	T455	accel.	0.134	0.410	-1.304	2.180	1.818	421	A+R
I.	T456	accel.	0.194	0.360	-1.357	2.269	1.829	303	Rock
I.	T457	accel.	0.019	0.439	-0.810	1.923	2.241	116	Alluv.
I.	T458	vel.	4.731	0.488	-1.175	2.113	1.890	433	A+R
I.	T459	vel.	5.769	0.460	-1.196	2.297	2.005	315	Rock
I.	T460	vel.	2.367	0.540	-1.060	1.589	1.548	116	Alluv.
I.	T461	disp.	0.658	0.580	-1.128	2.167	1.985	432	A+R
I.	T462	disp.	0.637	0.589	-1.141	2.300	2.075	314	Rock
I.	T463	disp.	0.243	0.488	-0.737	1.798	2.216	116	Alluv.
II.	T464	accel.	0.153	0.395	-1.325	2.263	1.853	320	A+R
II.	T465	accel.	0.259	0.315	-1.351	2.308	1.858	263	Rock
II.	T466	accel.	0.008	0.677	-0.984	1.905	1.925	57	Alluv.
II.	T467	vel.	5.202	0.473	-1.175	2.122	1.897	332	A+R
II.	T468	vel.	6.153	0.446	-1.182	2.187	1.940	275	Rock
II.	T469	vel.	2.116	0.578	-1.102	1.805	1.709	57	Alluv.
II.	T470	disp.	0.687	0.575	-1.140	2.168	1.972	331	A+R
II.	T471	disp.	0.641	0.585	-1.129	2.173	1.988	274	Rock
II.	T472	disp.	0.239	0.522	-0.807	2.168	2.609	57	Alluv.
III.	T473	accel.	0.138	0.413	-1.337	2.331	1.883	284	A+R
III.	T474	accel.	0.246	0.326	-1.371	2.404	1.897	227	Rock

Table 4: Prediction Equations for Component Ground Motions from Long (1992), continued

Group No.	Eqn. No.	Ground Motion Parameter	Constant	Yield exponent	Range exponent	σ gd. mot.	σ range	Number of data	Medium
III.	T475	accel.	0.008	0.677	-0.984	1.905	1.925	57	Alluv.
III.	T476	vel.	4.746	0.490	-1.191	2.175	1.920	296	A+R
III.	T477	vel.	5.873	0.458	-1.208	2.262	1.966	239	Rock
III.	T478	vel.	2.116	0.578	-1.102	1.805	1.709	57	Alluv.
III.	T479	disp.	0.606	0.599	-1.116	2.226	1.994	295	A+R
III.	T480	disp.	0.598	0.603	-1.165	2.247	2.004	238	Rock
III.	T481	disp.	0.239	0.522	-0.807	2.168	2.609	57	Alluv.

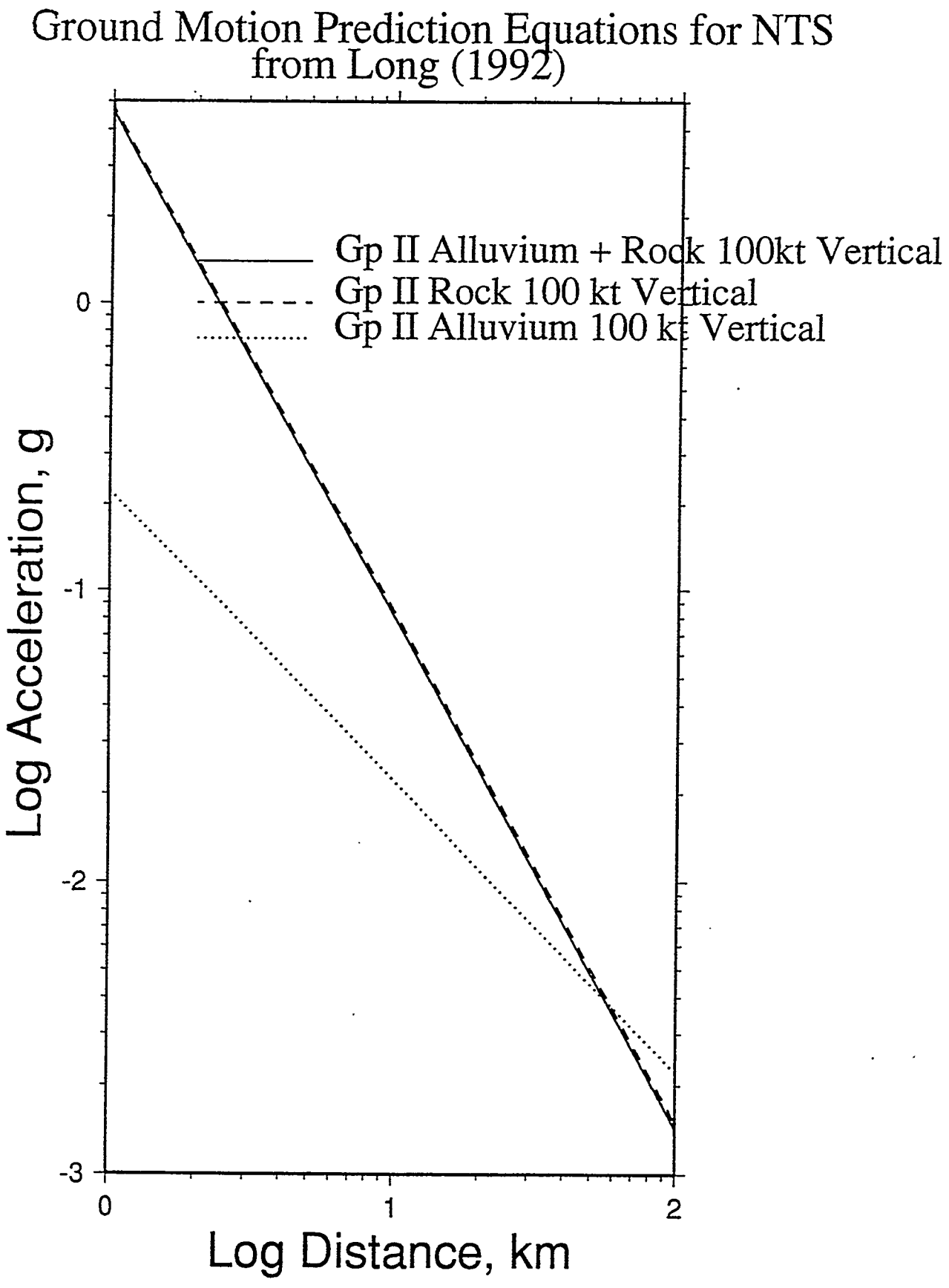

Figure 14: Comparison of data group II regression equations for rock plus alluvium, rock only, and alluvium only, yield = 100kt, vertical component (equations from Long, 1992)

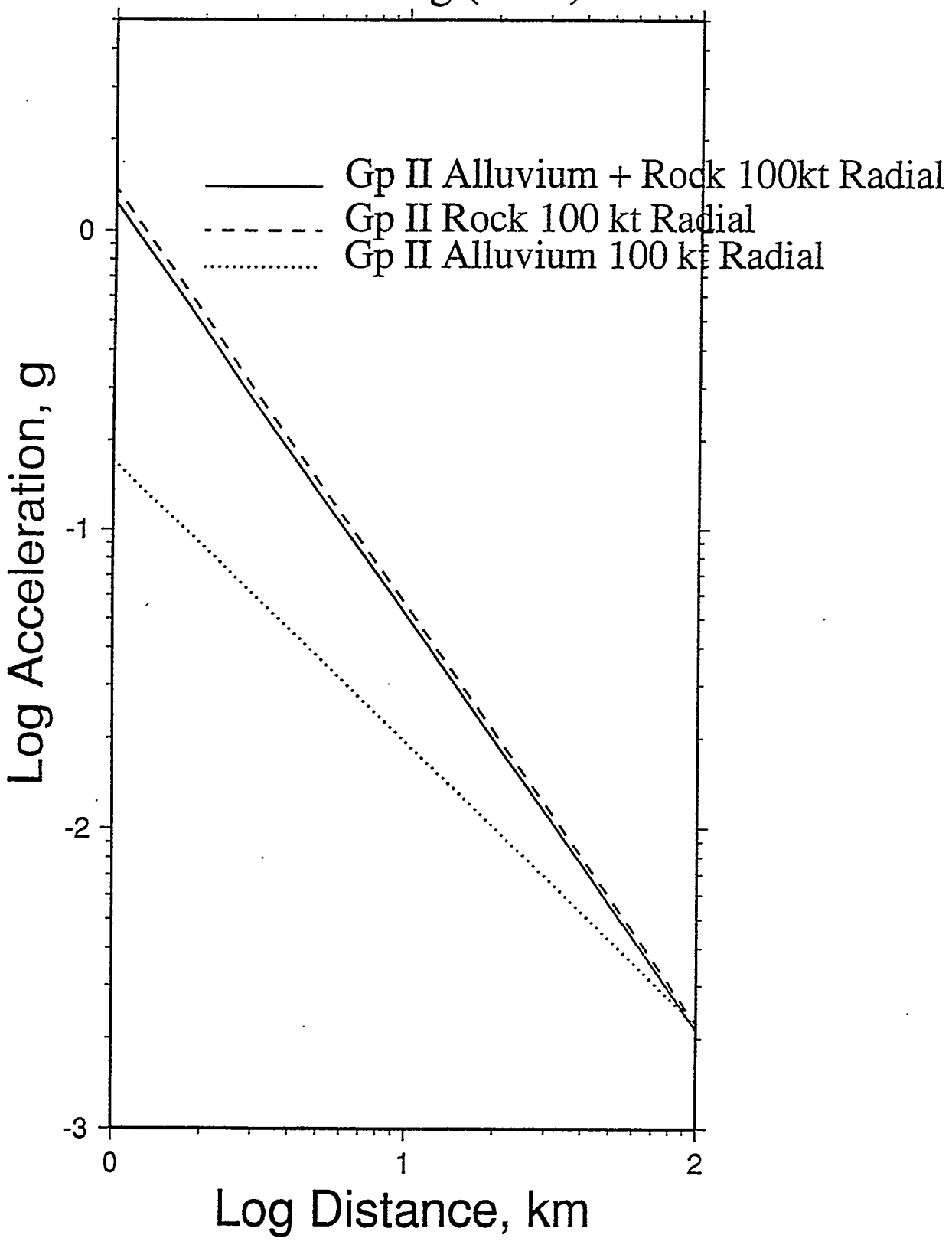

Figure 15: Same as figure 14 for the radial component.

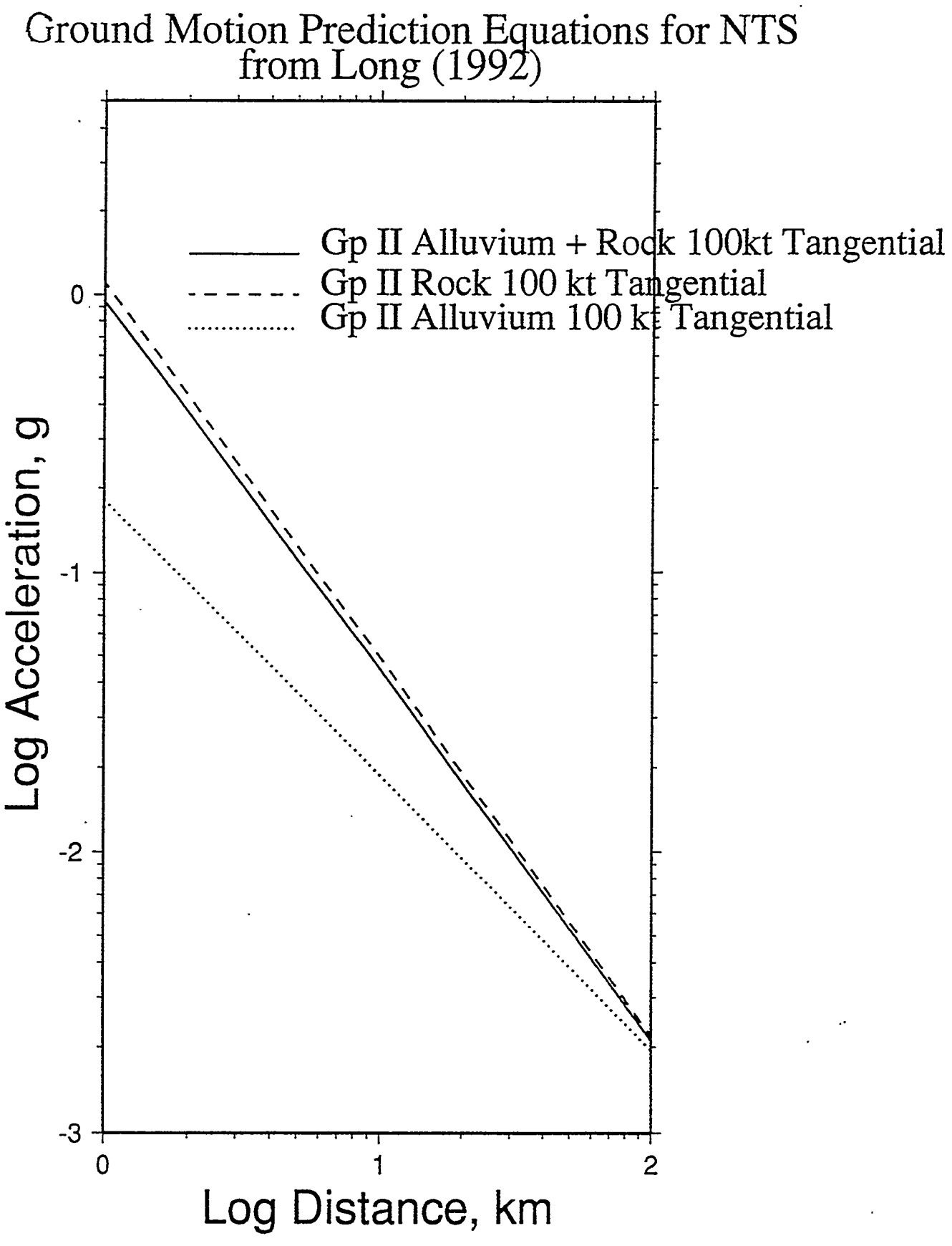

Figure 16: Same as figure 14 for the tangential component.

Phillips (1991a) also studied component ground motions for Pahute Mesa explosions at both surface and downhole locations; his focus in this report was the change in ground motion between the uphole and downhole recordings. He documents a very large amount of scatter in peak ground motion amplitudes among three stations with similar geological profiles and similar depths to downhole instruments, and concentrates on the response spectra, which will be discussed in a later section.

Comparison of the Long (1992) prediction equations with Yucca Flat UNE data

As was the case with the vector ground motions, no previous assessment of the applicability of the published component prediction equations (based on Pahute Mesa UNEs) has been conducted for the more limited Yucca Flat data. We examined the component ground motion for the same data set of 12 UNEs with yields between 70 and 150 kt as were discussed above. Figures 17-25 show the range of vertical, radial, and tangential component ground motion data points superimposed on 100kt yield prediction lines for Long's Group I, rock plus alluvium equations for acceleration, velocity, and displacement. As the illustrations demonstrate, the Yucca Flat UNE data fit well into the prediction range of the Pahute-based equations. Figures 26-34 show the results in more detail, by station, for the measured-to-predicted ratios in comparison with the Group I rock plus alluvium equations of Table 4. The average acceleration ratios are almost always within the standard deviation of the prediction equations, with station 3 being low, as usual. Station 11 generally has higher-than-expected accelerations. This station is very close to Yucca Flat; the Pahute Mesa-derived equations apparently are not totally consistent with the close-in Yucca Flat data. Velocities are similarly well predicted, again with the exception of station 3 and a few other isolated examples such as station 20 radial velocities. Some of the stations have quite a large scatter of peak velocity values. As was observed for the vector ground motions, the displacements show the greatest discrepancy between the observed and predicted values. Stations 20, 21, 23, and 28 (all Yucca Mountain stations) exhibit higher-than expected peak displacements usually in all three components. These ratios often have a large degree of scatter, however, such that the uncertainty ranges of the equations and the data do overlap. Again, the anomalously large amount of surface wave energy observed at Yucca Mountain stations may be responsible for the larger-than-expected displacements.

The comparison of the Yucca Flat UNE component ground motion data with the prediction equations of Long (1992) shows that these equations describe expected ground motions on the NTS in a reasonable fashion. There is no need to develop separate Yucca Flat-specific ground motion prediction equations for peak component acceleration, velocity, or displacement.

Response Spectra: Observations and Predictions

The response spectrum of a seismic event (e.g., Joyner and Boore, 1982) provides more information to the design engineer than simple peak ground motions; it adds the capability of determining the frequency of large excitations observed in the seismogram, or time history. Response spectra are widely used in earthquake engineering (Joyner and Boore, 1982; Boore et al., 1993; and others) and have also been used in some analyses of NTS UNE ground motion

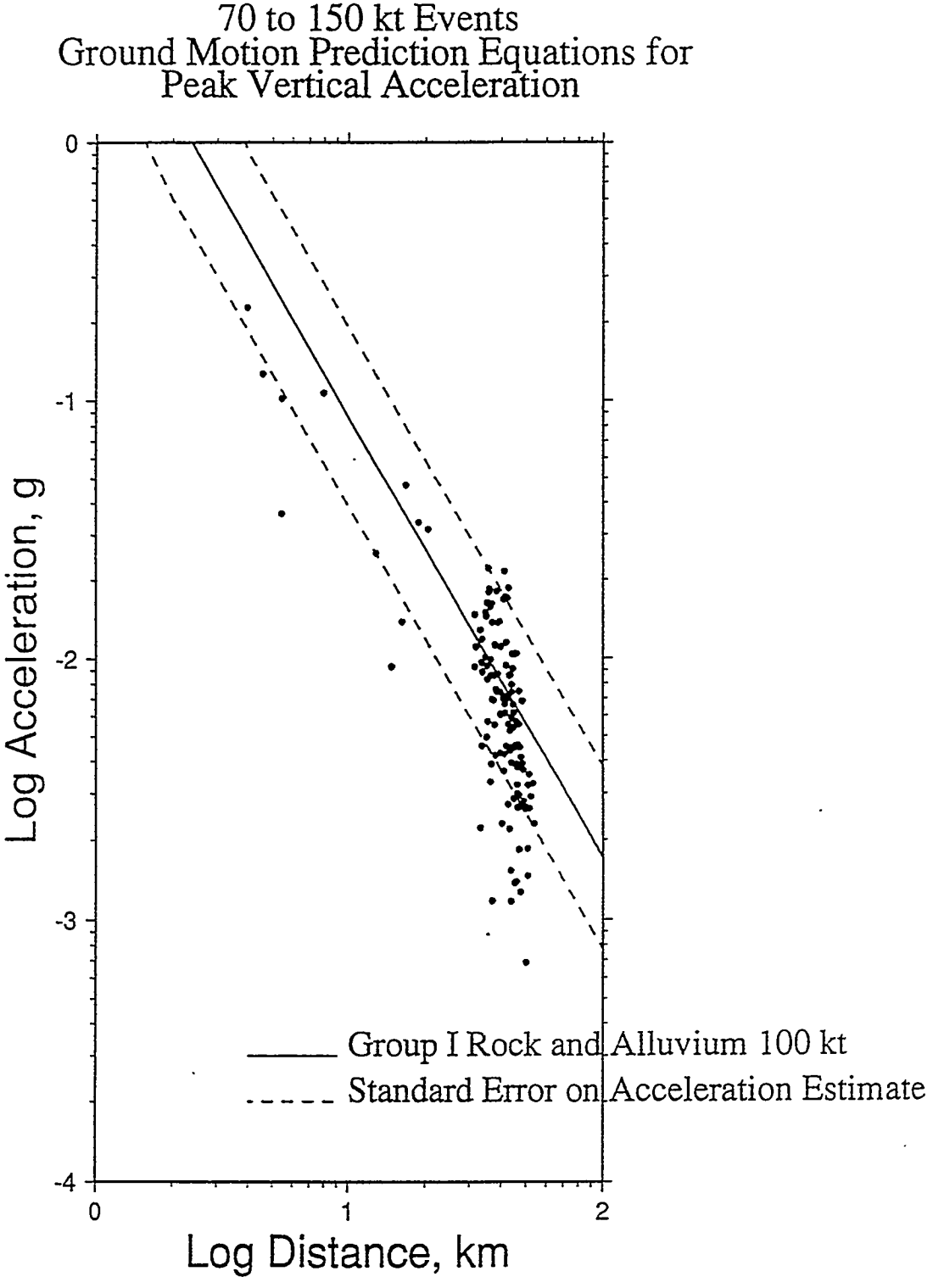

Figure 17: Yucca Flat vertical component acceleration data superimposed on Long's (1992) group I, rock plus alluvium prediction equation for a yield of 100 kt. Dashed lines indicate standard deviations of the prediction equation.

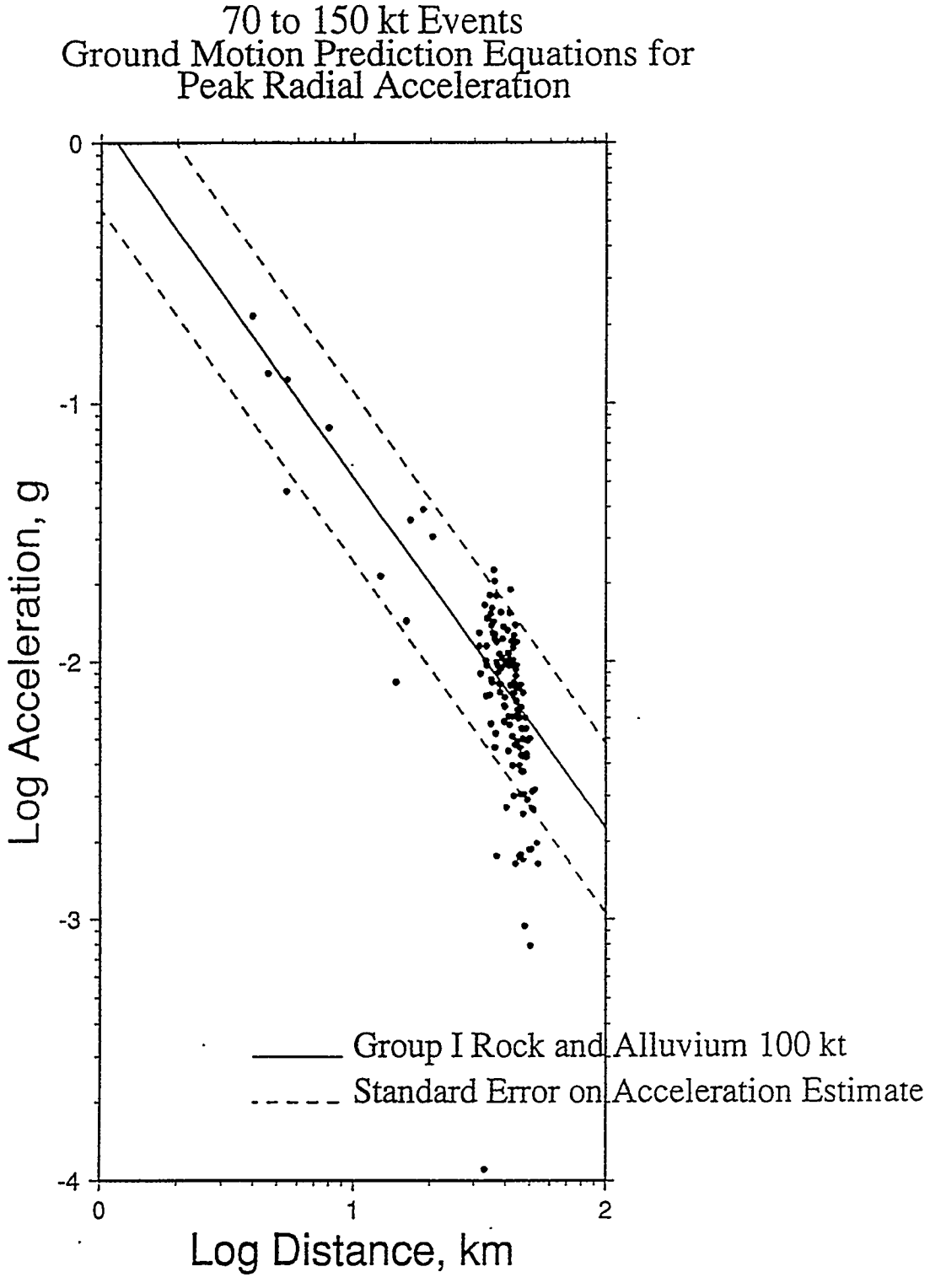

Figure 18: Same as figure 17 for radial component acceleration data.

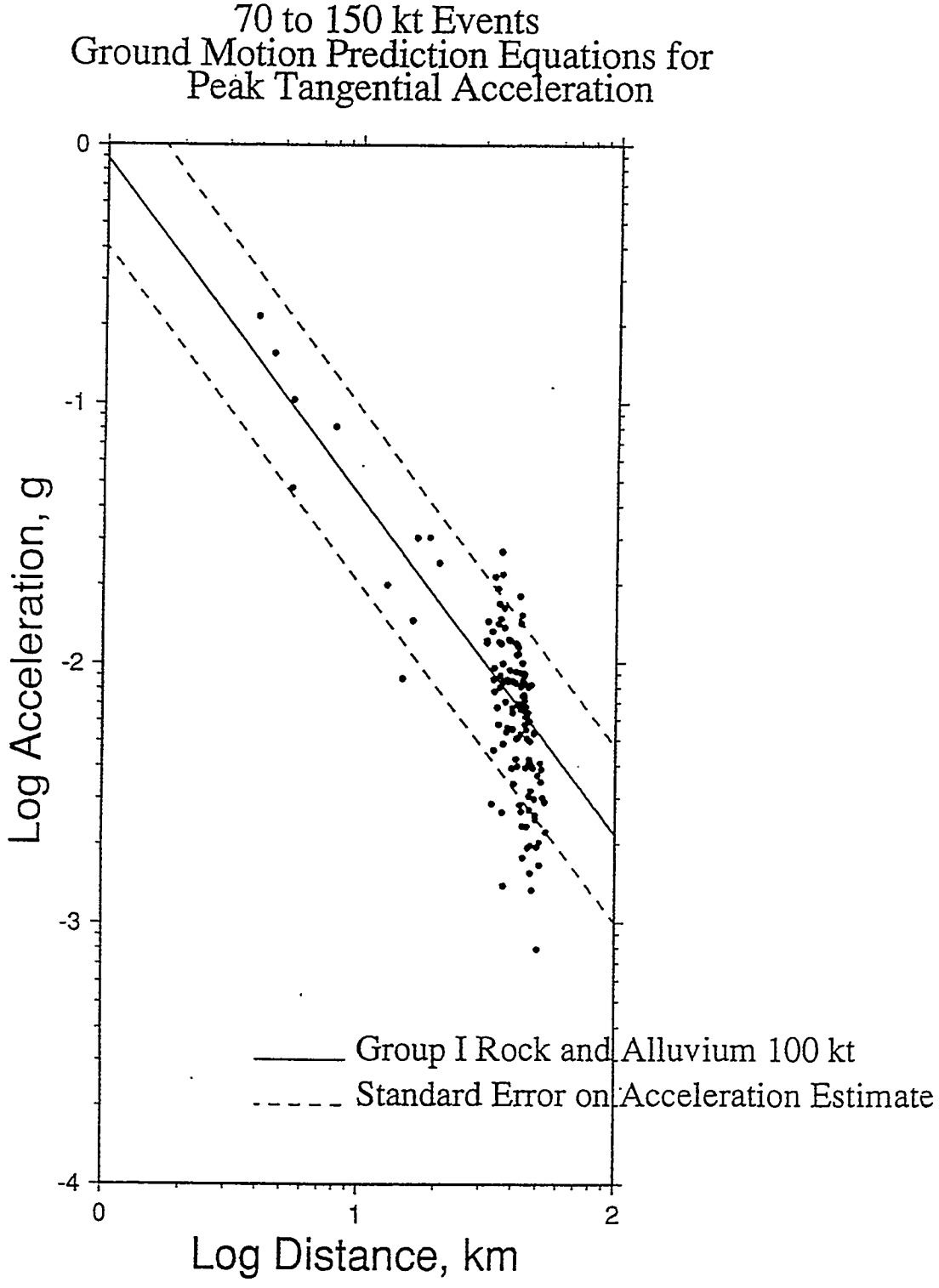

Figure 19: Same as figure 17 for tangential component acceleration data.

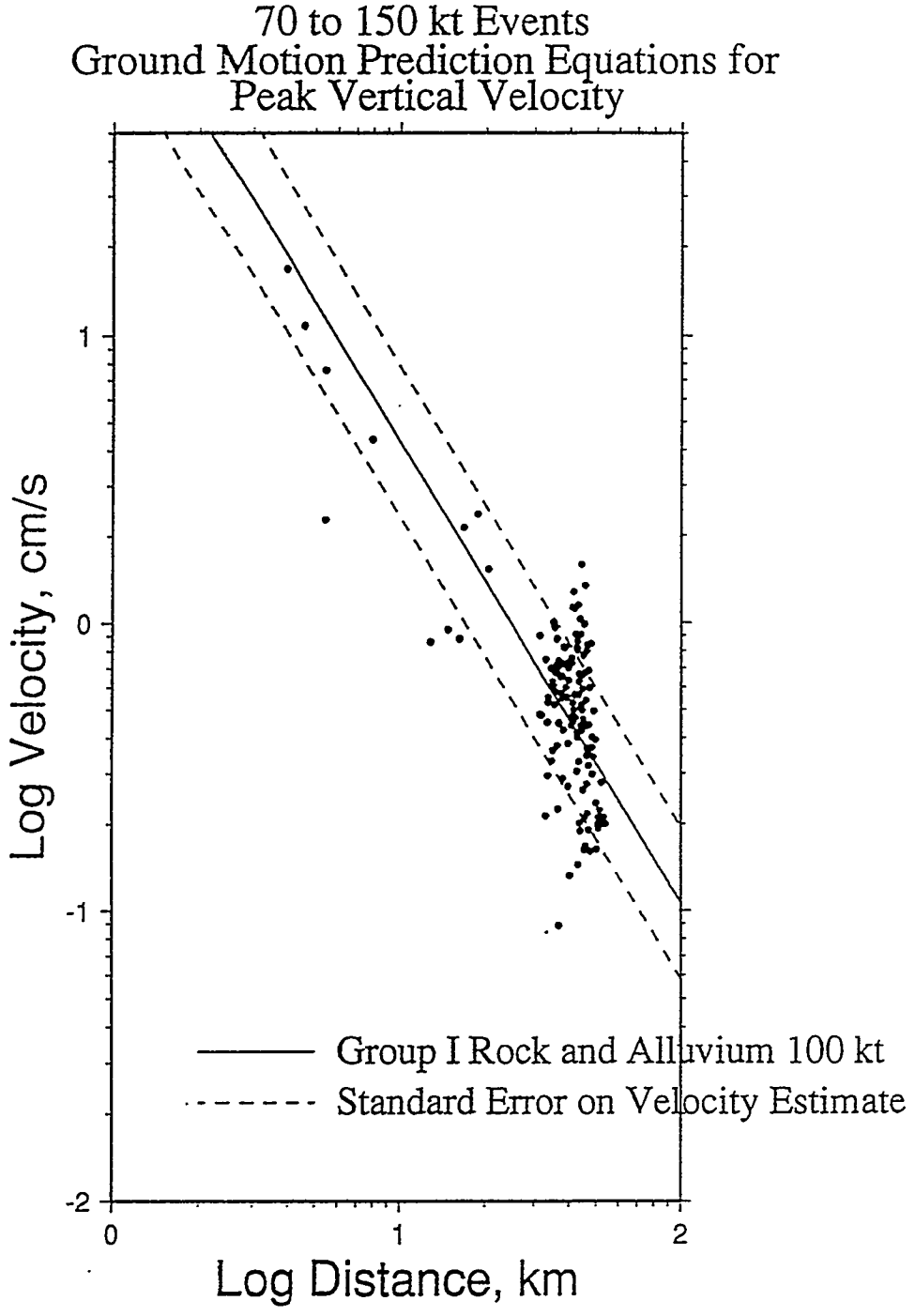

Figure 20: Same as figure 17 for vertical component velocity data.

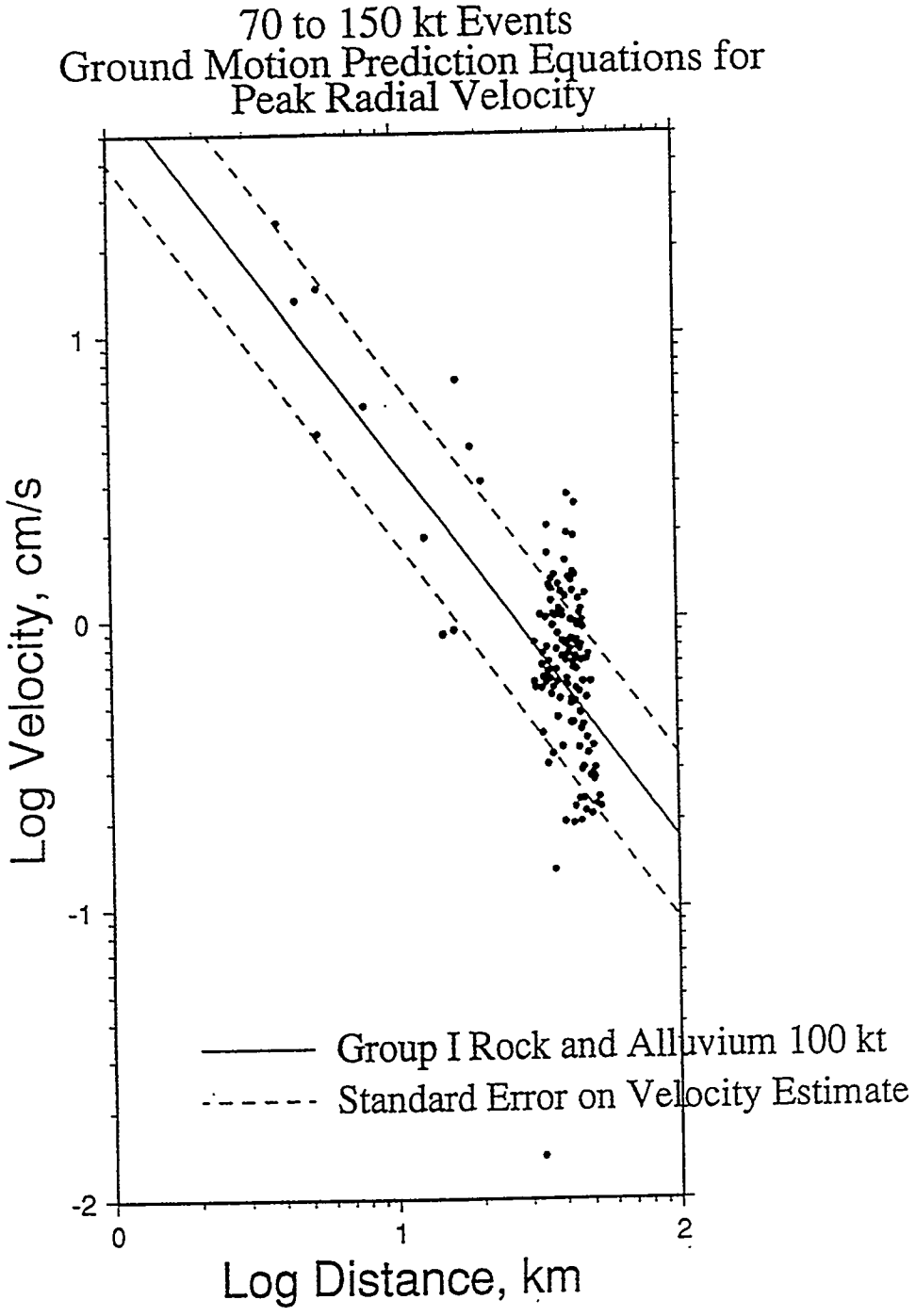

Figure 21: Same as figure 17 for radial component velocity data.

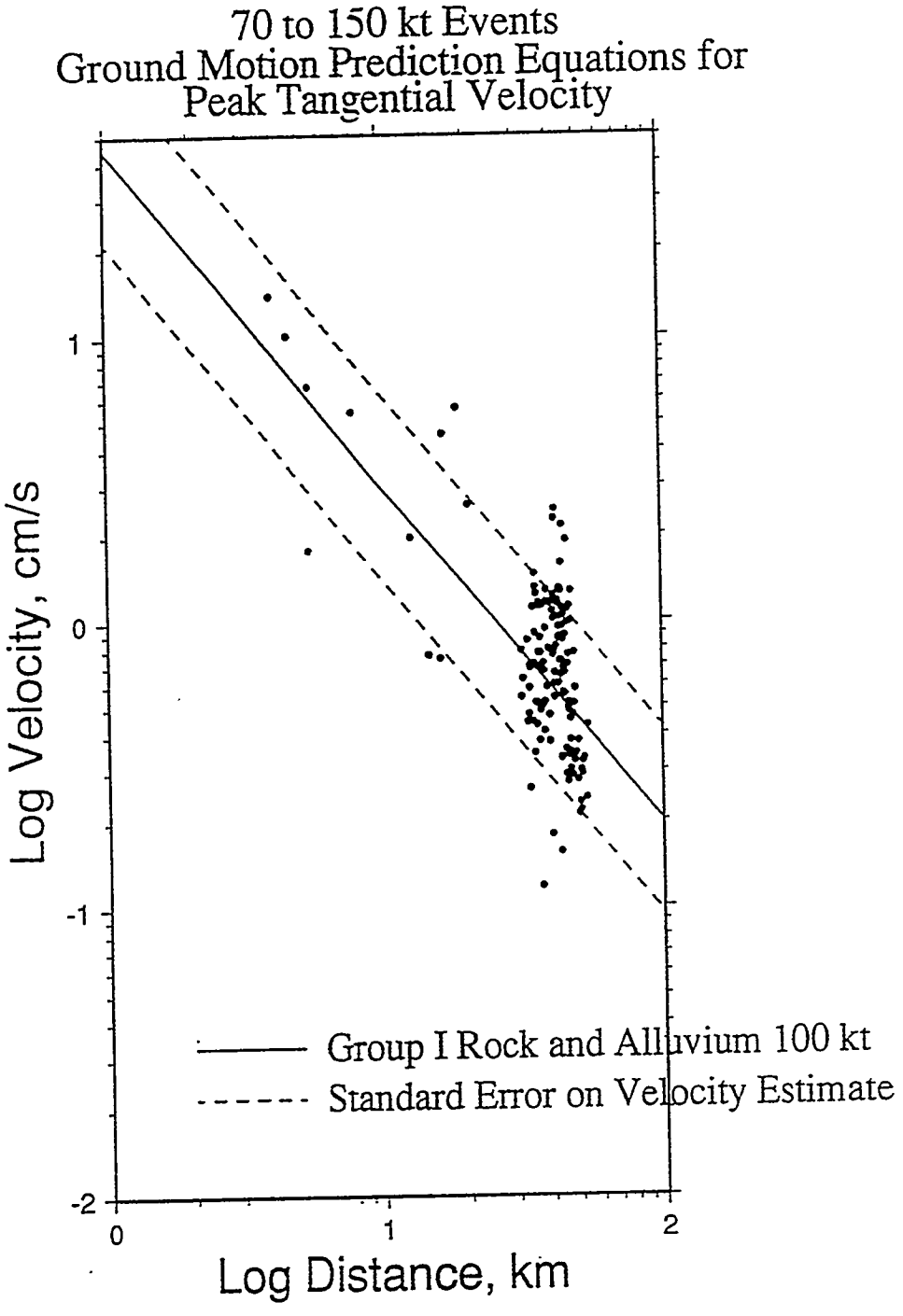

Figure 22: Same as figure 17 for tangential component velocity data.

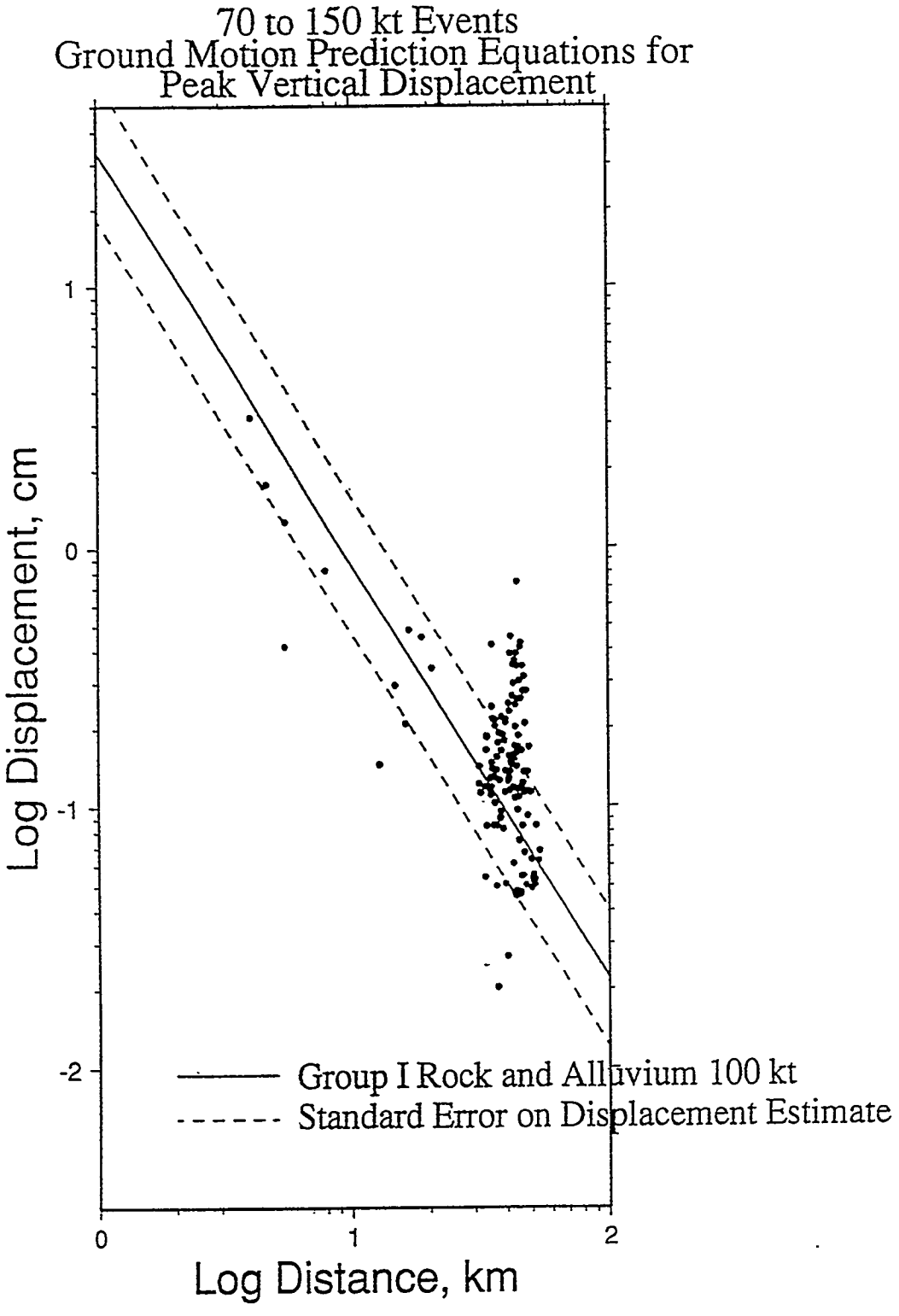

Figure 23: Same as figure 17 for vertical component displacement data.

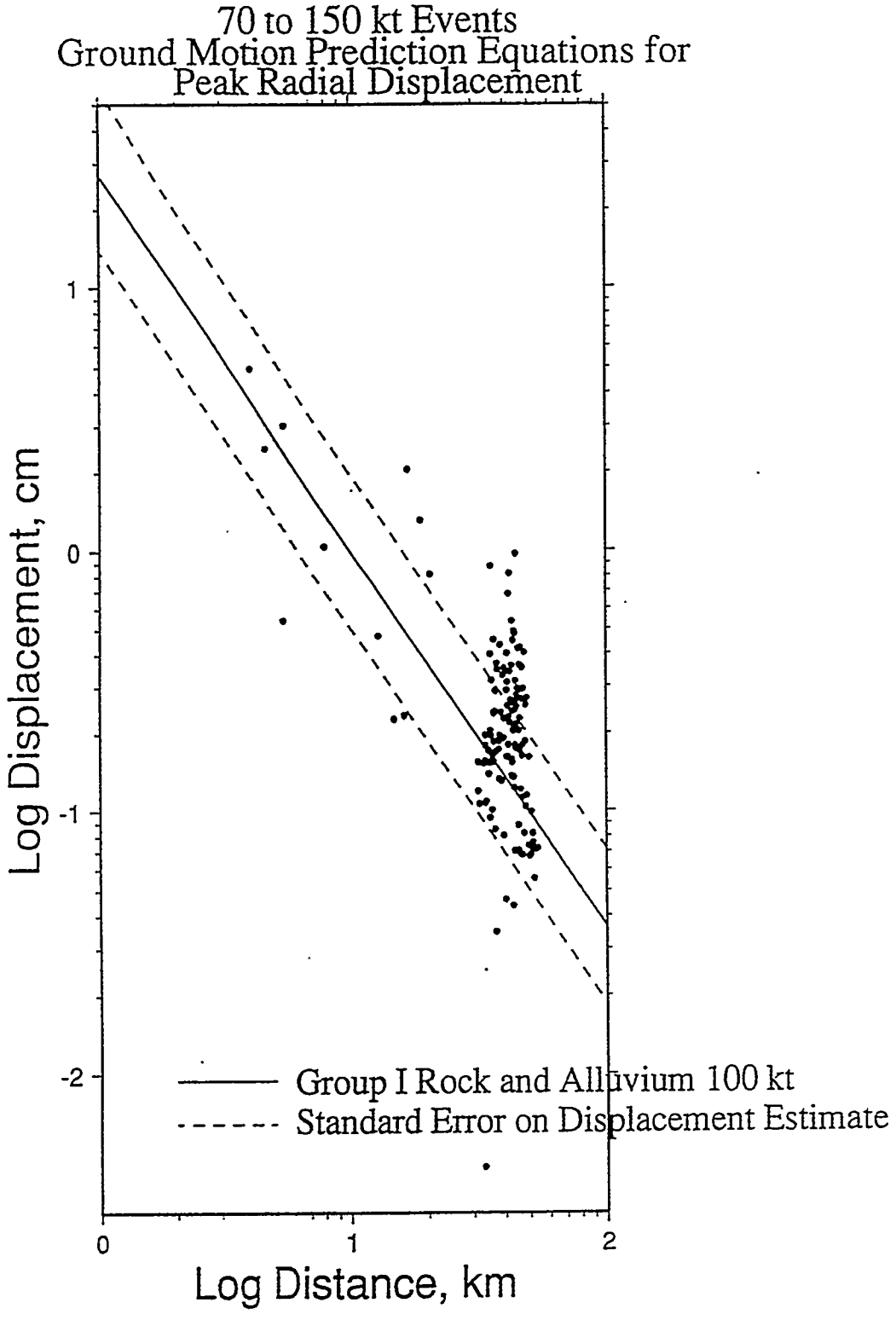

Figure 24: Same as figure 17 for radial component displacement data.

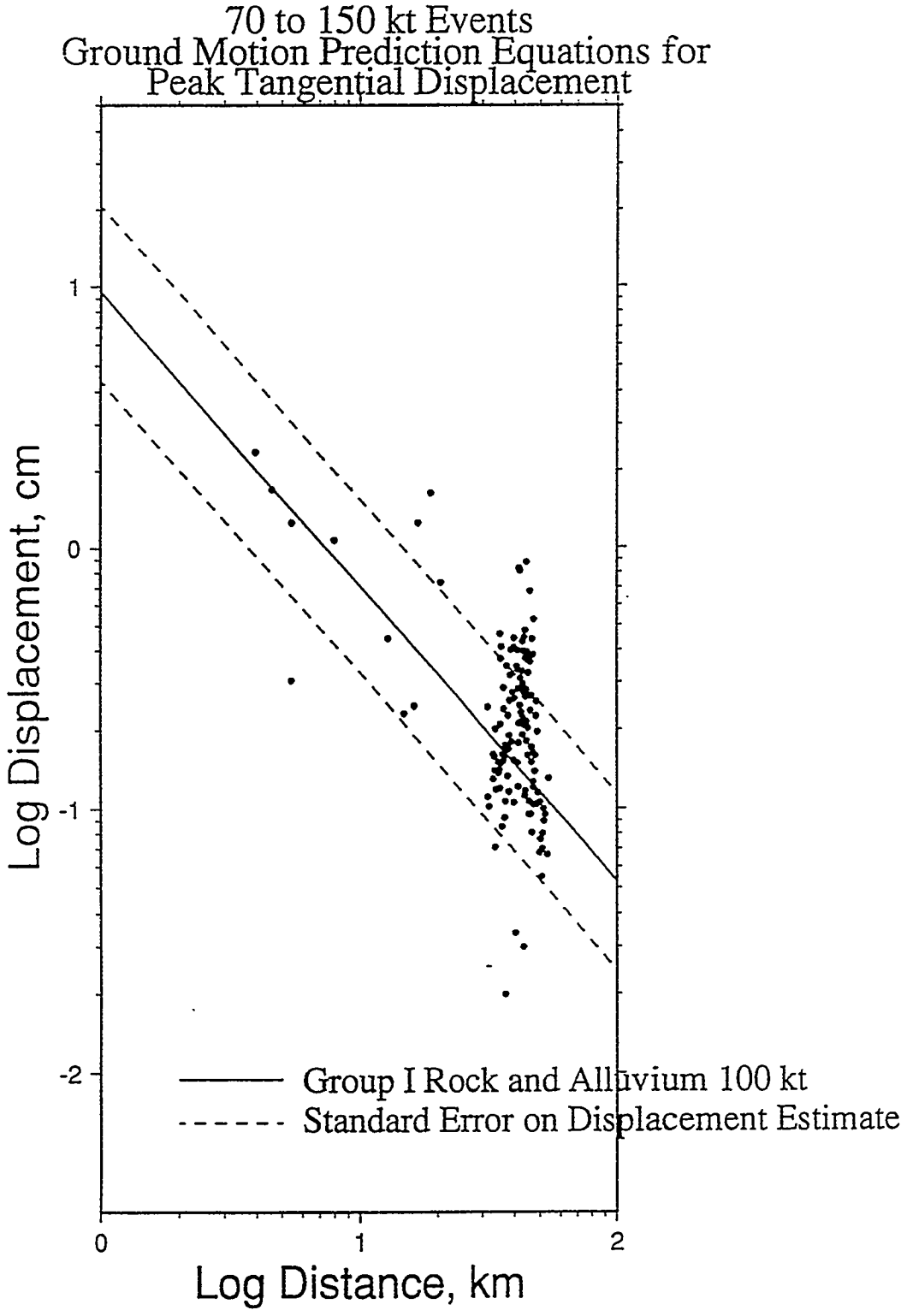

Figure 25: Same as figure 17 for tangential component displacement data.

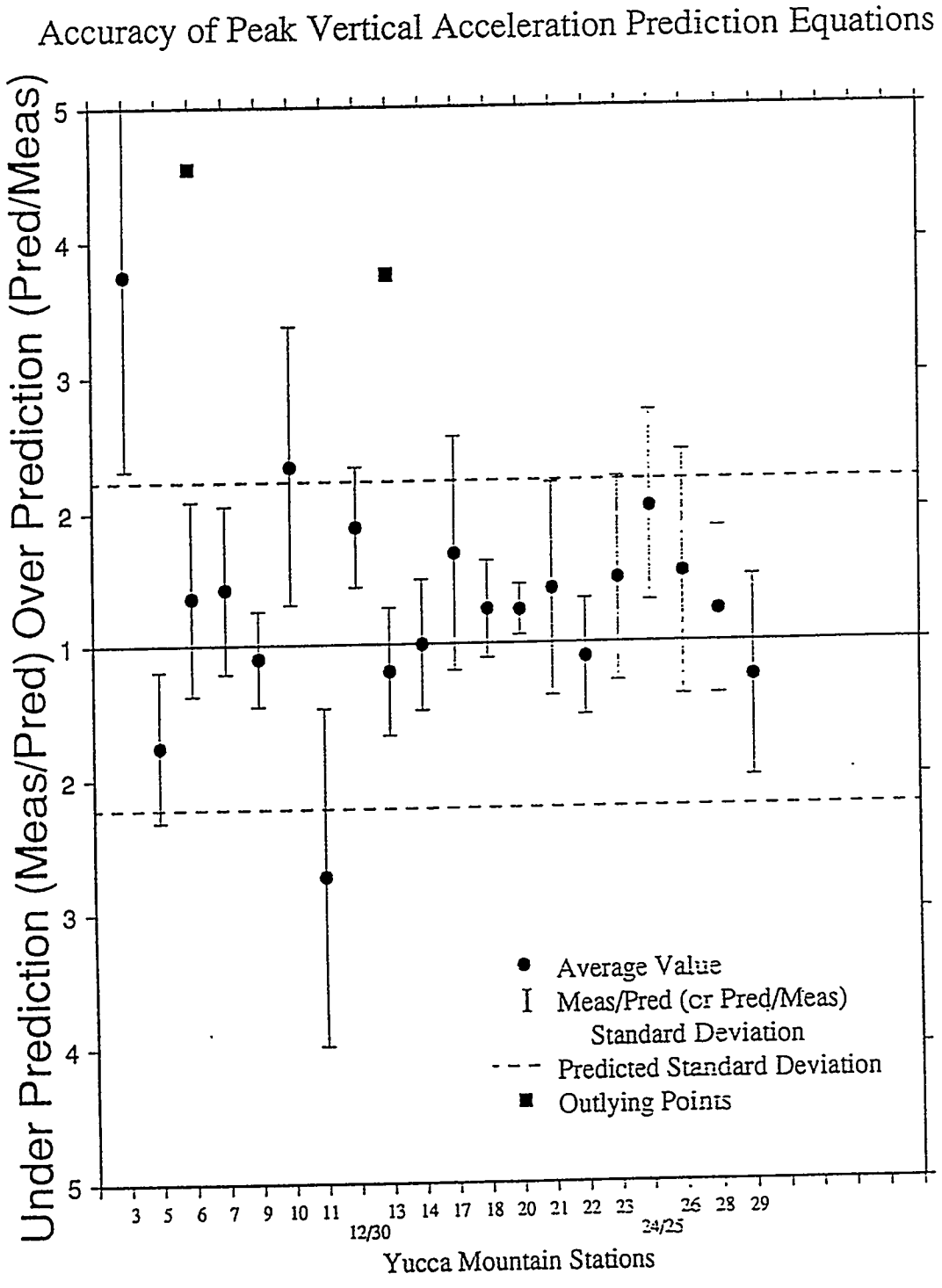

Figure 26: Comparison of ratio of measured-to-predicted vertical component acceleration for WTSI stations, Yucca Flat sources, and the Long (1992) group I equations.

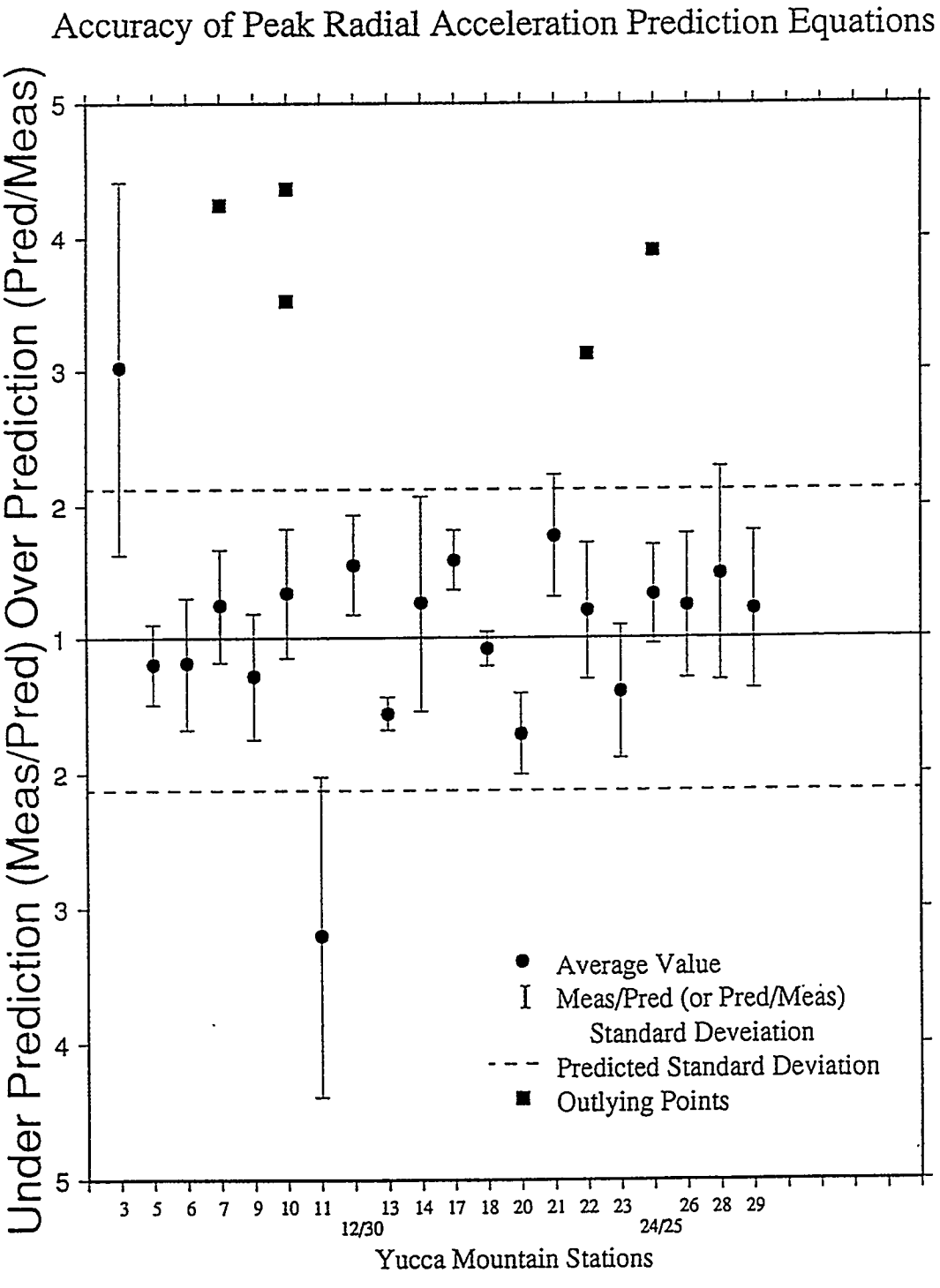

Figure 27: Same as figure 26 for the radial component acceleration data.

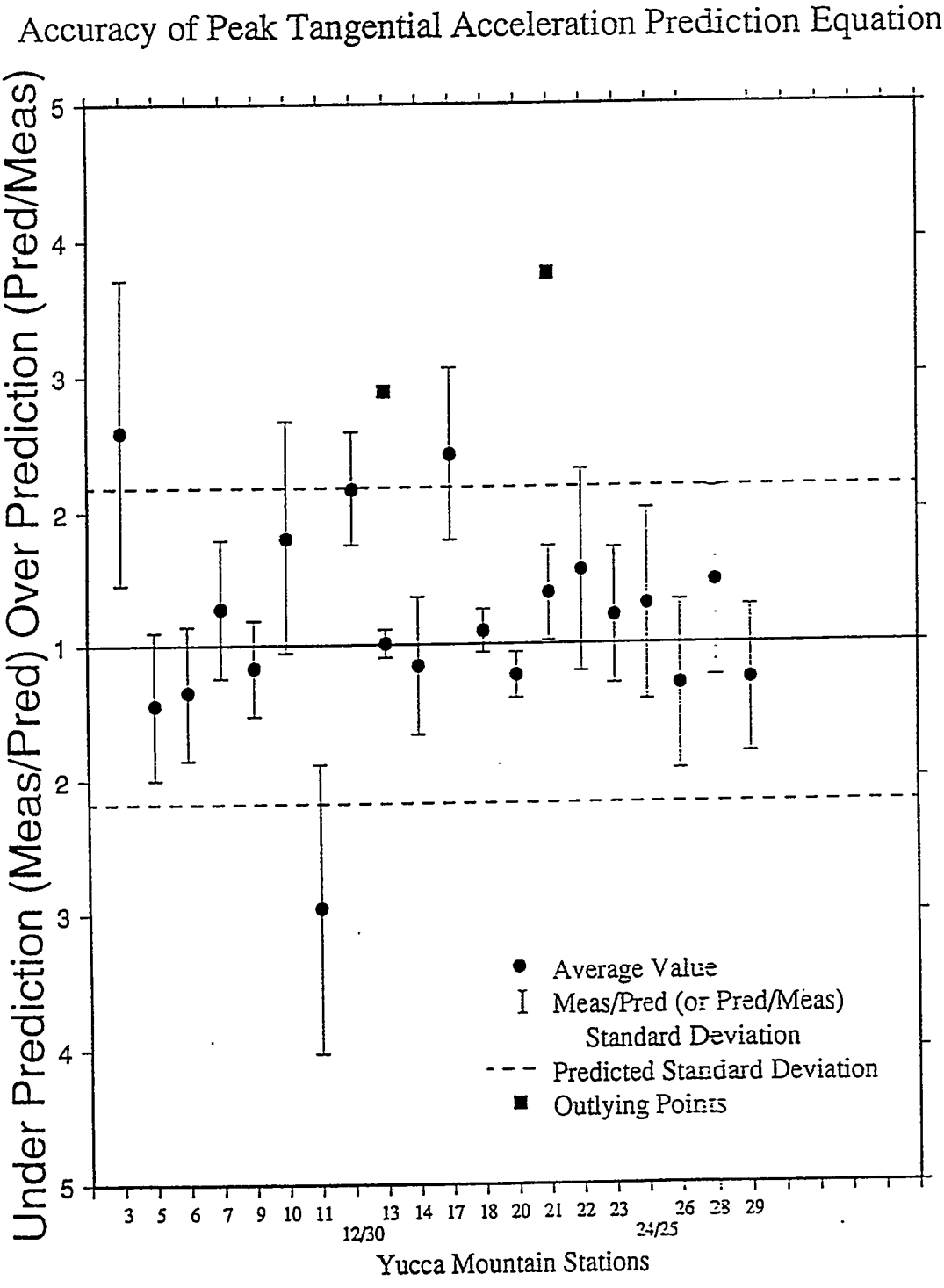

Figure 28: Same as figure 26 for the tangential component acceleration data.

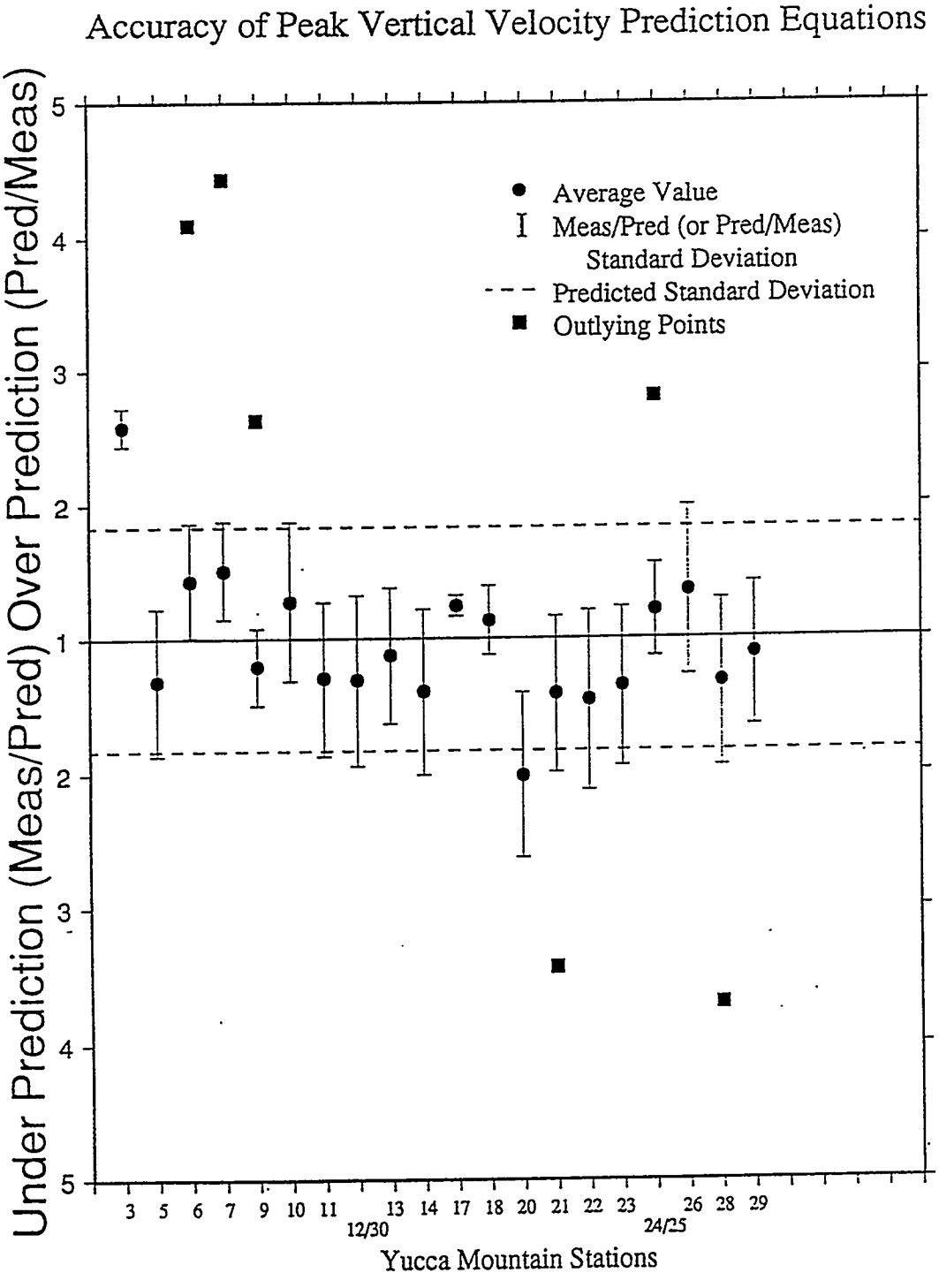

Figure 29: Same as figure 26 for the vertical component velocity data.

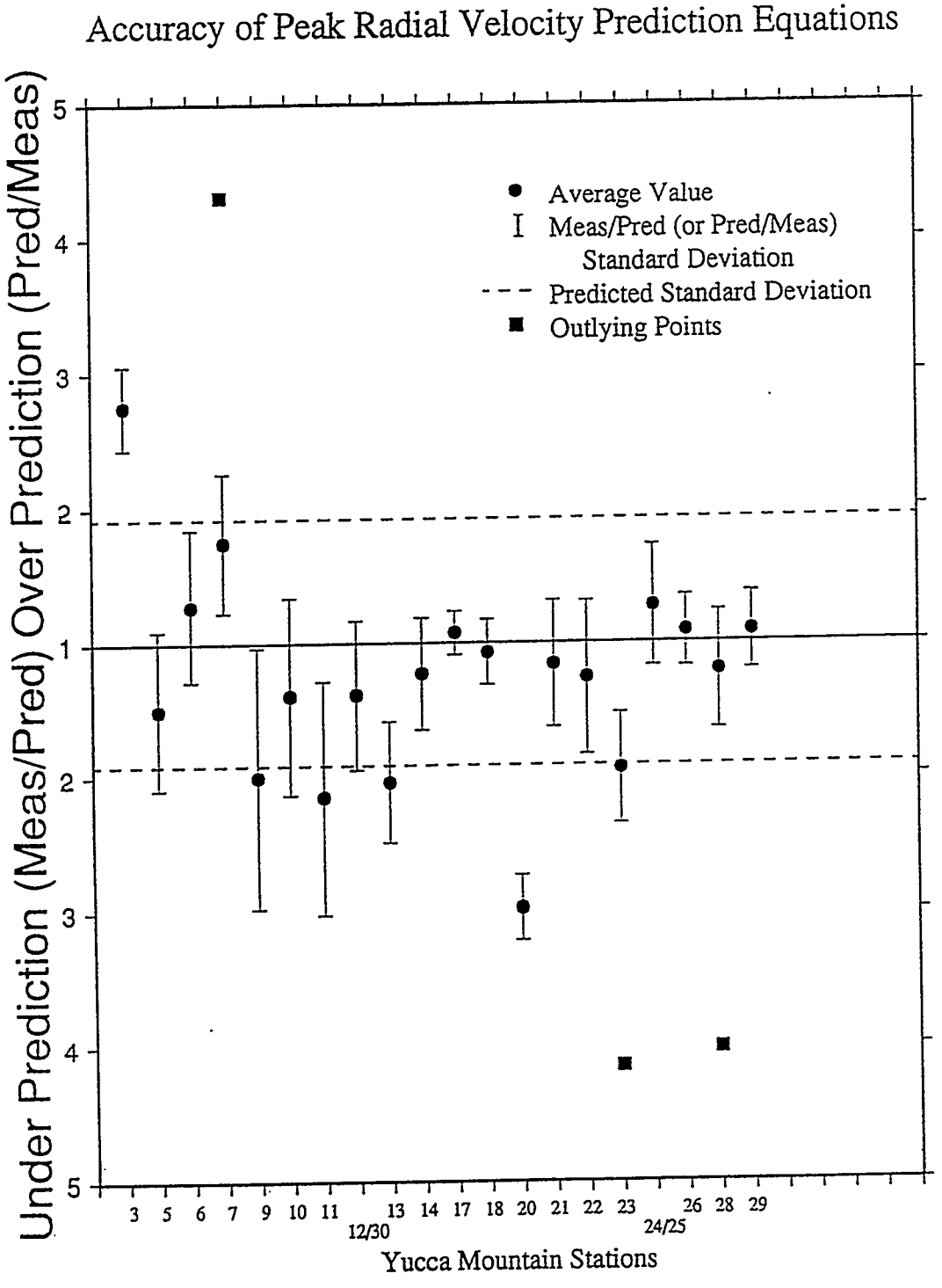

Figure 30: Same as figure 26 for the radial component velocity data.

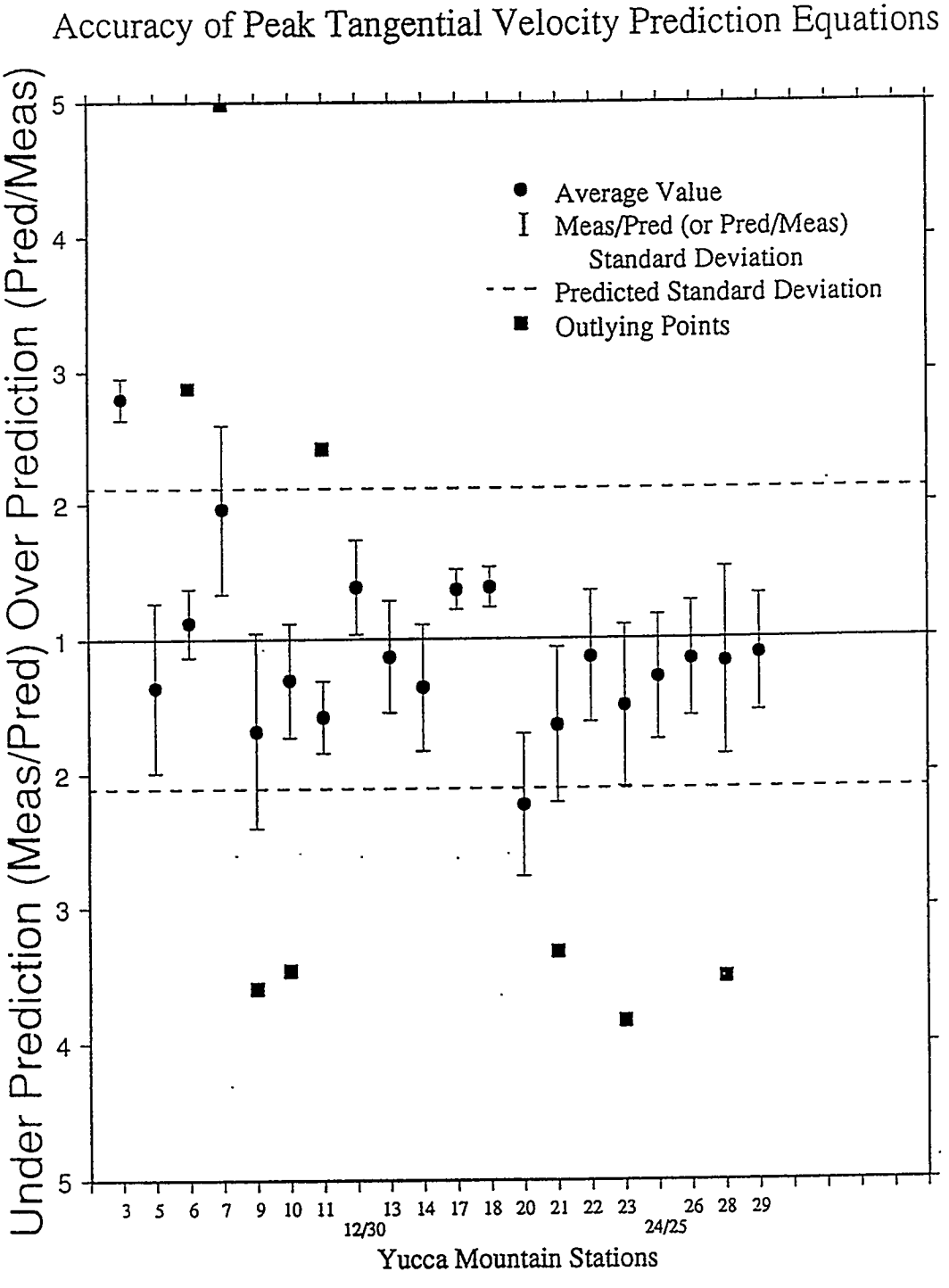

Figure 31: Same as figure 26 for the tangential component velocity data.

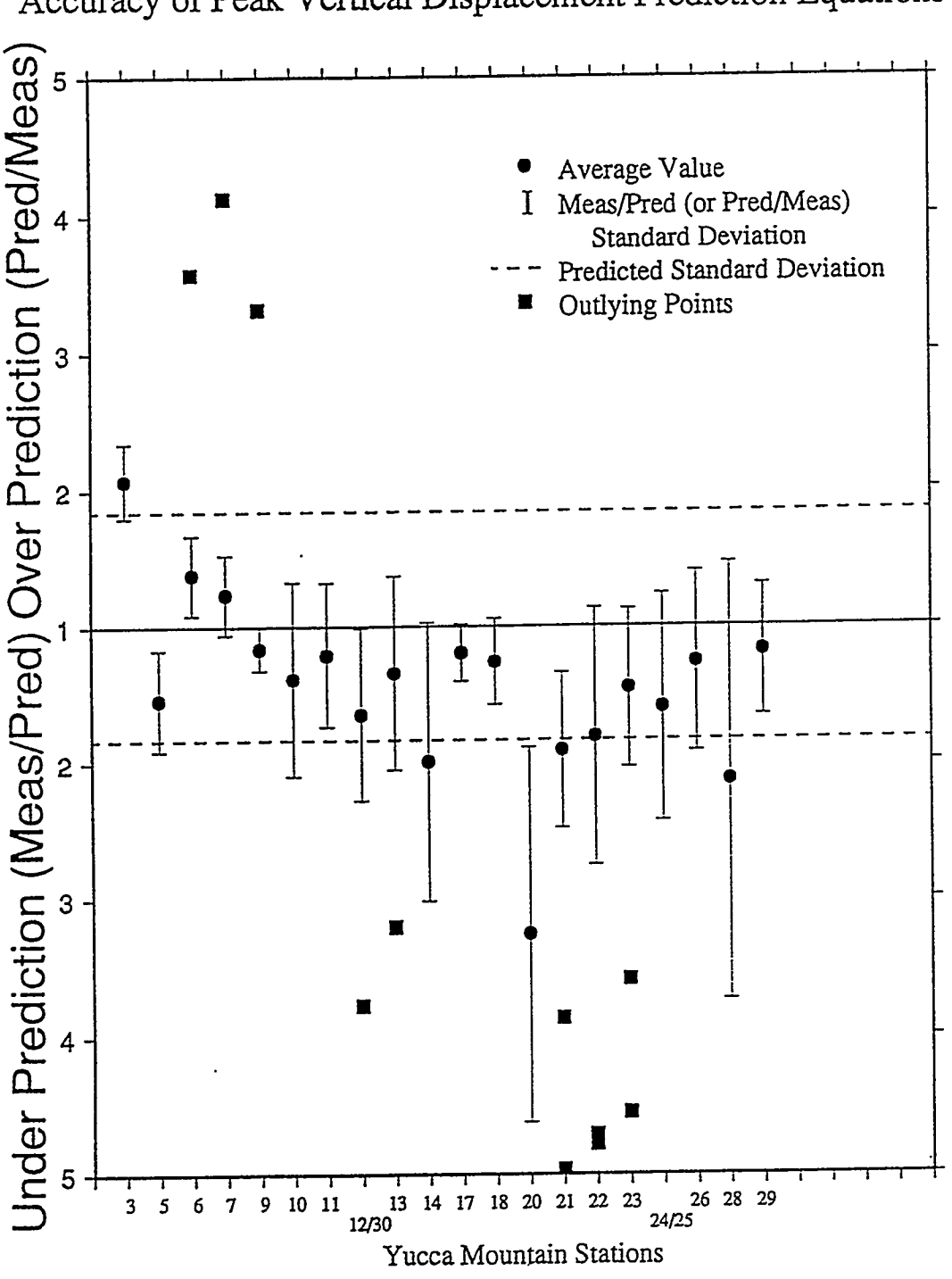

Figure 32: Same as figure 26 for the vertical component displacement data.

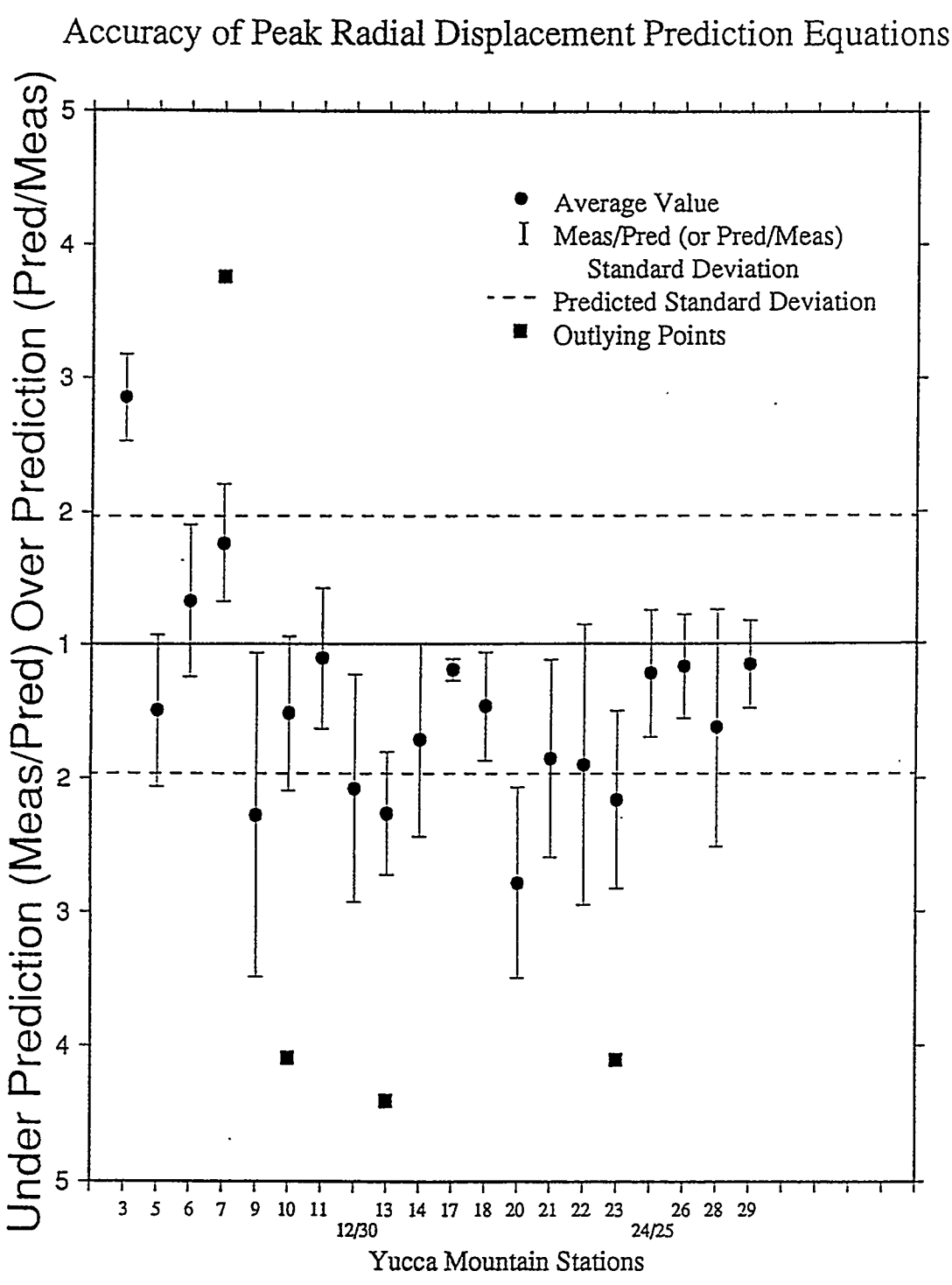

Figure 33: Same as figure 26 for the radial component displacement data.

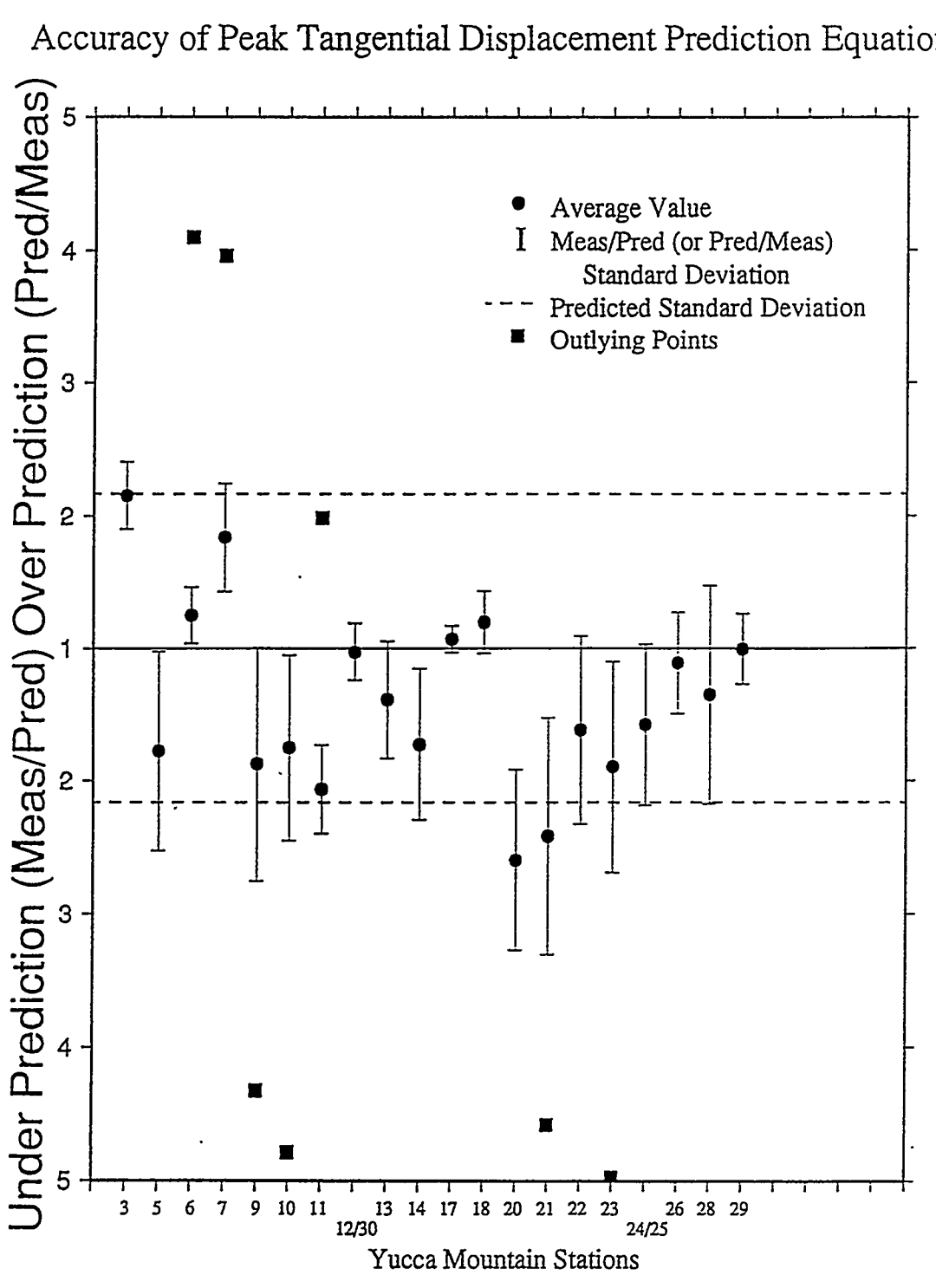

Figure 34: Same as figure 26 for the tangential component displacement data.

data. In his 1986 report, Vortman presented a few selected response spectra along with his vector ground motion predictions, however, he focused only on some anomalous observations at Jackass Flats and did not provide examples of typical UNE response spectra. He also did not attempt to develop a predictive capability for response spectra. Vortman and Long (1982a, b) presented ratios of surface to downhole response spectra for Pahute Mesa and Yucca Flat events recorded at stations around the NTS that had recording instrumentation at depth. They qualitatively discussed features of the various uphole/downhole station pair spectra for which data were available. At the time of their reports, data from Yucca Mountain stations were not yet available.

Two more recent reports have examined response spectra from Pahute Mesa UNEs in more detail. Phillips (1991a) examines response spectra from both surface and downhole stations specifically in the Yucca Mountain area. He analyzed data from eleven Pahute Mesa events, at distances of 42 to 50 km. For three of the stations (25, 28, and 30), downhole instrumentation was located at approximately the depth of the potential repository, about 350m below the ground surface. At the fourth station (29), the downhole accelerometers were at 82m depth, near the alluvium/tuff interface. Phillips (1991a) calculated ratios of response spectra as a function of frequency in an attempt to characterize the differences between surface and downhole records for Yucca Mountain stations. The 5% damping response spectra were calculated at 48 frequencies between 0.3 and 30 Hz.

Phillips' (1991a) surface/downhole response spectra observations included both general and station-specific comments. He noted that higher frequencies attenuate with depth more rapidly than lower frequencies, and that horizontal components suffer more attenuation with depth that does the vertical component for the same event at the same station. For the Pahute Mesa events, station 25 has the largest surface motions relative to the downhole motions. This may be due to an amplification effect from the shallow alluvium layer present at station 25. Phillips (1991a) also notes anomalous behavior in the high frequencies of the downhole horizontal components, particularly the transverse component, of station 28. In his attempt to understand the anomalous behavior at station 28, Phillips analyzed two Yucca Flat UNE response spectra (Hermosa and Cottage). These are the only Yucca Flat response spectra data included in any previously published UNE ground motion reports. He finds only a minimal anomalous effect for the Cottage event, and none for Hermosa. Instrumentation and installation problems were suspected at station 28 and the downhole accelerometer was removed and reinstalled in 1987. The anomalous horizontal high-frequency records persisted in the newer data, however, implying that the observed phenomenon is a real wave propagation effect and not due to instrumentation. No further study has been conducted of this downhole anomaly.

Figure 35 shows Phillips (1991a) figure 2.2-5, in which is plotted a comparison of the average surface-to-depth response spectra ratios for all four Yucca Mountain downhole stations. Due to the large variability between these relatively closely-spaced stations, all in similar materials and with the downhole measurements at similar depths (except station 29), Phillips concludes that the data do not allow development of a general regional model for attenuation with depth but must be dealt with on a station-by-station basis. He notes that response spectra prediction equations coupled with these surface-to-downhole ratios could be used to predict downhole

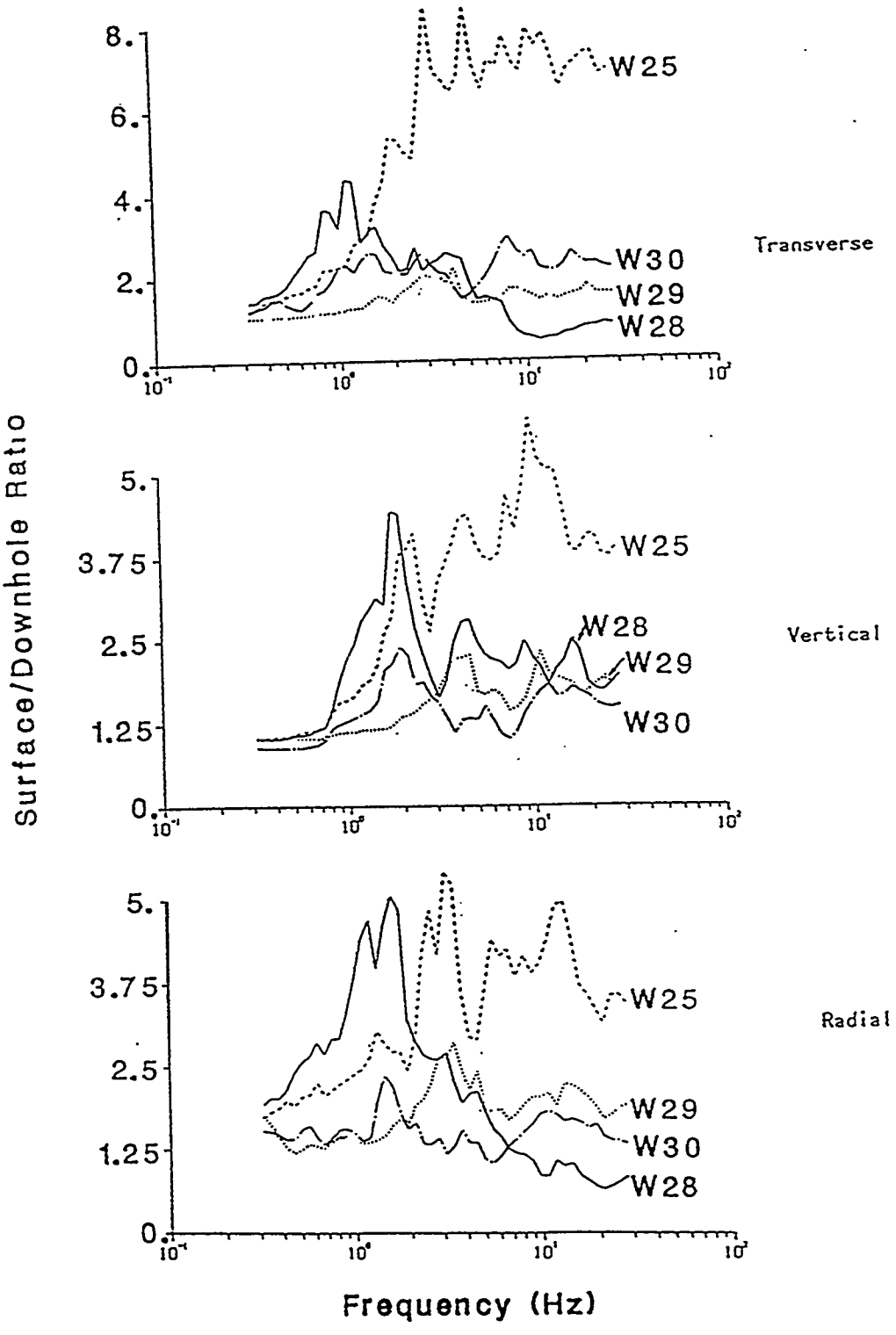

Figure 35: Comparison of average surface-to-downhole response spectra ratios at four Yucca Mountain stations (Figure 2.2-5 from Phillips, 1991a)

SUMMARY OF PREDICTION COEFFICIENTS FOR VERTICAL PSRVS FOR STATIONS ON ROCK.

Frequency	Best Estimate Equations			Lower Bound Equations			Upper Bound Equations		
(Hz)	a	b	K	a	b	K	a	b	K
0.314	0.629	-1.050	1.913	0.702	-1.171	0.670	0.557	-0.929	5.461
0.345	0.582	-1.030	2.808	0.652	-1.154	0.859	0.512	-0.906	8.221
0.380	0.535	-1.030	4.078	0.602	-1.157	1.348	0.469	-0.902	12.336
0.418	0.510	-1.038	5.231	0.574	-1.168	1.689	0.446	-0.908	16.195
0.459	0.498	-1.065	6.438	0.558	-1.183	2.119	0.438	-0.937	19.558
0.505	0.479	-1.109	8.168	0.533	-1.234	2.760	0.425	-0.984	24.176
0.556	0.500	-1.158	8.285	0.554	-1.282	2.813	0.446	-1.033	24.400
0.612	0.569	-1.211	6.394	0.627	-1.333	2.212	0.512	-1.088	18.487
0.673	0.644	-1.252	4.696	0.705	-1.371	1.673	0.583	-1.133	13.184
0.740	0.731	-1.253	3.056	0.798	-1.369	1.124	0.664	-1.138	8.306
0.814	0.766	-1.242	2.633	0.839	-1.361	0.940	0.692	-1.123	7.376
0.895	0.736	-1.252	3.543	0.809	-1.375	1.215	0.664	-1.128	10.329
0.985	0.680	-1.282	5.642	0.747	-1.410	1.873	0.613	-1.155	16.998
1.083	0.658	-1.341	7.390	0.722	-1.471	2.380	0.594	-1.210	22.940
1.192	0.659	-1.400	8.063	0.720	-1.528	2.661	0.599	-1.273	24.432
1.311	0.698	-1.442	6.818	0.759	-1.569	2.282	0.637	-1.316	20.366
1.442	0.726	-1.468	6.104	0.789	-1.595	2.023	0.663	-1.340	18.420
1.586	0.691	-1.476	7.605	0.752	-1.605	2.469	0.630	-1.346	23.424
1.745	0.629	-1.473	11.171	0.686	-1.606	3.504	0.572	-1.339	35.617
1.919	0.629	-1.449	10.606	0.687	-1.584	3.306	0.570	-1.315	34.027
2.111	0.659	-1.449	8.589	0.720	-1.584	2.670	0.598	-1.315	27.633
2.322	0.685	-1.455	7.079	0.750	-1.591	2.163	0.621	-1.318	23.163
2.555	0.726	-1.455	5.382	0.794	-1.592	1.642	0.658	-1.318	17.635
2.810	0.710	-1.475	5.823	0.776	-1.611	1.783	0.644	-1.338	19.017
3.091	0.707	-1.470	5.426	0.774	-1.607	1.642	0.641	-1.332	17.927
3.400	0.659	-1.479	6.726	0.722	-1.619	2.006	0.597	-1.340	22.549
3.740	0.618	-1.484	7.883	0.677	-1.626	2.296	0.558	-1.342	27.065
4.114	0.623	-1.473	7.013	0.684	-1.618	1.999	0.562	-1.328	24.609
4.526	0.622	-1.466	6.590	0.684	-1.614	1.828	0.559	-1.319	23.761
4.978	0.621	-1.488	6.734	0.684	-1.638	1.830	0.558	-1.337	24.783
5.476	0.595	-1.508	7.690	0.656	-1.660	2.052	0.535	-1.356	28.816
6.024	0.602	-1.485	6.490	0.664	-1.637	1.734	0.541	-1.333	24.293
6.626	0.614	-1.454	5.099	0.678	-1.606	1.363	0.549	-1.302	19.080
7.289	0.642	-1.437	3.811	0.710	-1.590	1.011	0.573	-1.284	14.371
8.018	0.644	-1.422	3.290	0.714	-1.574	0.874	0.575	-1.269	12.379
8.820	0.616	-1.441	3.629	0.682	-1.596	0.948	0.550	-1.286	13.896
9.702	0.608	-1.455	3.448	0.672	-1.609	0.901	0.543	-1.300	13.188
10.672	0.618	-1.469	2.940	0.682	-1.623	0.776	0.553	-1.316	11.139
11.739	0.667	-1.473	1.996	0.737	-1.626	0.529	0.598	-1.319	7.527
12.913	0.690	-1.492	1.614	0.761	-1.646	0.424	0.619	-1.338	6.136
14.204	0.700	-1.518	1.421	0.771	-1.673	0.373	0.629	-1.364	5.411
15.625	0.692	-1.535	1.350	0.761	-1.688	0.356	0.623	-1.381	5.117
17.187	0.691	-1.553	1.229	0.759	-1.705	0.328	0.623	-1.401	4.610
18.906	0.700	-1.573	1.077	0.767	-1.724	0.290	0.633	-1.422	3.998
20.796	0.714	-1.589	0.900	0.783	-1.741	0.240	0.646	-1.437	3.371
22.876	0.716	-1.606	0.820	0.784	-1.759	0.218	0.648	-1.453	3.091
25.164	0.727	-1.622	0.713	0.797	-1.776	0.187	0.658	-1.467	2.717
27.680	0.744	-1.624	0.584	0.816	-1.780	0.151	0.673	-1.468	2.254

Table 5: Response spectra equation coefficients for rock and alluvium site conditions and vertical, radial, and transverse components, from Phillips (1991b). See text for explanation of table headings.

SUMMARY OF PREDICTION COEFFICIENTS FOR VERTICAL PSRVs FOR STATIONS ON ALLUVIUM.

Frequency	Best Estimate Equations			Lower Bound Equations			Upper Bound Equations		
(Hz)	a	b	K	a	b	k	a	b	K
0.314	0.609	-1.116	2.410	0.663	-1.214	1.007	0.556	-1.018	5.763
0.345	0.564	-1.105	3.532	0.616	-1.206	1.439	0.513	-1.005	8.670
0.380	0.526	-1.112	4.968	0.575	-1.217	1.958	0.476	-1.008	12.608
0.418	0.507	-1.116	6.083	0.555	-1.221	2.384	0.459	-1.011	15.521
0.459	0.499	-1.121	6.855	0.544	-1.223	2.794	0.453	-1.019	17.314
0.505	0.490	-1.127	7.710	0.534	-1.228	3.116	0.445	-1.025	19.078
0.556	0.505	-1.161	7.825	0.549	-1.262	3.156	0.461	-1.059	19.401
0.612	0.562	-1.214	6.475	0.608	-1.314	2.676	0.516	-1.115	15.668
0.673	0.634	-1.253	4.835	0.682	-1.348	2.077	0.586	-1.158	11.258
0.740	0.709	-1.244	3.330	0.761	-1.336	1.476	0.657	-1.153	7.511
0.814	0.726	-1.242	3.246	0.781	-1.336	1.397	0.670	-1.147	7.538
0.895	0.686	-1.266	4.775	0.739	-1.364	2.003	0.633	-1.169	11.361
0.985	0.628	-1.309	7.915	0.675	-1.409	3.257	0.580	-1.209	19.237
1.083	0.615	-1.350	9.558	0.661	-1.452	3.855	0.568	-1.248	23.695
1.192	0.631	-1.379	9.096	0.676	-1.479	3.730	0.585	-1.279	22.179
1.311	0.677	-1.405	7.122	0.725	-1.503	2.972	0.630	-1.307	17.071
1.442	0.696	-1.419	6.542	0.745	-1.519	2.700	0.647	-1.320	15.850
1.586	0.652	-1.427	8.481	0.699	-1.530	3.398	0.605	-1.324	21.173
1.745	0.601	-1.433	11.887	0.645	-1.538	4.676	0.557	-1.329	30.220
1.919	0.610	-1.416	10.863	0.656	-1.521	4.259	0.565	-1.311	27.708
2.111	0.643	-1.406	8.514	0.692	-1.512	3.288	0.594	-1.299	22.048
2.322	0.674	-1.402	6.716	0.727	-1.512	2.528	0.621	-1.292	17.845
2.555	0.697	-1.398	5.622	0.752	-1.510	2.083	0.641	-1.287	15.177
2.810	0.677	-1.404	6.022	0.732	-1.518	2.170	0.622	-1.289	16.714
3.091	0.672	-1.392	5.641	0.728	-1.509	1.974	0.615	-1.274	16.118
3.400	0.628	-1.395	6.730	0.683	-1.517	2.273	0.573	-1.274	19.926
3.740	0.584	-1.393	7.883	0.637	-1.518	2.589	0.532	-1.268	24.005
4.114	0.592	-1.381	6.922	0.647	-1.509	2.211	0.537	-1.253	21.667
4.526	0.588	-1.376	6.620	0.644	-1.508	2.050	0.532	-1.245	21.377
4.978	0.589	-1.400	6.776	0.645	-1.534	2.043	0.532	-1.265	22.476
5.476	0.570	-1.415	7.401	0.626	-1.552	2.181	0.515	-1.278	25.119
6.024	0.581	-1.401	6.269	0.638	-1.538	1.835	0.524	-1.263	21.413
6.626	0.601	-1.369	4.681	0.662	-1.507	1.361	0.540	-1.230	16.097
7.289	0.635	-1.353	3.409	0.701	-1.493	0.980	0.569	-1.214	11.854
8.018	0.643	-1.352	2.946	0.709	-1.491	0.855	0.577	-1.214	10.153
8.820	0.613	-1.380	3.342	0.674	-1.519	0.974	0.551	-1.242	11.473
9.702	0.604	-1.397	3.213	0.663	-1.534	0.947	0.545	-1.260	10.899
10.672	0.615	-1.402	2.681	0.675	-1.537	0.801	0.556	-1.266	8.976
11.739	0.655	-1.411	1.951	0.718	-1.545	0.591	0.593	-1.277	6.447
12.913	0.672	-1.432	1.643	0.735	-1.566	0.498	0.609	-1.298	5.421
14.204	0.676	-1.458	1.499	0.737	-1.591	0.457	0.614	-1.325	4.915
15.625	0.667	-1.479	1.440	0.727	-1.611	0.443	0.607	-1.346	4.688
17.187	0.666	-1.495	1.307	0.724	-1.628	0.405	0.607	-1.365	4.220
18.906	0.669	-1.515	1.179	0.727	-1.646	0.366	0.611	-1.383	3.801
20.796	0.683	-1.521	0.963	0.742	-1.653	0.295	0.623	-1.388	3.139
22.876	0.682	-1.535	0.880	0.741	-1.668	0.268	0.623	-1.401	2.890
25.164	0.692	-1.544	0.763	0.752	-1.678	0.231	0.632	-1.410	2.528
27.680	0.709	-1.542	0.617	0.771	-1.677	0.184	0.647	-1.406	2.065

Table 5, continued

SUMMARY OF PREDICTION COEFFICIENTS FOR RADIAL PSRVS FOR STATIONS ON ROCK.

Frequency	Best Estimate Equations			Lower Bound Equations			Upper Bound Equations		
Hz	a	b	K	a	b	K	a	b	K
0.314	0.713	-1.233	3.089	0.778	-1.344	1.240	0.649	-1.121	7.694
0.345	0.660	-1.180	4.318	0.725	-1.296	1.683	0.596	-1.065	11.082
0.380	0.575	-1.177	7.812	0.634	-1.298	2.858	0.516	-1.057	21.162
0.418	0.487	-1.227	16.294	0.537	-1.353	5.852	0.437	-1.102	45.369
0.459	0.439	-1.269	25.222	0.483	-1.397	8.808	0.395	-1.142	71.415
0.505	0.430	-1.310	30.450	0.471	-1.435	10.974	0.389	-1.184	84.494
0.556	0.468	-1.320	25.468	0.511	-1.440	9.540	0.425	-1.200	67.988
0.612	0.507	-1.409	24.965	0.551	-1.530	9.274	0.463	-1.287	67.208
0.673	0.545	-1.457	22.042	0.591	-1.579	8.123	0.499	-1.334	59.811
0.740	0.558	-1.434	18.881	0.604	-1.553	7.147	0.511	-1.315	49.883
0.814	0.557	-1.427	18.392	0.602	-1.542	7.154	0.512	-1.311	47.286
0.895	0.543	-1.422	20.399	0.587	-1.538	7.896	0.498	-1.306	52.698
0.985	0.527	-1.432	24.097	0.571	-1.551	9.154	0.483	-1.313	63.431
1.083	0.511	-1.464	29.640	0.555	-1.589	10.626	0.467	-1.338	82.678
1.192	0.508	-1.495	31.513	0.552	-1.624	11.063	0.465	-1.367	89.763
1.311	0.546	-1.491	23.649	0.593	-1.620	8.319	0.499	-1.363	67.225
1.442	0.579	-1.455	17.084	0.631	-1.585	5.949	0.528	-1.326	49.062
1.586	0.532	-1.453	21.040	0.579	-1.582	7.356	0.485	-1.324	60.178
1.745	0.508	-1.459	23.596	0.552	-1.584	8.511	0.465	-1.334	65.419
1.919	0.519	-1.446	20.615	0.562	-1.566	7.764	0.476	-1.326	54.736
2.111	0.546	-1.391	14.381	0.594	-1.512	5.358	0.499	-1.270	38.599
2.322	0.562	-1.369	11.609	0.611	-1.489	4.353	0.512	-1.248	30.960
2.555	0.590	-1.362	9.161	0.642	-1.482	3.443	0.538	-1.242	24.375
2.810	0.557	-1.408	11.472	0.606	-1.530	4.209	0.509	-1.285	31.263
3.091	0.557	-1.451	12.131	0.605	-1.576	4.371	0.509	-1.326	33.668
3.400	0.561	-1.462	11.428	0.609	-1.589	4.069	0.512	-1.336	32.097
3.740	0.570	-1.436	9.513	0.620	-1.562	3.405	0.520	-1.310	26.579
4.114	0.573	-1.446	9.025	0.623	-1.572	3.237	0.523	-1.321	25.164
4.526	0.566	-1.446	8.725	0.619	-1.581	2.905	0.513	-1.311	26.208
4.978	0.556	-1.462	9.073	0.611	-1.605	2.815	0.502	-1.318	29.245
5.476	0.554	-1.482	8.922	0.607	-1.624	2.798	0.500	-1.340	28.450
6.024	0.562	-1.480	7.391	0.615	-1.618	2.384	0.510	-1.341	22.914
6.626	0.580	-1.458	5.682	0.636	-1.598	1.807	0.524	-1.317	17.868
7.289	0.627	-1.462	4.151	0.686	-1.600	1.346	0.568	-1.324	12.807
8.018	0.632	-1.444	3.445	0.693	-1.583	1.109	0.571	-1.305	10.705
8.820	0.621	-1.472	3.445	0.681	-1.612	1.098	0.562	-1.331	10.813
9.702	0.602	-1.516	3.762	0.656	-1.652	1.238	0.548	-1.380	11.436
10.672	0.630	-1.522	2.919	0.687	-1.659	0.952	0.573	-1.384	8.952
11.739	0.651	-1.542	2.419	0.709	-1.681	0.781	0.592	-1.404	7.491
12.913	0.671	-1.552	1.952	0.730	-1.689	0.639	0.612	-1.415	5.967
14.204	0.687	-1.572	1.652	0.746	-1.707	0.549	0.628	-1.437	4.967
15.625	0.679	-1.586	1.569	0.736	-1.720	0.525	0.621	-1.452	4.687
17.187	0.682	-1.615	1.465	0.739	-1.751	0.482	0.624	-1.479	4.452
18.906	0.687	-1.638	1.319	0.743	-1.773	0.440	0.630	-1.504	3.949
20.796	0.686	-1.656	1.210	0.742	-1.791	0.402	0.630	-1.521	3.641
22.876	0.686	-1.687	1.178	0.741	-1.823	0.390	0.631	-1.552	3.559
25.164	0.702	-1.700	1.006	0.759	-1.837	0.328	0.645	-1.562	3.083
27.680	0.708	-1.712	0.903	0.766	-1.851	0.289	0.650	-1.572	2.821

Table 5, continued

SUMMARY OF PREDICTION COEFFICIENTS FOR RADIAL PSRVS FOR STATIONS ON ALLUVIUM.

Frequency	Best Estimate Equations			Lower Bound Equations			Upper Bound Equations		
(Hz)	a	b	K	a	b	K	a	b	K
0.314	0.658	-1.303	4.843	0.706	-1.400	2.144	0.609	-1.207	10.938
0.345	0.617	-1.246	6.232	0.666	-1.346	2.680	0.567	-1.146	14.493
0.380	0.529	-1.247	11.573	0.573	-1.351	4.806	0.485	-1.142	27.865
0.418	0.441	-1.293	23.488	0.478	-1.401	9.485	0.404	-1.186	58.163
0.459	0.392	-1.332	36.201	0.423	-1.439	14.672	0.360	-1.225	89.318
0.505	0.390	-1.371	41.932	0.420	-1.476	17.354	0.360	-1.267	101.319
0.556	0.427	-1.382	35.502	0.459	-1.484	15.092	0.396	-1.281	83.514
0.612	0.449	-1.462	37.576	0.480	-1.563	16.025	0.418	-1.361	88.114
0.673	0.493	-1.504	31.700	0.526	-1.605	13.589	0.460	-1.404	73.946
0.740	0.507	-1.484	27.297	0.541	-1.583	11.819	0.473	-1.385	63.047
0.814	0.505	-1.466	26.348	0.539	-1.564	11.510	0.471	-1.368	60.313
0.895	0.492	-1.453	28.692	0.526	-1.554	12.253	0.457	-1.352	67.186
0.985	0.489	-1.458	31.210	0.523	-1.559	13.316	0.455	-1.358	73.153
1.083	0.473	-1.499	39.073	0.505	-1.602	16.372	0.440	-1.396	93.249
1.192	0.457	-1.532	44.836	0.488	-1.635	18.740	0.426	-1.429	107.275
1.311	0.501	-1.529	32.497	0.534	-1.632	13.663	0.467	-1.427	77.289
1.442	0.540	-1.495	22.689	0.577	-1.589	9.452	0.502	-1.391	54.461
1.586	0.490	-1.498	28.830	0.524	-1.602	12.068	0.456	-1.395	68.871
1.745	0.462	-1.507	33.437	0.493	-1.608	14.271	0.431	-1.406	78.345
1.919	0.484	-1.483	26.786	0.515	-1.580	11.743	0.452	-1.385	61.100
2.111	0.508	-1.434	18.354	0.543	-1.534	8.344	0.472	-1.334	44.894
2.322	0.522	-1.407	15.559	0.559	-1.508	6.652	0.485	-1.307	36.389
2.555	0.555	-1.389	11.746	0.595	-1.490	5.016	0.515	-1.288	27.506
2.810	0.512	-1.410	14.839	0.550	-1.516	6.076	0.473	-1.304	36.239
3.091	0.504	-1.434	15.725	0.543	-1.543	6.249	0.466	-1.325	39.570
3.400	0.513	-1.431	13.967	0.553	-1.543	5.450	0.473	-1.320	35.794
3.740	0.515	-1.401	11.999	0.556	-1.514	4.650	0.474	-1.289	30.962
4.114	0.520	-1.404	11.023	0.562	-1.516	4.262	0.478	-1.291	28.512
4.526	0.516	-1.399	10.463	0.560	-1.519	3.787	0.471	-1.279	28.908
4.978	0.511	-1.409	10.469	0.557	-1.536	3.578	0.465	-1.282	30.631
5.476	0.514	-1.423	9.929	0.561	-1.553	3.315	0.467	-1.294	29.743
6.024	0.534	-1.397	7.408	0.583	-1.528	2.460	0.484	-1.267	22.302
6.626	0.549	-1.381	5.857	0.601	-1.512	1.947	0.497	-1.251	17.615
7.289	0.597	-1.388	4.285	0.653	-1.516	1.446	0.542	-1.259	12.697
8.018	0.607	-1.381	3.540	0.663	-1.508	1.211	0.552	-1.254	10.345
8.820	0.597	-1.406	3.542	0.650	-1.532	1.219	0.543	-1.279	10.289
9.702	0.586	-1.439	3.589	0.636	-1.561	1.274	0.536	-1.316	10.110
10.672	0.608	-1.451	2.915	0.660	-1.574	1.032	0.556	-1.328	8.232
11.739	0.627	-1.474	2.457	0.680	-1.597	0.871	0.575	-1.352	6.927
12.913	0.638	-1.494	2.147	0.690	-1.616	0.770	0.586	-1.373	5.985
14.204	0.644	-1.519	1.941	0.695	-1.639	0.710	0.594	-1.400	5.306
15.625	0.635	-1.540	1.880	0.684	-1.658	0.696	0.587	-1.423	5.079
17.187	0.634	-1.572	1.792	0.682	-1.690	0.663	0.587	-1.454	4.846
18.906	0.637	-1.593	1.624	0.683	-1.710	0.607	0.590	-1.476	4.347
20.796	0.638	-1.605	1.450	0.684	-1.722	0.539	0.591	-1.488	3.898
22.876	0.638	-1.631	1.391	0.684	-1.749	0.516	0.592	-1.514	3.747
25.164	0.649	-1.644	1.220	0.685	-1.762	0.450	0.602	-1.526	3.312
27.680	0.655	-1.654	1.092	0.702	-1.774	0.397	0.607	-1.535	3.001

Table 5, continued

SUMMARY OF PREDICTION COEFFICIENTS FOR TRANSVERSE PSRVS FOR STATIONS ON ROCK.

Frequency	Best Estimate Equations			Lower Bound Equations			Upper Bound Equations		
(Hz)	a	b	K	a	b	K	a	b	K
0.314	0.511	-0.986	3.999	0.575	-1.110	1.469	0.447	-0.863	10.888
0.345	0.489	-1.035	5.986	0.548	-1.160	2.159	0.429	-0.910	16.595
0.380	0.488	-1.077	7.440	0.544	-1.201	2.719	0.432	-0.953	20.356
0.418	0.480	-1.128	9.779	0.533	-1.251	3.571	0.427	-1.004	26.782
0.459	0.449	-1.173	14.200	0.497	-1.299	5.119	0.401	-1.048	39.390
0.505	0.436	-1.226	18.401	0.482	-1.356	6.413	0.390	-1.097	52.800
0.556	0.454	-1.264	18.726	0.501	-1.394	6.504	0.408	-1.134	53.918
0.612	0.467	-1.324	20.747	0.513	-1.453	7.264	0.422	-1.195	59.258
0.673	0.515	-1.369	18.092	0.564	-1.499	6.237	0.466	-1.238	52.479
0.740	0.535	-1.397	17.652	0.584	-1.526	6.164	0.485	-1.268	50.546
0.814	0.573	-1.399	14.438	0.626	-1.528	5.041	0.520	-1.269	41.350
0.895	0.563	-1.409	15.813	0.617	-1.542	5.356	0.510	-1.276	46.690
0.985	0.513	-1.415	21.868	0.562	-1.552	7.212	0.463	-1.279	66.310
1.083	0.458	-1.444	32.051	0.502	-1.581	10.477	0.415	-1.306	98.050
1.192	0.443	-1.502	39.729	0.484	-1.639	13.036	0.403	-1.365	121.075
1.311	0.478	-1.519	32.222	0.520	-1.655	10.671	0.435	-1.383	97.301
1.442	0.539	-1.476	20.007	0.589	-1.613	6.589	0.489	-1.340	60.754
1.586	0.538	-1.456	18.433	0.590	-1.594	5.987	0.488	-1.318	56.749
1.745	0.550	-1.419	15.408	0.602	-1.553	5.165	0.498	-1.285	45.965
1.919	0.521	-1.387	16.069	0.571	-1.520	5.452	0.471	-1.254	47.358
2.111	0.531	-1.385	14.489	0.581	-1.517	4.972	0.480	-1.254	42.219
2.322	0.563	-1.408	12.268	0.616	-1.541	4.139	0.510	-1.274	36.360
2.555	0.607	-1.391	8.772	0.665	-1.523	2.993	0.549	-1.259	25.712
2.810	0.609	-1.393	8.296	0.668	-1.528	2.771	0.550	-1.258	24.833
3.091	0.600	-1.411	8.647	0.657	-1.547	2.854	0.542	-1.275	26.202
3.400	0.582	-1.438	9.235	0.637	-1.574	3.043	0.527	-1.301	28.028
3.740	0.611	-1.432	7.132	0.669	-1.569	2.332	0.552	-1.294	21.812
4.114	0.581	-1.459	9.281	0.616	-1.602	2.911	0.506	-1.317	29.587
4.526	0.580	-1.462	10.233	0.583	-1.608	3.108	0.477	-1.315	33.691
4.978	0.558	-1.429	7.496	0.617	-1.581	2.172	0.498	-1.277	25.866
5.476	0.581	-1.428	6.079	0.641	-1.576	1.820	0.521	-1.279	20.305
6.024	0.588	-1.427	4.900	0.659	-1.570	1.526	0.538	-1.284	15.739
6.626	0.597	-1.409	4.241	0.657	-1.552	1.328	0.536	-1.267	13.541
7.289	0.637	-1.394	3.017	0.701	-1.535	0.954	0.572	-1.252	9.545
8.018	0.661	-1.385	2.314	0.729	-1.527	0.727	0.593	-1.243	7.360
8.820	0.668	-1.409	2.078	0.735	-1.550	0.660	0.601	-1.268	6.544
9.702	0.674	-1.436	1.918	0.740	-1.578	0.604	0.607	-1.294	6.089
10.672	0.695	-1.452	1.581	0.763	-1.594	0.497	0.627	-1.310	5.034
11.739	0.710	-1.463	1.298	0.780	-1.608	0.397	0.639	-1.317	4.244
12.913	0.727	-1.471	1.067	0.798	-1.616	0.328	0.655	-1.326	3.474
14.204	0.743	-1.482	0.876	0.815	-1.626	0.271	0.671	-1.338	2.832
15.625	0.724	-1.515	0.917	0.792	-1.657	0.288	0.656	-1.373	2.913
17.187	0.699	-1.557	1.017	0.763	-1.698	0.321	0.636	-1.415	3.222
18.906	0.718	-1.593	0.909	0.781	-1.737	0.281	0.651	-1.448	2.947
20.796	0.730	-1.608	0.777	0.796	-1.753	0.238	0.664	-1.463	2.536
22.876	0.745	-1.626	0.661	0.812	-1.772	0.201	0.678	-1.480	2.168
25.164	0.757	-1.641	0.583	0.825	-1.789	0.175	0.688	-1.493	1.949
27.680	0.756	-1.661	0.557	0.824	-1.810	0.164	0.688	-1.511	1.887

Table 5, continued

SUMMARY OF PREDICTION COEFFICIENTS FOR TRANSVERSE PSRVS FOR STATIONS ON ALLUVIUM

Frequency	Best Estimate Equations			Lower Bound Equations			Upper Bound Equations		
(Hz)	a	b	K	a	b	K	a	b	K
0.314	0.468	-0.999	5.065	0.519	-1.108	2.031	0.417	-0.890	12.633
0.345	0.445	-1.042	7.575	0.491	-1.152	3.016	0.398	-0.933	19.024
0.380	0.448	-1.080	9.111	0.493	-1.187	3.674	0.403	-0.972	22.598
0.418	0.457	-1.131	10.846	0.500	-1.238	4.421	0.414	-1.024	26.610
0.459	0.416	-1.180	16.678	0.454	-1.288	6.735	0.378	-1.072	41.300
0.505	0.389	-1.244	24.044	0.423	-1.353	9.599	0.354	-1.135	60.224
0.556	0.405	-1.291	25.304	0.439	-1.400	10.115	0.371	-1.182	63.301
0.612	0.418	-1.365	28.958	0.451	-1.471	11.776	0.385	-1.258	71.207
0.673	0.468	-1.405	24.738	0.503	-1.511	10.088	0.432	-1.298	60.662
0.740	0.484	-1.426	24.401	0.519	-1.530	10.189	0.449	-1.323	58.440
0.814	0.520	-1.418	19.855	0.558	-1.522	8.242	0.482	-1.313	47.832
0.895	0.520	-1.417	20.232	0.559	-1.523	8.277	0.481	-1.310	49.455
0.985	0.471	-1.433	28.548	0.507	-1.541	11.531	0.436	-1.325	70.676
1.083	0.425	-1.476	41.369	0.456	-1.584	16.610	0.393	-1.367	103.037
1.192	0.402	-1.537	53.928	0.430	-1.645	21.647	0.373	-1.428	134.345
1.311	0.437	-1.550	43.051	0.467	-1.657	17.520	0.407	-1.443	105.786
1.442	0.487	-1.529	29.483	0.522	-1.636	11.952	0.453	-1.422	72.732
1.586	0.486	-1.511	27.476	0.522	-1.620	10.963	0.451	-1.401	68.859
1.745	0.488	-1.481	24.723	0.523	-1.587	10.130	0.453	-1.375	60.336
1.919	0.471	-1.444	23.967	0.505	-1.548	9.982	0.437	-1.340	57.546
2.111	0.487	-1.447	21.047	0.523	-1.552	8.715	0.452	-1.342	50.832
2.322	0.519	-1.455	17.408	0.557	-1.562	7.075	0.480	-1.348	42.833
2.555	0.550	-1.429	13.137	0.591	-1.536	5.329	0.509	-1.322	32.387
2.810	0.548	-1.420	12.372	0.591	-1.531	4.866	0.506	-1.309	31.455
3.091	0.536	-1.432	12.940	0.578	-1.546	4.967	0.493	-1.318	33.714
3.400	0.518	-1.439	13.202	0.560	-1.553	5.039	0.477	-1.324	34.590
3.740	0.545	-1.418	10.043	0.590	-1.535	3.750	0.500	-1.301	26.898
4.114	0.496	-1.429	12.582	0.537	-1.550	4.565	0.454	-1.309	34.674
4.526	0.475	-1.430	13.109	0.517	-1.555	4.593	0.434	-1.306	37.411
4.978	0.512	-1.399	9.209	0.559	-1.528	3.108	0.465	-1.270	27.293
5.476	0.543	-1.393	7.098	0.593	-1.521	2.422	0.493	-1.265	20.797
6.024	0.561	-1.386	5.658	0.611	-1.511	1.979	0.510	-1.261	16.172
6.626	0.557	-1.374	5.045	0.607	-1.499	1.763	0.506	-1.249	14.441
7.289	0.592	-1.374	3.820	0.645	-1.498	1.339	0.538	-1.249	10.902
8.018	0.623	-1.360	2.788	0.681	-1.486	0.961	0.565	-1.233	8.093
8.820	0.636	-1.369	2.355	0.695	-1.496	0.809	0.577	-1.242	6.856
9.702	0.642	-1.391	2.151	0.700	-1.517	0.746	0.584	-1.266	6.199
10.672	0.658	-1.415	1.873	0.717	-1.542	0.649	0.599	-1.290	5.408
11.739	0.671	-1.432	1.572	0.730	-1.559	0.539	0.611	-1.305	4.587
12.913	0.680	-1.455	1.390	0.739	-1.581	0.483	0.622	-1.329	4.001
14.204	0.693	-1.475	1.190	0.751	-1.599	0.419	0.635	-1.351	3.378
15.625	0.669	-1.510	1.261	0.723	-1.632	0.457	0.615	-1.388	3.584
17.187	0.642	-1.554	1.443	0.692	-1.675	0.522	0.592	-1.433	3.990
18.906	0.653	-1.567	1.317	0.703	-1.708	0.476	0.603	-1.465	3.645
20.796	0.669	-1.599	1.099	0.720	-1.720	0.397	0.618	-1.478	3.043
22.876	0.683	-1.611	0.926	0.735	-1.732	0.334	0.632	-1.490	2.567
25.164	0.692	-1.628	0.833	0.744	-1.750	0.298	0.640	-1.506	2.324
27.680	0.691	-1.645	0.790	0.743	-1.768	0.282	0.640	-1.523	2.215

Table 5, continued

response spectra for both Pahute Mesa and Yucca Flat explosions, but does not develop the equations in this study.

In a later report, Phillips (1991b) develops a prediction procedure for UNE surface response spectra. His data base is drawn primarily from the same events studied by Vortman (1986) and includes events from Pahute Mesa only. Table 5 reproduces his prediction equations, which are functions of frequency, yield, distance, and pseudo velocity and are applicable for ranges of 1-60 km and a variety of yields. The coefficients a, b, and K in Table 5 are empirically determined for the equation $P=KW^aR^b$, where P is the pseudo velocity in cm/sec, W is yield in kilotons, and R is distance in km. Phillips (1991b) considers vertical, radial, and transverse components separately. He presents many examples of UNE response spectra as compared to predicted values and includes 95% confidence intervals in the comparisons. Phillips also uses the surface/downhole response spectra ratios developed in the earlier report (1991a) to predict downhole response spectra at the Yucca Mountain stations and finds reasonable agreement between the observations and predictions. As a final test of the response spectra prediction equations, he tests the predictions against four events not included in the data used for equation regression. Results from these tests (his figures 4-1 through 4-25) show that the response spectra predictions are reasonable approximations of expected motions for a range of yields and distances.

Phillips (1991b) notes that pseudo velocities recorded at Yucca Mountain stations were generally somewhat higher than those at other NTS stations, particularly for low frequencies (less than 4 Hz). He attributes this amplification to the considerable topography surrounding the Yucca Mountain stations analyzed; all four stations considered (14, 21, 22, 23) are located on the Yucca Mountain ridge itself. While Phillips did not conduct a quantitative analysis to model the observed pseudo velocity effect, his arguments appear to be reasonable. Further, the response spectral values recorded at Yucca Mountain generally fall within the 95% confidence limits of the prediction equations.

Phillips also attempts to compare response spectra for the UNEs with an "equivalent" earthquake. He used the magnitude-yield relationship of Vortman (1992) and the earthquake response spectrum prediction method of Joyner and Boore (1982) for western North American earthquakes to simulate an earthquake response spectrum equivalent to that of the "design basis UNE" (a 700kt blast located 22.8 km from Yucca Mountain). For stations on "rock", Phillips found that the equivalent earthquake (moment magnitude of 6.4) would produce response spectral values higher than the UNE by a factor of about 2.7 and shifted towards lower frequencies. For alluvium sites, the spectral shapes are quite similar but again the UNE spectrum is lower by about a factor of three. Clearly, earthquakes of sizes considered reasonable for the southern Basin and Range (magnitudes of 6.5 - 7.5, Pezzopane et al., 1994) will represent the controlling ground motions for the Yucca Mountain site.

Response Spectra from Yucca Flat UNEs recorded at Yucca Mountain

Previous studies of UNE response spectra have not included data from Yucca Flat UNEs. Because Yucca Flat explosions are in the same size and distance range from Yucca Mountain

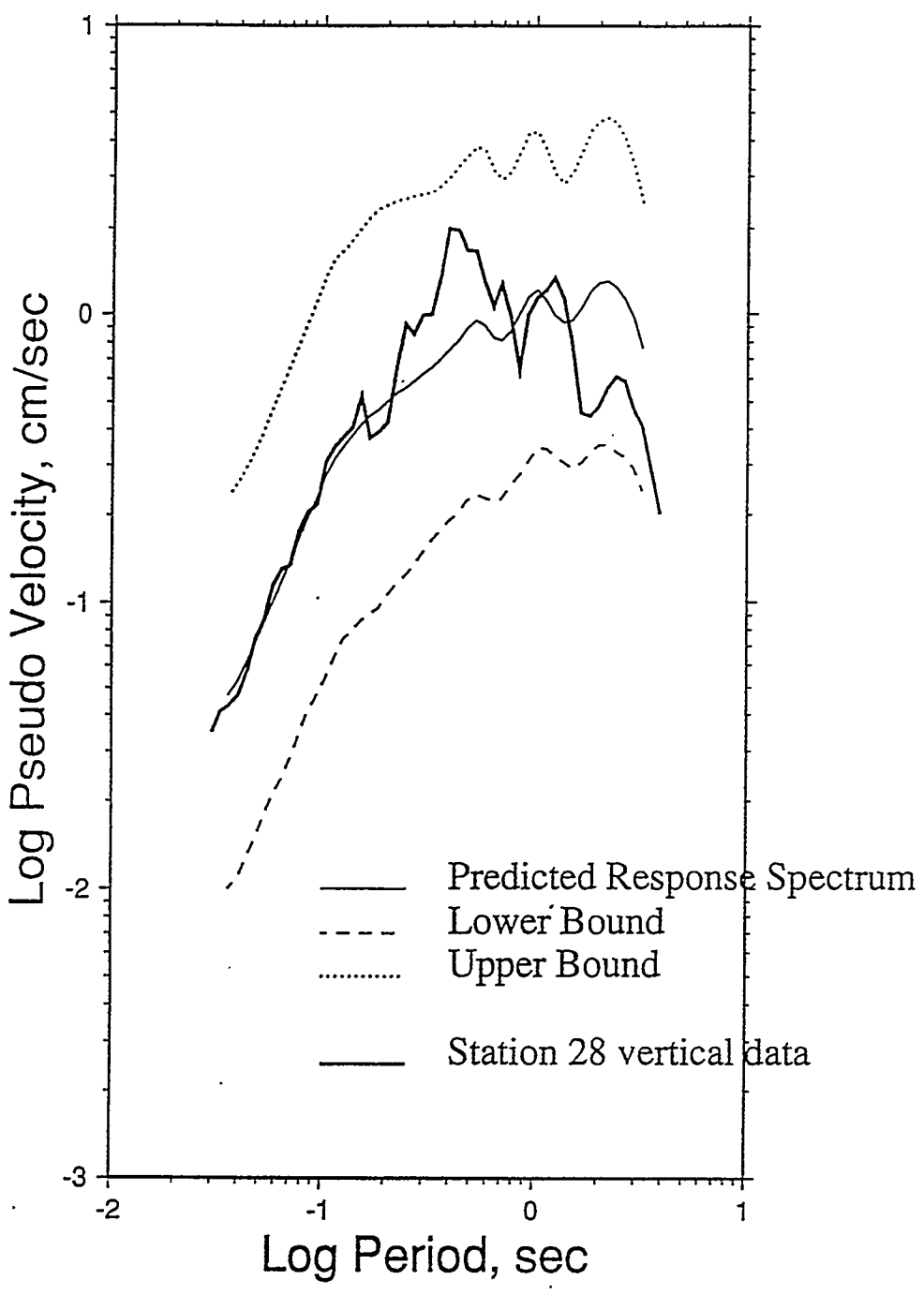

Figure 36: Response spectrum (vertical component) for a Yucca Flat event recorded at station 28 compared to the prediction equations of Phillips (1991b, Table 5)

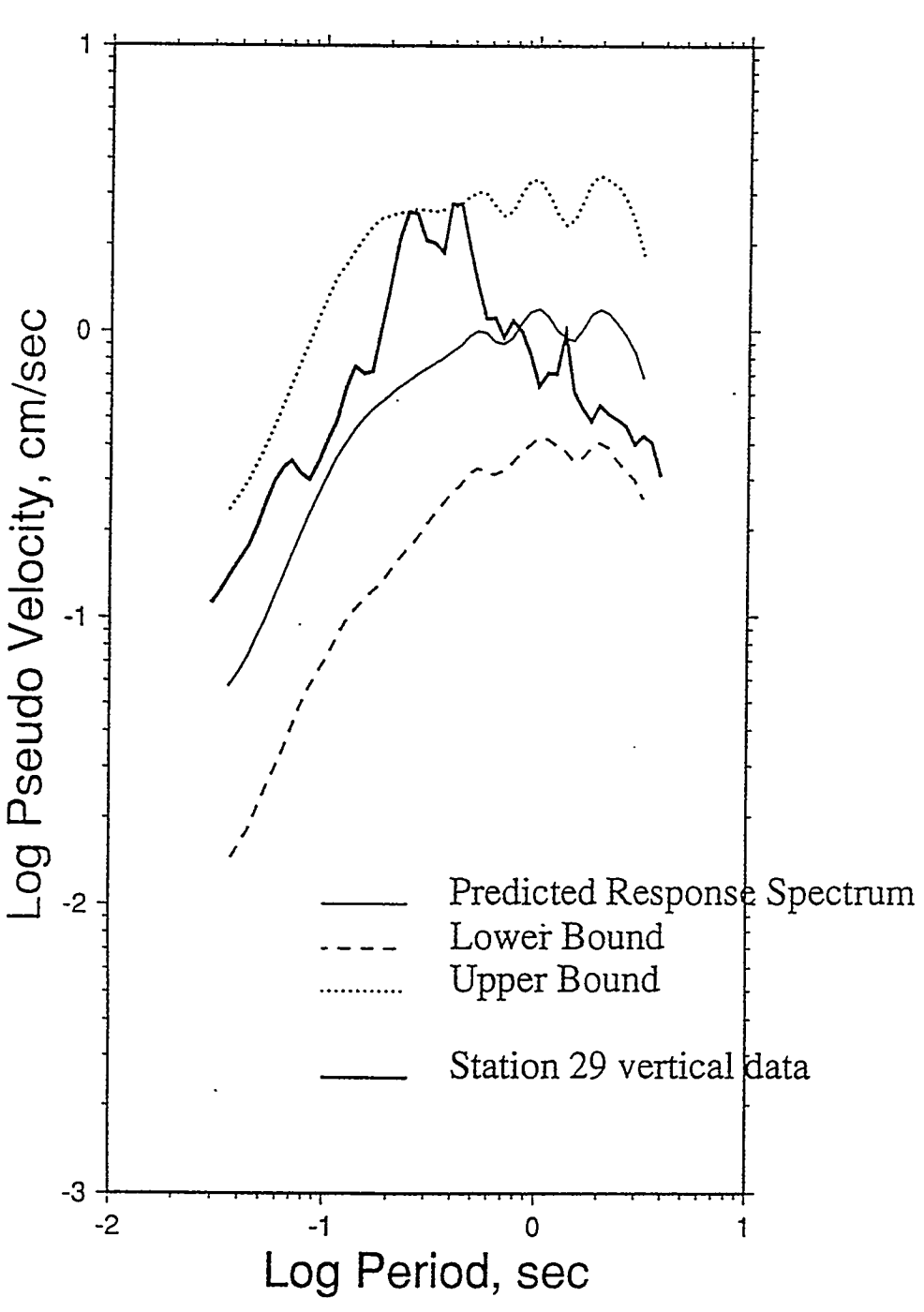

Figure 37: Response spectrum (vertical component) for the same Yucca Flat event as in figure 36 recorded at station 29 compared to the prediction equations of Phillips (1991b, Table 5)

as the Pahute Mesa events, we expect their pseudo velocity values to be similar to the predicted values, or at least within the 95% confidence intervals. Figure 36 shows the response spectra for the vertical component of a Yucca Flat event recorded at Yucca Mountain station 28 (a "rock" station) compared to the predicted values from the equations of Phillips (1991b). As the figure demonstrates, the observed pseudo velocities lie within the 95% confidence bounds of the prediction equations. The high frequencies are very well predicted, while the lowest frequencies are somewhat smaller than predicted, but still within the uncertainty. Another vertical response spectrum for the same event at a different station (29, on alluvium) is plotted in Figure 37. For alluvium stations, the Yucca Flat sources tend to follow the predictions at high frequencies, have a peak higher than predicted form about 2-5 Hz, and fall lower than the predictions at low frequencies. The observed spectra fall within the 95% confidence regions defined by Phillips. These response spectra are typical of Yucca Flat UNEs recorded at Yucca Mountain, and demonstrate that Phillips' (1991b) prediction equations are quite adequate for characterizing Yucca Flat UNE sources as well as Pahute Mesa UNE sources.

Surface/Downhole Data Pairs

The WTSI data set is unusual in the number and variety of downhole UNE records available for analysis. Many of the recording sites were located at boreholes equipped with identical surface and borehole-mounted triaxial accelerometers. The depths at which the downhole instrumentation was installed were dependent on many factors, including local geology, and there was little consistency between sites. This did result, however, in borehole instrumentation depths ranging from a few tens of meters to more than 700 meters.

Early attempts at relating surface and downhole ground motions included the work of Vortman and Long (1982a, b) and Long et al. (1983). These studies were completed prior to the station installations at Yucca Mountain and are generally applicable to the NTS, but not to Yucca Mountain in particular. Vortman and Long (1982a) compared ground motion at the surface and at depth for nine different locations with instrumentation depths ranging from 61m (station 10') to 762 m (station 13) for Pahute Mesa UNE sources only. Downhole instruments were located in alluvium (stations 10' and 4), granite (station 3), Paleozoic sediments (stations 8 and 11) and tuff (stations 5, 9, 10, and 13). Vortman and Long (1982a) also treated stations 15 and 16 as a surface/downhole pair, even though both were surface installations. They were located 2.3 km apart and had an elevation difference of 581m. The fact that station 16 is in fact located on the Earth's surface clearly makes it inappropriate to use its data in this manner, and the results from station 15/16 are ignored in the following discussion.

Vortman and Long's (1982a) analysis included (1) comparisons of peak ground motion parameters as a function of station depth, (2), comparisons of averages of the several largest peak (time domain) motion parameters as a function of depth and (3) ratios of surface/downhole response spectra and comparison as a function of depth. For the Pahute Mesa data, they documented very large data scatter in plots of peak vector acceleration, velocity, and displacement as a function of depth. Despite the large variation, Vortman and Long fit least-squares regression lines through the average peak ground motion values'

variation with depth; correlation coefficients were very low, ranging from 0.28 for acceleration to 0.49 for velocity. These poor correlations indicate that the data are not sufficient to establish a real relationship for attenuation with depth at NTS. Vortman and Long note that the surface/downhole ground motion ratios seem to be most affected by the geologic medium in which the instruments occur, rather than following a general relationship. Their attempts at characterizing the average of multiple peaks of ground motion with depth did not meet with any more success. Correlation coefficients rose slightly to around 0.4, but are still too low to indicate a meaningful relationship between vector ground motion and depth as measured from these data. They also examined the variation with depth of top/bottom ratios for vector response spectra mean values (averaged over the entire frequency range), and determined a least squares fit that had a correlation coefficient of 0.57. A large amount of effort went into this study, however it appears that it demonstrates little other than to establish the large variability in both peak ground motions and spectra of UNEs recorded at borehole stations.

Vortman and Long (1982b) conducted a parallel study using Yucca Flat UNE data. These results are very similar to those obtained using Pahute Mesa sources. While a general decrease in peak ground motion with increasing depth was observed, the data scatter is very significant. For example, the correlation coefficient for the peak vector displacement data as a function of depth was 0.087. A correlation coefficient this low implies essentially no demonstrated correlation bertween peak displacement and depth. Regressions using averages of several peaks and averages of response spectra ratios were also extremely scattered. The Yucca Flat data set includes more data than did the Pahute Mesa data set and exhibits correspondingly more variability, as Vortman and Long (1982b) noted. Their equations for variation of ground motion with depth are not included here.

The next study to attempt to document and understand downhole motions was that of Long et al. (1983). Using optimum finite impulse response filters for each station with downhole instrumentation, they developed a series of least-squares linear prediction mathematical transfer functions. A filter that would transform the surface waveform into the downhole waveform was computed for each borehole record pair and then the available filters were averaged in order to provide a more general predictive filter for each station. Long et al. (1983) analyzed data from both Pahute Mesa and Yucca Flat, and determined the success in the predictions based on the root-mean-square error between the actual and predicted waveform. This is a time-domain technique, and while the filters were derived from velocity waveforms, published comparisons were made with displacement waveforms, which emphasize the lower frequencies in the data. Long et al. (1983) had reasonable success in predicting downhole displacement waveforms for stations 10', 3, and 4, and less success with stations 8, 9, 11, and 13 for both Pahute Mesa and Yucca Flat sources. No Yucca Mountain stations had enough data available at that time to design a Yucca Mountain-specific filter. In all cases the vertical transfer functions were more successful than the predictions for either the radial or transverse components. Long et al. (1983) do not provide a tabulation of their filter coefficients in their report. While the filters appear to do a reasonably good job of predicting downhole displacement waveforms, they are based solely on signal processing techniques and contain no geologic information that would help in generalizing to other locations. Thus the usefulness of

this technique is limited to existing boreholes for which a suite of surface/downhole record pairs exists.

Most recently, Durrani and Walck (1996) have examined and analyzed the surface/downhole data now available from boreholes in the immediate vicinity of Yucca Mountain. The WTSI project took advantage of several existing boreholes at Yucca Mountain and established downhole instruments near the expected depth of the potential repository (about 350m below ground surface) in three wells for which detailed geological (and some geophysical) information was available: USW G-1 (station 25), USW G-2 (station 28) and USW GU3 (station 12/30). An additional, shallower borehole site was established near the proposed site of the repository surface facilities (station 29, with a downhole accelerometer at 82m depth). Stations 28, 25, and 30 define a north-south line through the Yucca Mountain ridge.

Durrani and Walck also developed site-specific transfer functions, however they took a different approach from that of Long et al. (1983) by incorporating available geological and geophysical information into seismic velocity models for each borehole location. They calculated one-dimensional seismic transfer functions using the propagator matrix method (e.g., Shearer et al., 1987) and used the transfer function to transform observed surface records into simulated downhole records. The geologic/seismologic models were then adjusted in a forward modeling process using data from 37 Pahute Mesa and Yucca Flat UNEs until the synthetic downhole waveforms best matched the observed waveforms, in the judgment of the analysts. The details of the modeling, as Durrani and Walck (1996) describe, show that the differences between the surface and borehole records from quite similar geologic environments and at similar depths can be quite pronounced. The four Yucca Mountain stations (28, 25, 30, 29) were each modeled separately (Table 6; Figures 38 and 39). The agreement between the observations and synthetic waveforms were particularly good for the shallow borehole station 29; both vertical and radial records were well-matched (Figure 40 and 41). Generally, like the study of Long et al., the modeling was more successful for the vertical than for the radial records (Figures 42-47). The match of the synthetic downhole vertical waveforms to those observed is excellent and the radial components still match well in overall amplitude and frequency content. The proposed models are consistent with both the known seismological and geological data for the area.

Durrani and Walck (1996) then used the models developed for the three deep borehole stations to propose a two-dimensional north-south seismic model for the uppermost 350m of the Yucca Mountain ridge (Figure 48). Finally, they used a one-dimensional slice through the two-dimensional model to represent the seismic velocities in the immediate vicinity of the potential repository. Surface recordings from station 21 (see Figure 1) and the transfer function generated using this model (Table 7) were used to predict downhole waveforms that would be observed at the repository site from a UNE of comparable size and distance to those in the data base. This geologic/seismologic model also provides a means for predicting repository-level ground motions for earthquakes, given a specified surface ground motion time history or spectrum.

Other Factors affecting Ground Motion Prediction at Yucca Mountain

Station	Rock Type	Thickness km	Depth km	P-wave velocity km/s	S-wave velocity km/s
28	Alluvium	0.0	0.0	N/A	N/A
	Tiva Canyon	0.075	0.075	1.50	1.07
	Bedded Tuff	0.156	0.231	2.30	1.33
	Topopah Spg. (Tsw1)	0.204	0.435	3.10	1.79
	Topopah Spg. (Tsw2)	1.000	1.435	3.90	2.25
25	Alluvium	.018	0.018	0.7	0.4
	Tiva Canyon	0.0	0.0	N/A	N/A
	Bedded Tuff	0.122	0.140	2.30	1.64
	Topopah Spg. (Tsw1)	0.170	0.310	3.10	1.79
	Topopah Spg. (Tsw2)	0.101	0.411	3.90	2.25
30	Alluvium	0.0	0.0	N/A	N/A
	Tiva Canyon/ Bedded Tuff	0.129	0.129	2.30	1.33
	Topopah Spg. (Tsw1)	0.301	0.430	3.10	1.79
	Topopah Spg. (Tsw2)	1.000	1.430	3.90	2.25
29	Alluvium	0.046	0.046	1.10	0.64
	Unit "X"	0.036	0.082	1.50	0.87
	Tiva Canyon	1.000	1.082	2.30	1.33

Table 6: One-dimensional geological/seismological models for WTSI Yucca Mountain stations 28, 25, 30, and 29, from Durrani and Walck (1996)

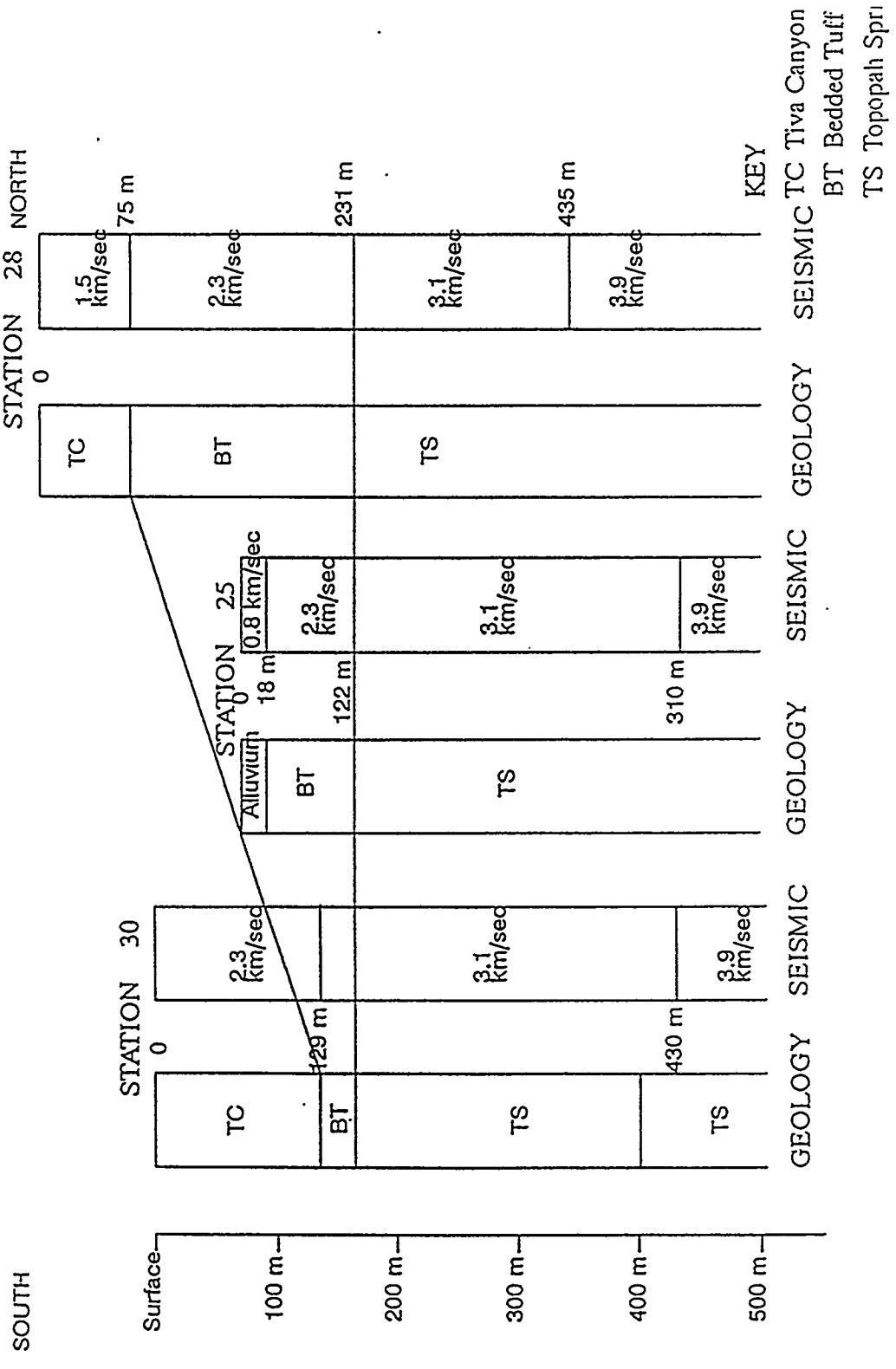

Figure 38: One-dimensional P-wave velocity models respresenting the near-surface seismic velocities for three Yucca Mountain borehole stations (from south to north) 30, 25, and 28. Downhole station depths are 352m, 358m (305m after 4/87) and 375m (358m after 4/87), respectively. Depth scale is shown separately for each hole.

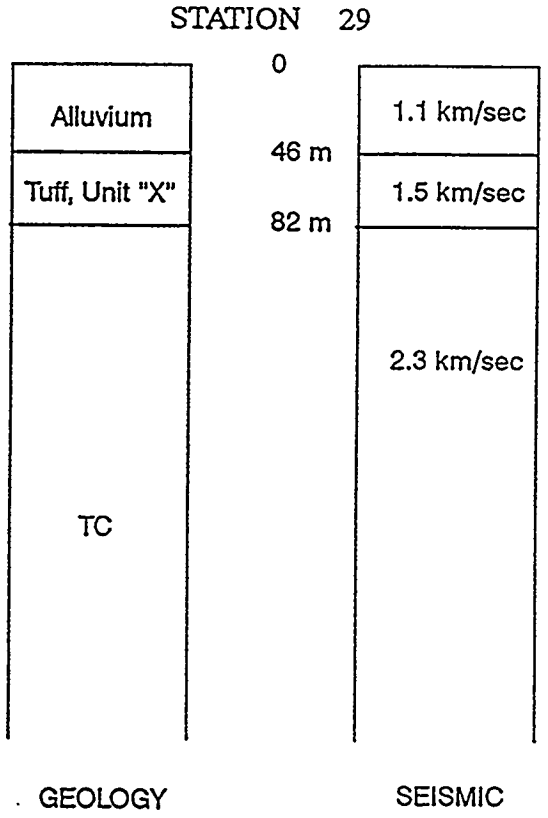

Figure 39: P-wave velocity model for station 29, located to the east of the Yucca Mountain ridge. Downhole instrumentation is located at 82m depth. TC denotes the Tiva Canyon Member of the Paintbrush Tuff.

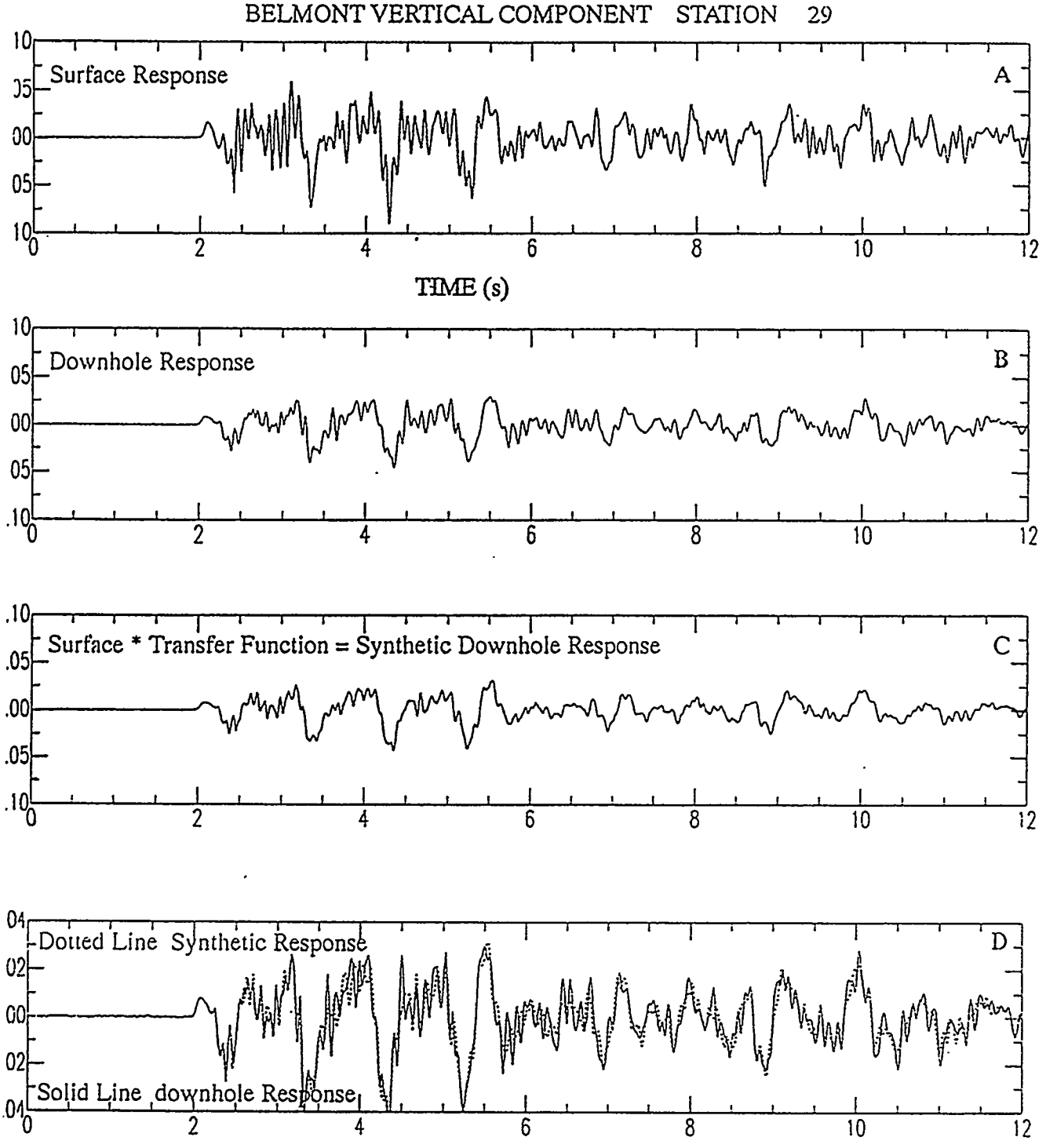

Figure 40: Results of velocity modeling for station 29, Pahute Mesa event Belmont, vertical component. A shows the observed vertical surface acceleration; B is the observed downhole record. C displays the synthetic downhole response obtained by convolving the transfer function generated from the velocity model in figure 39 with the observed surface record (A). D is an overlay of the observed and synthetic downhole traces: dotted line is the synthetic and solid line is the data.

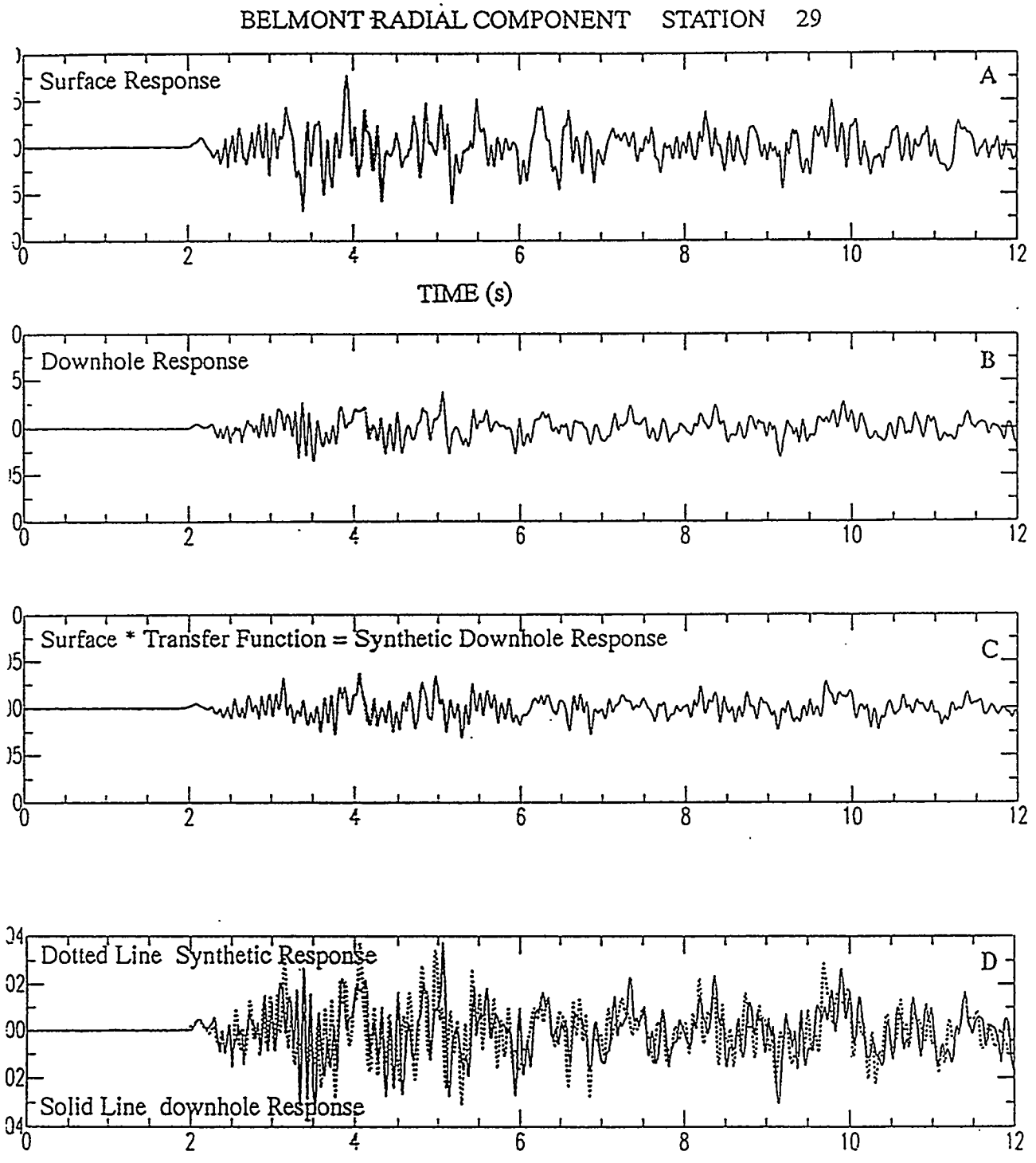

Figure 41: Same as figure 40 for station 29, Pahute Mesa event Belmont, radial component.

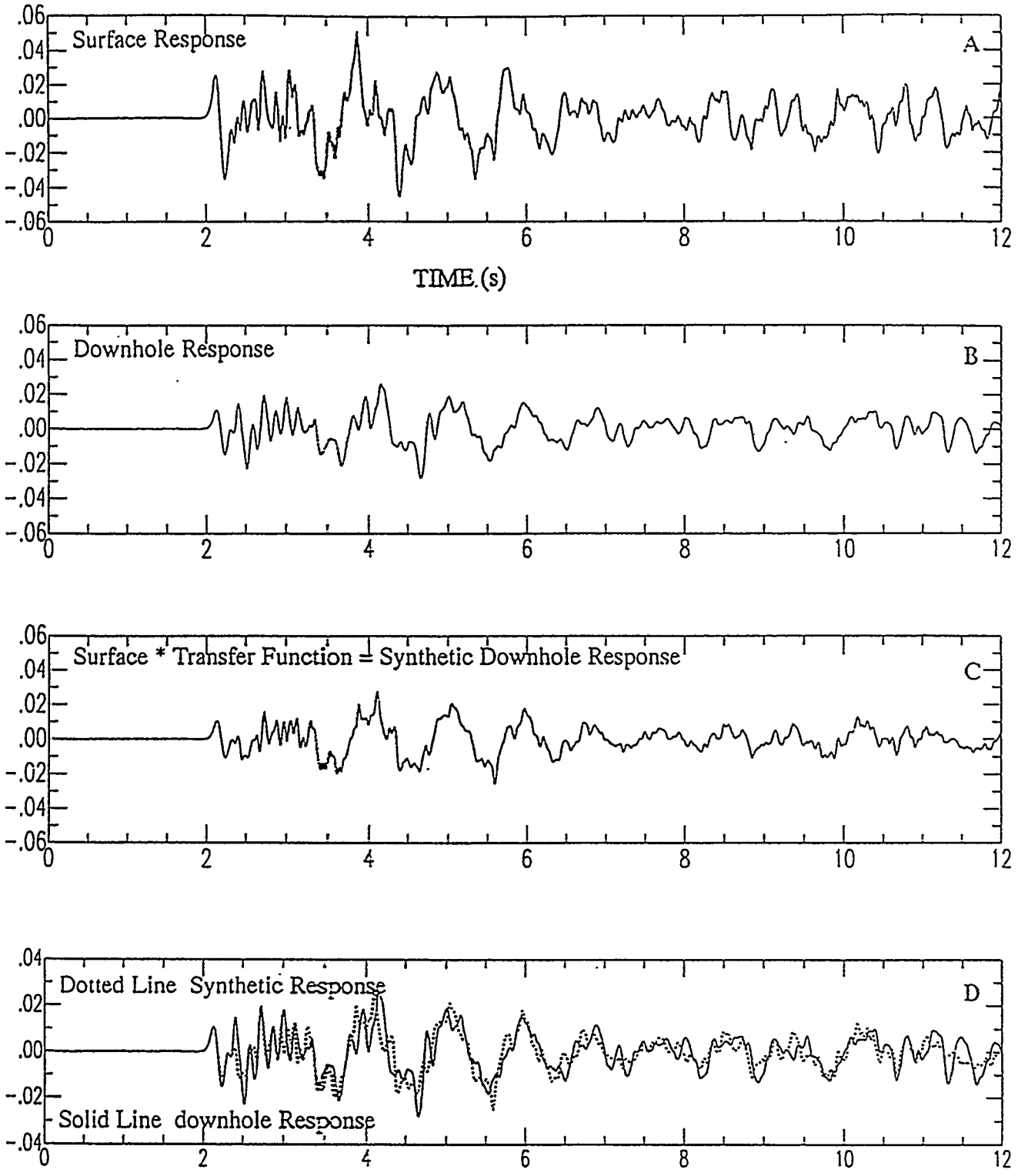

Figure 42: Same as figure 40 for station 30, Pahute Mesa event Delamar, vertical component.

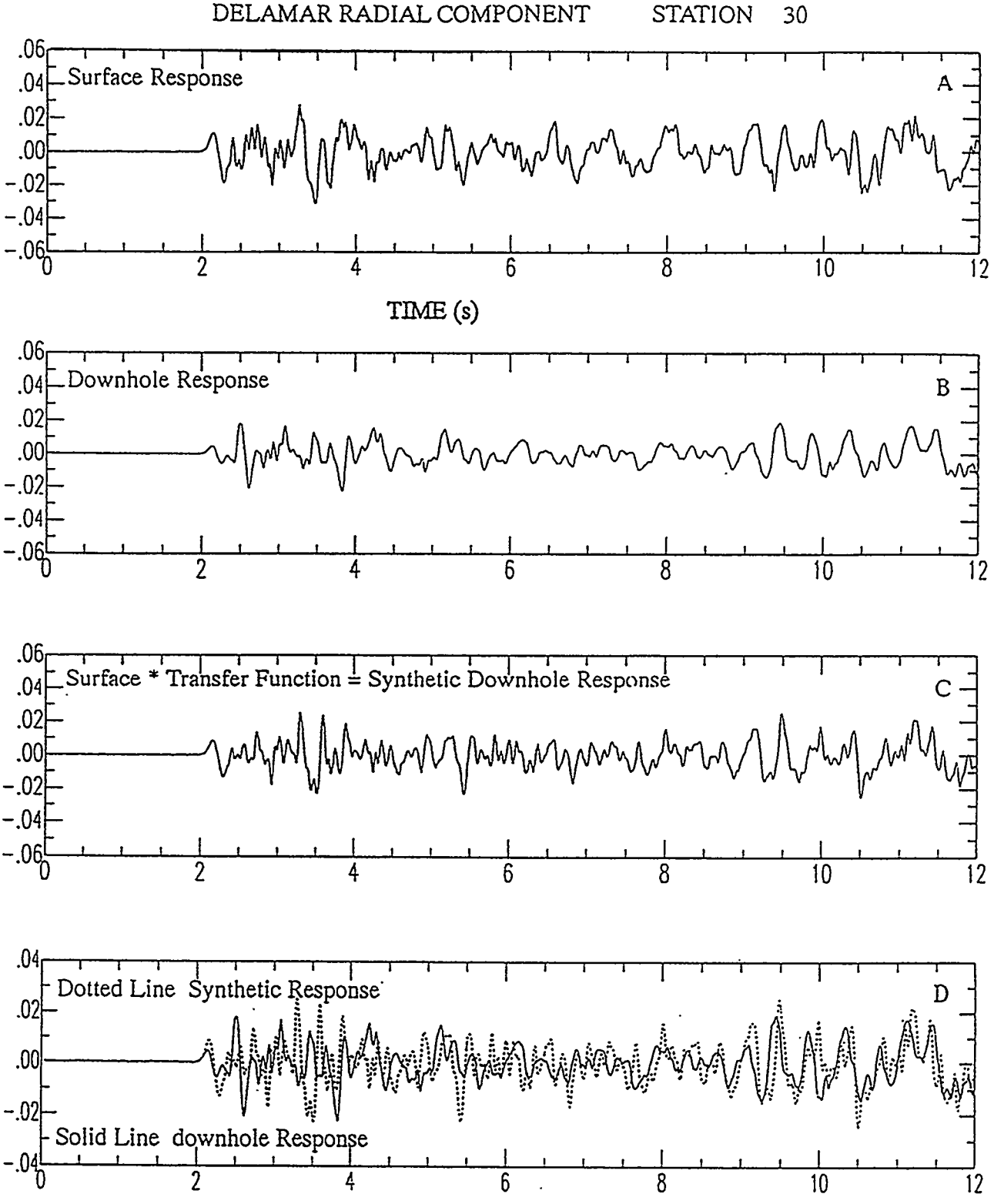

Figure 43: Same as figure 40 for station 30, Pahute Mesa event Delamar, radial component.

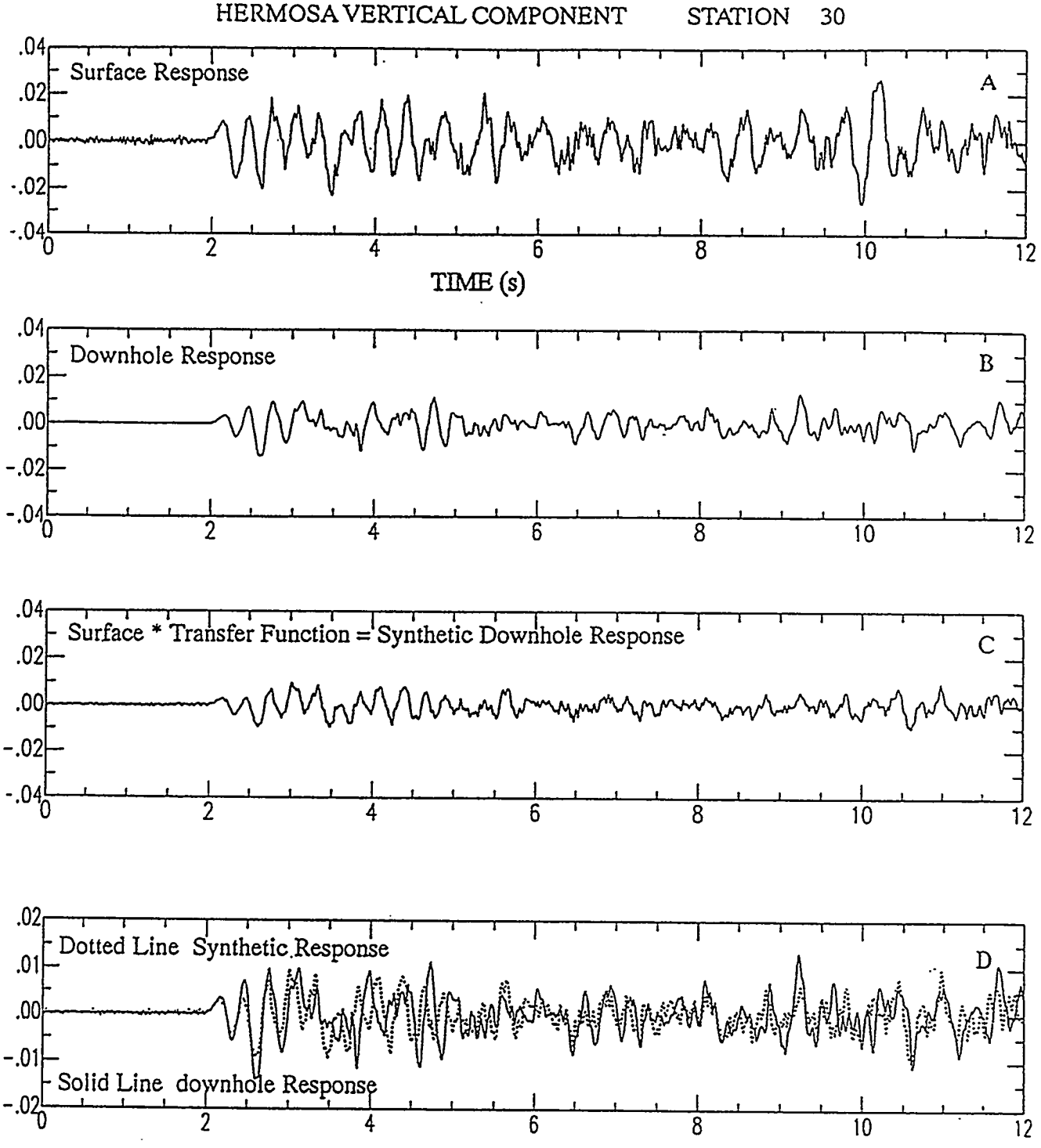

Figure 44: Same as figure 40 for station 30, Yucca Flat event Hermosa, vertical component.

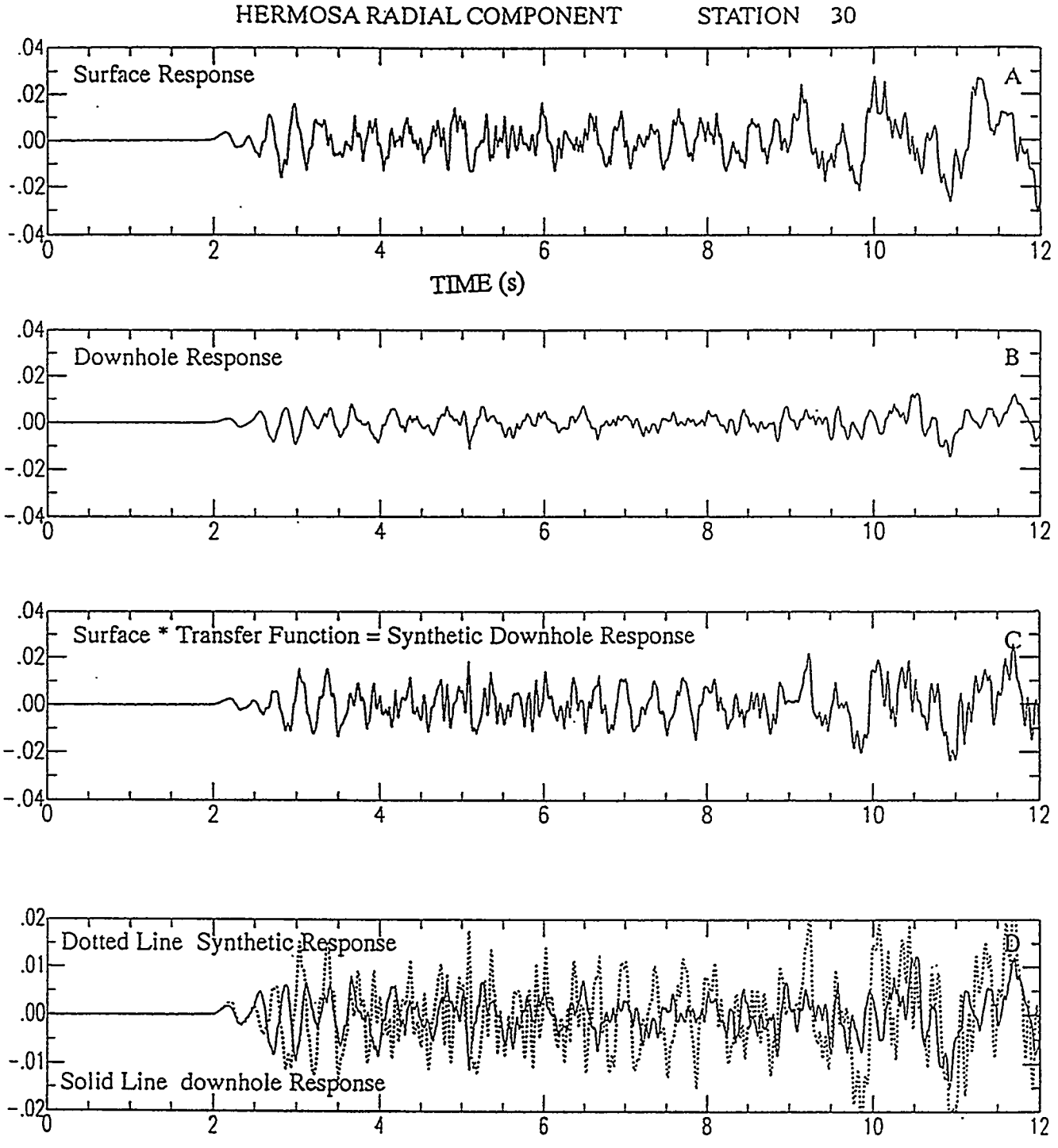

Figure 45: Same as figure 40 for station 30, Yucca Flat event Hermosa, radial component.

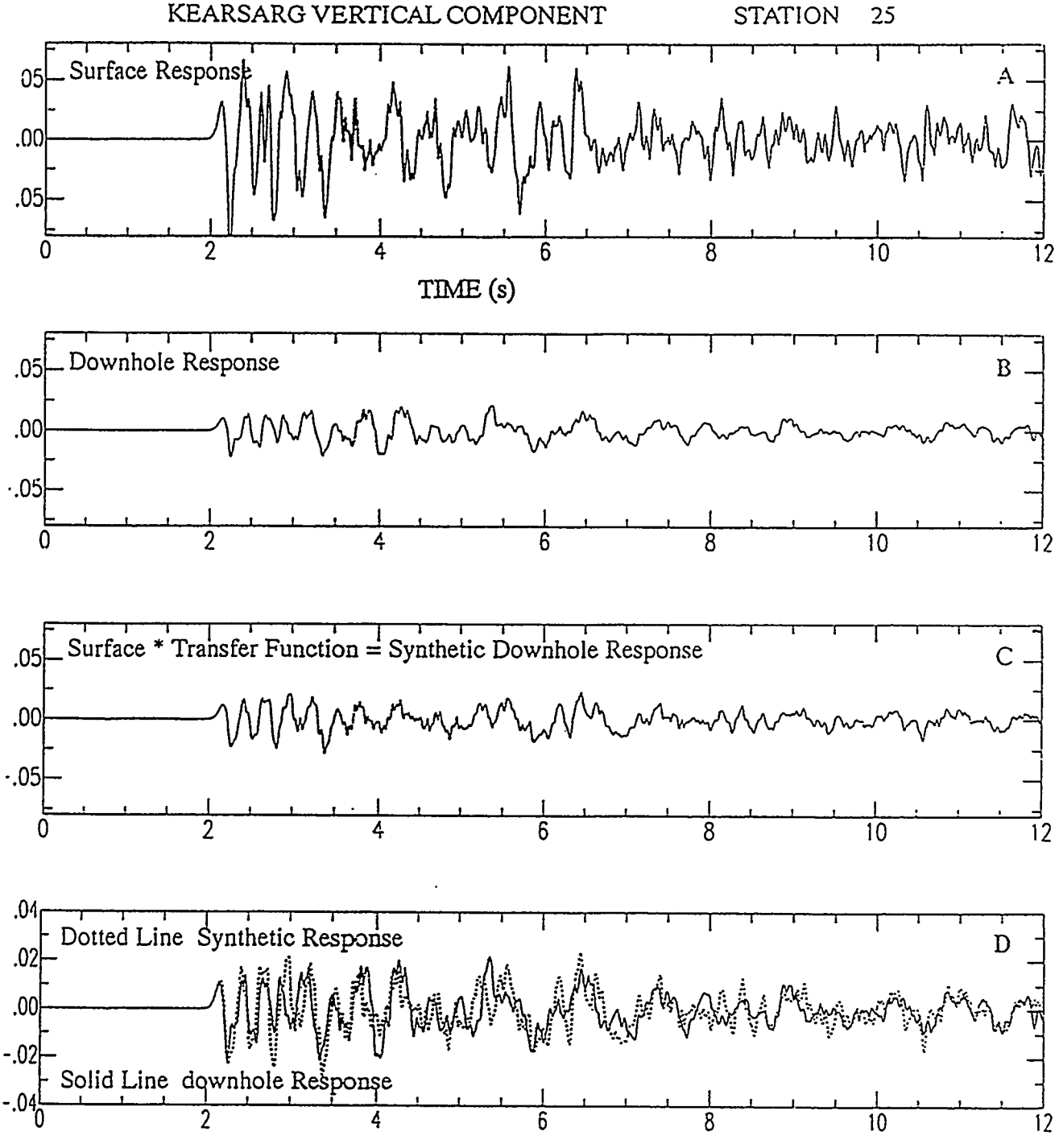

Figure 46: Same as figure 40 for station 25, Pahute Mesa event Kearsarg, vertical component.

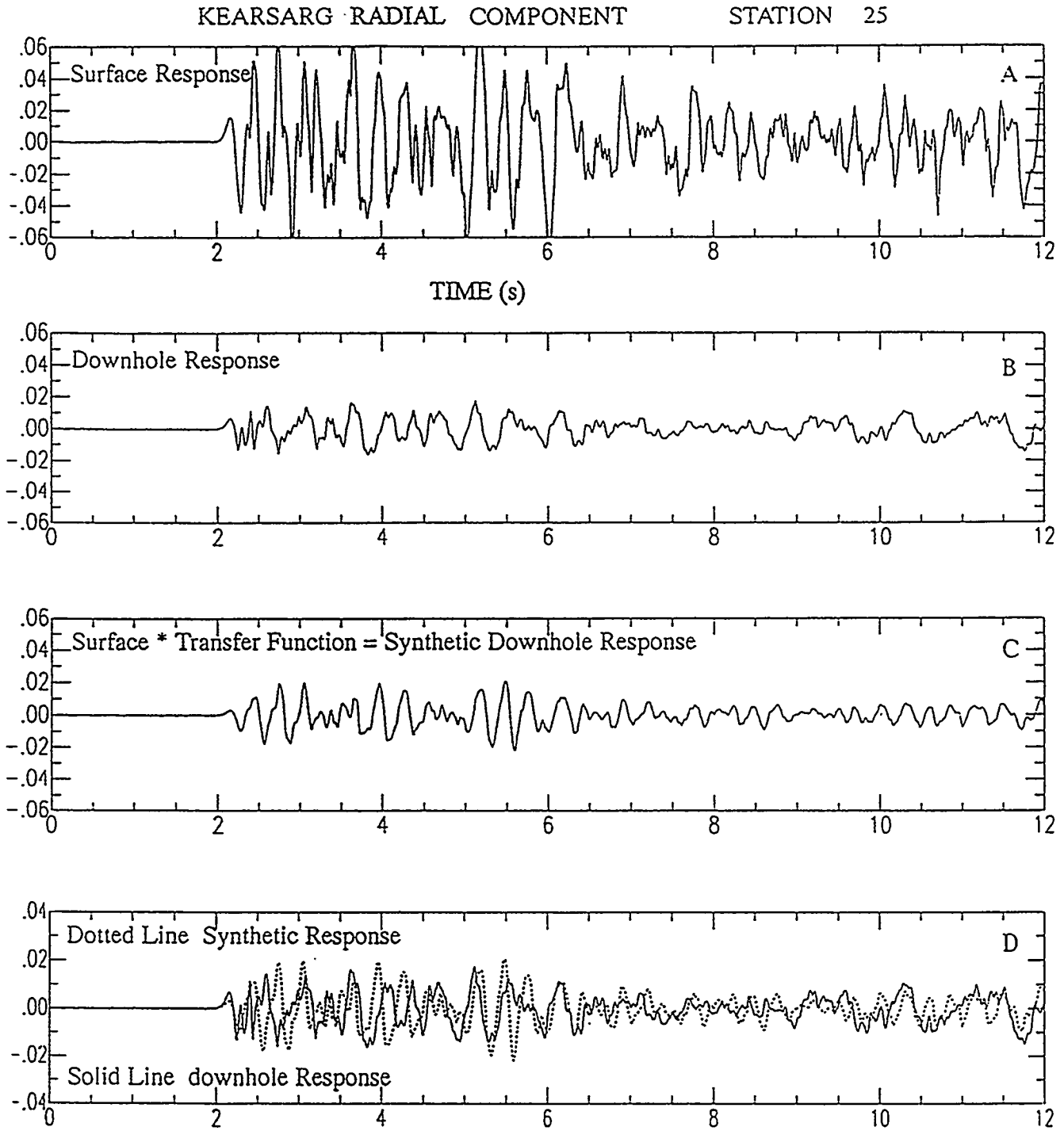

Figure 47: Same as figure 40 for station 25, Pahute Mesa event Kearsarg, radial component.

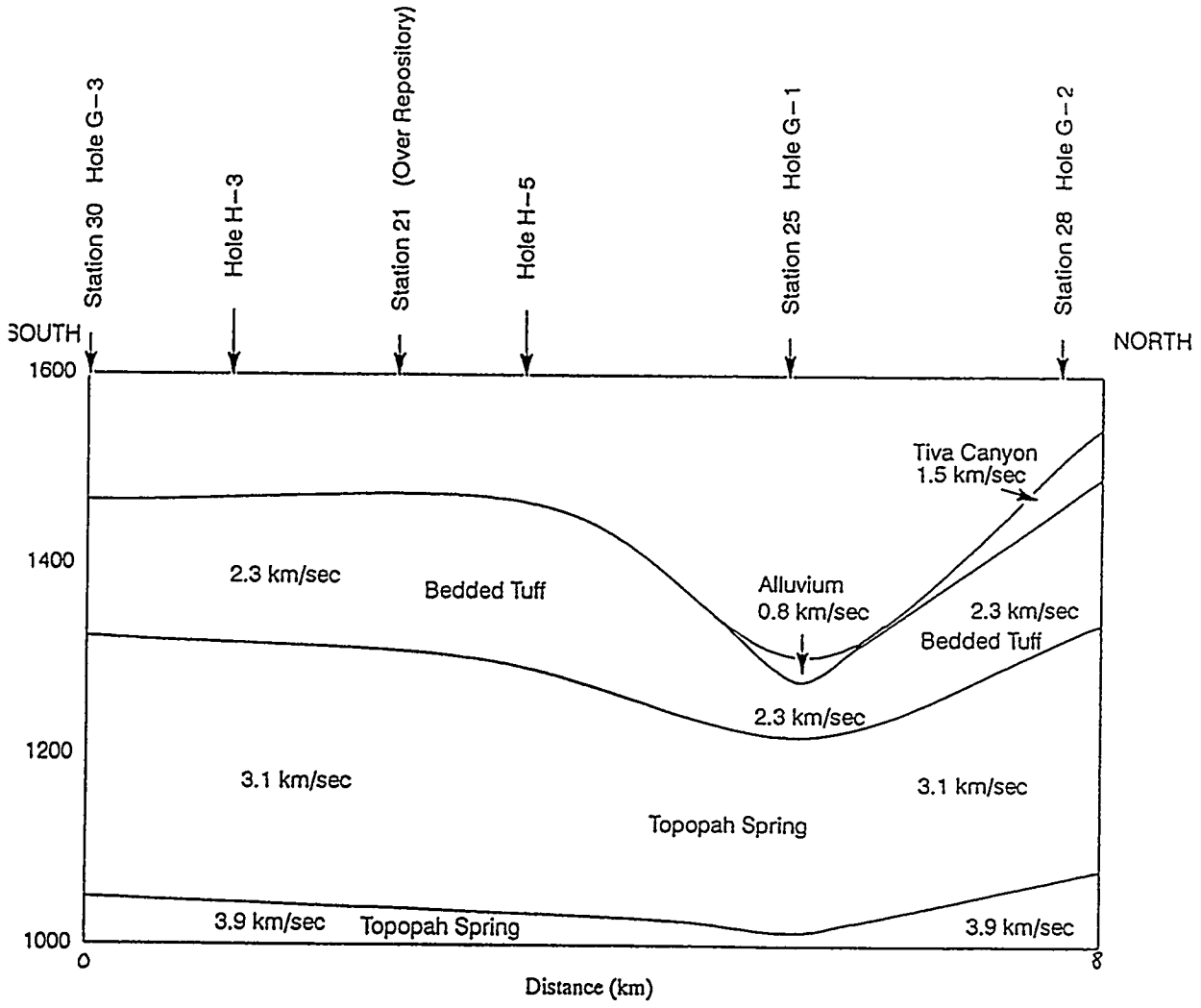

Figure 48: A simple two-dimensional compressional velocity model running approximately north-south through Yucca Mountain from station 30 at the south to station 28 at the north.

Station	Rock Type	Thickness km	Depth km	P-wave velocity km/s	S-wave velocity km/s
21	Alluvium	0.0	0.0	N/A	N/A
	Tiva Canyon/ Bedded Tuff	0.140	0.140	2.30	1.33
	Topopah Spg. (Tsw1)	0.290	0.430	3.10	1.79
	Topopah Spg. (Tsw2)	1.000	1.430	3.90	2.25

Table 7: One-dimensional geological/seismological model at the location of WTSI station 21 (directly above the potential repository) from Durrani and Walck (1996)

Ground motions recorded at Yucca Mountain are complex, and arise from a number of factors including the nature of the seismic source, effects of the recording site, and seismological effects encountered along the travel path in addition to the normal, predictable effects due to wave propagation in an elastic medium. The studies of UNE ground motion conducted to date have relied primarily on fits of empirical data to simple models. They have included only one type of source, the underground nuclear explosion, even though the recorded ground motions from UNEs compared to those from appropriately-sized earthquakes recorded elsewhere make it clear that earthquakes will be the dominant source of seismic energy recorded at the repository. The distribution of sources in azimuth and distance has been quite limited due to the similarity in distance to the two primary nuclear testing areas, and only a small difference in azimuth between Pahute Mesa and Yucca Flat. Site effects have not been given much attention, and true strong ground motion data for Yucca Mountain is in short supply, due to the very low seismicity rate; UNEs produce only weak ground motions at the site. Finally, the propagation paths along which seismic energy travels to Yucca Mountain vary dramatically as a function of azimuth. Researchers at the U. S. Geological Survey (Mooney and Schapper[2]; Hoffman and Mooney, 1984) have conducted several seismic refraction surveys that document highly varying crustal velocities in the vicinity of Yucca Mountain. Nuclear explosions have also been used as a seismic energy source to determine crustal structure in the context of the Yucca Mountain Project. Walck and Phillips (1990) studied records from 21 UNEs in western Pahute Mesa, eastern Pahute Mesa, and Yucca Flat; they developed three two-dimensional crustal velocity models that match the travel times and relative amplitudes of vertical acceleration records recorded at Yucca Mountain. These models, appropriate for paths from the testing areas to Yucca Mountain (Figure 49) demonstrate a notable amount of lateral variation in the shallow crust at NTS. Comparison of the top two panels of Figure 49 with the bottom panel shows that velocities of near 6 km/sec are reached at very shallow depths beneath Yucca Flat, but not below the Silent Canyon Caldera deposits of Pahute Mesa. Large lateral velocity variations such as these can have important effects on observed ground motions. For example, vertical accelerations from Pahute Mesa UNEs recorded at the Yucca Mountain station 25 are larger than would be predicted using the Vortman (1986) or Long (1992) prediction equations, however, vertical accelerations from Yucca Flat UNEs recorded at station 25 are within the expected range. Walck and Phillips (1990) attribute the large Pahute Mesa amplitudes to a path effect associated with the Timber Mountain Caldera along the Pahute Mesa - Yucca Mountain travel path that focuses energy near the northern end of Yucca Mountain. Yucca Flat UNEs exhibit relatively large motions for stations east of the repository (14, 26, 29) which most likely results from another focusing effect due to laterally varying crustal structure. These focusing effects are dependent on both the source and receiver location and understanding of them requires fairly detailed modeling of crustal velocity structure. Thus in order to make realistic ground motion estimates for Yucca Mountain, the lateral variations due to the complex geology and tectonics of the area surrounding Yucca Mountain require either very large uncertainties to be associated with the ground motion

[2]Mooney, W. D. and S. G. Schapper, Seismic refraction investigations, *in* Oliver, H. W., D. A., Ponce and W. C. Hunter, Major results of geophysical investigations at Yucca Mountain and vicinity, southern Nevada, Open-File Report 95-74, U. S. Geological Survey, 125, in press.

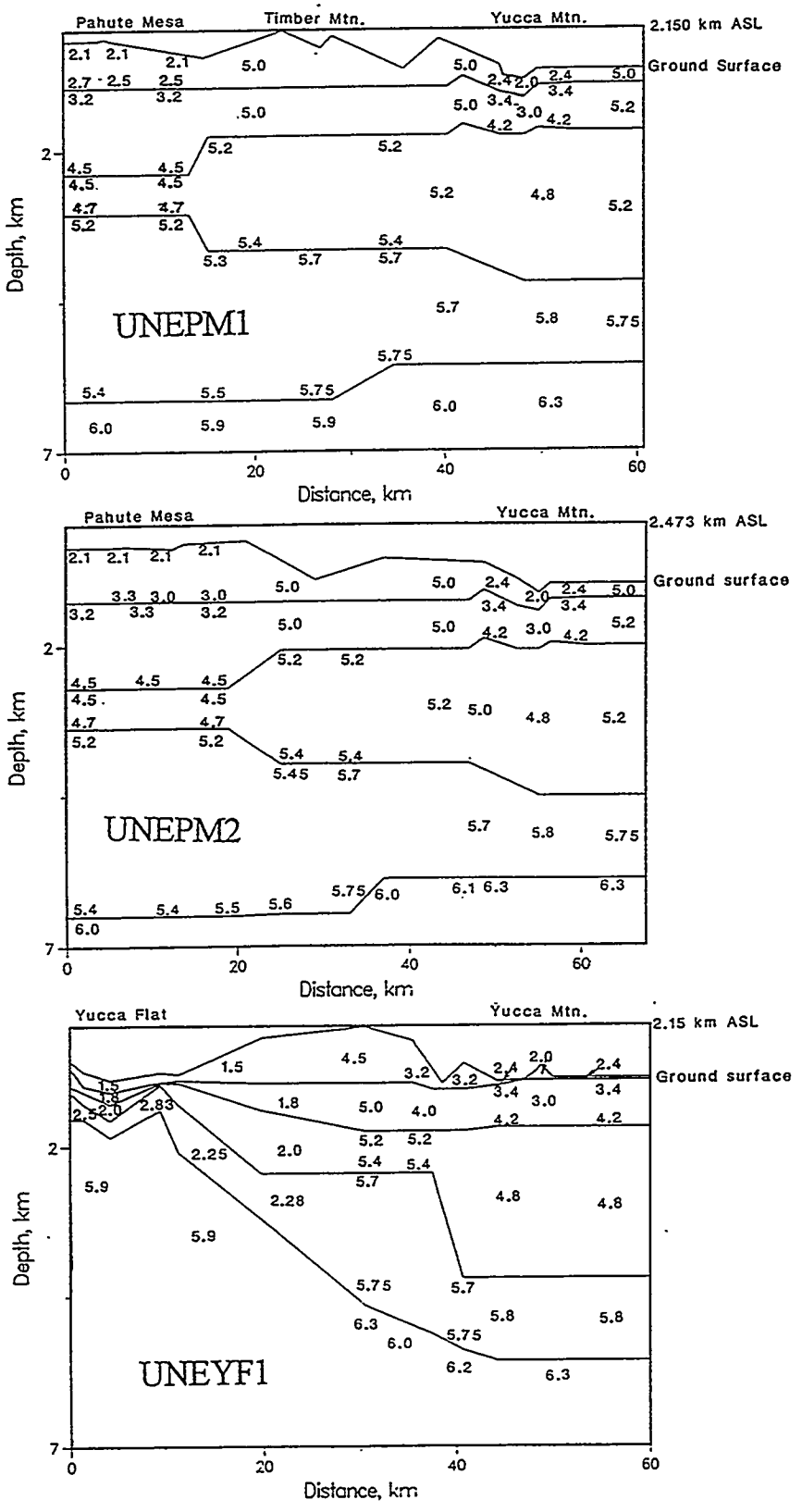

Figure 49: NTS crustal velocity models from Walck and Phillips (1990) representing paths from western Pahute Mesa (UNEPM1), eastern Pahute Mesa (UNEPM2) and Yucca Flat (UNEYF1) to Yucca Mountain. Note the variations among the models. Velocities are in km/sec. Solid lines are layer boundaries. Multiple velocity values within layers indicate vertical velocity gradients. Model datum is indicated at the top right of each panel. There is significant vertical exaggeration.

estimates, or detailed modeling of the local environment, including site effects assessment and also knowledge of the azimuthally-varying path effects.

Conclusions

This report summarizes data analyses of underground nuclear ground motions recorded on and near the Nevada Test Site collected by the Weapons Test Seismic Investigations project at Sandia National Laboratories. The analyses were conducted over a period of more than 10 years, and discuss a number of different aspects of UNE ground motions. Equations that predict UNE peak ground motion as a function of event yield (size) and distance are summarized in Tables 2 (vector motions; Vortman, 1986) and 4 (component motions; Long, 1992). Equations that predict response spectral pseudo velocity values as a function of yield and distance are summarized in Table 5 (Phillips; 1991b). In addition, Phillips (1991a) has documented response spectra ratios for surface and downhole stations that allows use of the spectra prediction equations for downhole motions at specific sites and depths. All of these equations are valid for ground motions from both the Pahute Mesa and Yucca Flat source areas, as demonstrated in this report.

Several studies have also addressed the variation of ground motion as a function of depth at the test site. The large amount of scatter in the data has precluded the formation of general relationships for the decrease in peak ground motion amplitudes as a function of depth for NTS. A seismic model for the near-surface regime at Yucca Mountain has been developed, however, which is appropriate for predicting vertical and radial levels of motion at depth given a surface seismogram or spectrum (Durrani and Walck, 1996; Tables 6, 7).

Finally, the ground motion estimates presented here all have rather large ranges of uncertainty. The error bars take into account variations in source coupling, variations in travel path effects, and also receiver site effects. Differences between explosion and earthquake sources, however, have not been included in the uncertainty estimates for these ground motion parameters.

References

Boore, D. M., W. B. Joyner, A. A. Oliver III, and R. A. Page, Estimation of ground motion parameters, Geological Survey Circular 795, U. S. Geological Survey, 1978.

Boore, D. M., W. B. Joyner, and T. E. Fumal, Estimation of response spectra and peak accelerations from western North American earthquakes: an interim report, Open File Report OFR 93-509, U. S. Geological Survey, 1993.

Brune, J. N., W. Nicks, and A. Aburto, Microearthquakes at Yucca Mountain, Nevada, *Bulletin of the Seismological Society of America*, **82**, 164 - 174, 1992.

Environmental Research Corporation, Prediction of ground motion characteristics of underground nuclear detonations, NVO-1163-239, ERC, Las Vegas, NV, 1974.

Durrani, B. A. and M. C. Walck, Near-surface velocity modeling at Yucca Mountain using borehole and surface records from underground nuclear explosions, SAND95-1606, Sandia National Laboratories, Albuquerque, NM, 1996.

Gibson, J. D., F. H. Swan, J. R. Wesling, T. F. Bullard, R. C. Perman, M. M. Angell, and L. A. DiSilvestro, Summary and evaluation of existing geological and geophysical data near prospective surface facilities in Midway Valley, Yucca Mountain Project, Nye County, Nevada, SAND90-2491, Sandia National Laboratories, Albuquerque, NM, 1992.

Gomberg, J., Seismicity and detection/location threshold in the Southern Great Basin Seismic Network, *Journal of Geophysical Research*, **96**, 16401 - 16414, 1991.

Hoffman, L. R. and W. D. Mooney, A seismic study of Yucca Mountain and vicinity, southern Nevada; data report and preliminary results, Open File Report 83-588, U. S. Geological Survey, Menlo Park, CA, 1984.

Joyner, W. B. and D. M. Boore, Prediction of earthquake response spectra, Open File Report 82-977, U. S. Geological Survey, Menlo Park, CA, 1982.

Long, J. W., Component ground motion at the Nevada Test Site from Pahute Mesa underground nuclear explosions, SAND86-0439, Sandia National Laboratories, Albuquerque, NM, 1992.

Long, J. W., K. A. Sabisch, S. D. Stearns, and L. J. Vortman, Prediction of downhole waveforms, SAND82-2478, Sandia National Laboratories, Albuquerque, NM, 1983.

Pezzopane, S. K., C. M. Menges, and J. W. Whitney, Quaternary paleoseismology and Neogene tectonics at Yucca Mountain, Nevada, Open-File Report 94-568, U. S. Geological Survey, 149-151, 1994.

Phillips, J. S., Analysis of component surface/downhole ground motions at Yucca Mountain for underground nuclear explosions in Pahute Mesa, SAND87-2381, Sandia National Laboratories, Albuquerque, NM, 1991a.

Phillips, J. S., Prediction of pseudo relative velocity response spectra at Yucca Mountain for underground nuclear explosions conducted in the Pahute Mesa testing area at the Nevada Test Site, SAND88-3032, Sandia National Laboratories, Albuquerque, NM, 1991b.

Shearer, P. M. and J. A. Orcutt, Surface and near-surface effects on seismic waves -- theory and borehole seismometer results, *Bulletin of the Seismological Society of America*, 77, 1168 - 1196, 1987.

Stump, B. W. and R. E. Reinke, Free-field and free surface ground motions from nuclear explosions, their spatial variations, and the constraint of physical source mechanisms, *in* Taylor, S. R., H. J. Patton, and P. G. Richards, eds., Explosion Source Phenomenology, Geophysical Monograph 65, American Geophysical Union, Washington, DC, 47-61, 1991.

Trifunac, M. D., Preliminary analysis of the peaks of strong earthquake ground motion -- dependence of peaks on earthquake magnitude, epicentral distance, and recording site conditions, *Bulletin of the Seismological Society of America*, **66**, 189 - 219, 1976.

Vortman, L. J., Prediction of ground motion from underground nuclear weapons tests as it relates to siting of a nuclear waste storage facility at NTS and compatibility with the weapons test program, SAND80-1020/1, Sandia National Laboratories, Albuquerque, NM, 1980.

Vortman, L. J., Ground motion produced at Yucca Mountain from Pahute Mesa underground nuclear explosions, SAND85-1605, Sandia National Laboratories, Albuquerque, NM, 1986.

Vortman, L. J., An evaluation of the seismicity of the Nevada Test Site and vicinity, SAND86-7006, Sandia National Laboratories, Albuquerque, NM, 1991.

Vortman, L. J. and J. W. Long, Effects of repository depth on ground motion, the Pahute Mesa data, SAND82-0174, Sandia National Laboratories, Albuquerque, NM, 1982a.

Vortman, L. J. and J. W. Long, Effects of ground motion on repository depth -- the Yucca Flat data, SAND82-1647, Sandia National Laboratories, Albuquerque, NM, 1982b.

Walck, M. C., Modeling of anomalous ground motion observed at Jackass Flats, Nevada Test Site (abstract), *Seismological Research Letters*, **59** (1): 31, 1988.

Walck, M. C. and J. S. Phillips, Two-dimensional velocity models for paths from Pahute Mesa and Yucca Flat to Yucca Mountain, SAND88-3033, Sandia National Laboratories, Albuquerque, NM, 1990.

YUCCA MOUNTAIN SITE CHARACTERIZATION PROJECT
SAND95-1938 - DISTRIBUTION LIST

1 D. A. Dreyfus (RW-1)
Director
OCRWM
US Department of Energy
1000 Independence Avenue SW
Washington, DC 20585

1 L. H. Barrett (RW-2)
Acting Deputy Director
OCRWM
US Department of Energy
1000 Independence Avenue SW
Washington, DC 20585

1 S. Rousso (RW-40)
Office of Storage and Transportation
OCRWM
US Department of Energy
1000 Independence Avenue SW
Washington, DC 20585

1 R. A. Milner (RW-30)
Office of Program Management
and Integration
OCRWM
US Department of Energy
1000 Independence Avenue SW
Washington, DC 20585

1 D. R. Elle, Director
Environmental Protection Division
DOE Nevada Field Office
US Department of Energy
P.O. Box 98518
Las Vegas, NV 89193-8518

1 T. Wood (RW-14)
Contract Management Division
OCRWM
US Department of Energy
1000 Independence Avenue SW
Washington, DC 20585

4 Victoria F. Reich, Librarian
Nuclear Waste Technical Review Board
1100 Wilson Blvd., Suite 910
Arlington, VA 22209

1 Wesley Barnes, Project Manager
Yucca Mountain Site Characterization
Office
US Department of Energy
P.O. Box 98608--MS 523
Las Vegas, NV 89193-8608

1 Director, Public Affairs Office
c/o Technical Information Resource Center
DOE Nevada Operations Office
US Department of Energy
P.O. Box 98518
Las Vegas, NV 89193-8518

8 Technical Information Officer
DOE Nevada Operations Office
US Department of Energy
P.O. Box 98518
Las Vegas, NV 89193-8518

1 J. R. Dyer, Deputy Project Manager
Yucca Mountain Site Characterization Office
US Department of Energy
P.O. Box 98608 -- MS 523
Las Vegas, NV 89193-88608

1 M. C. Brady
Laboratory Lead for YMP
M&O/Sandia National Laboratories
1261 Town Center Drive
Bldg. 4, Room 421A
Las Vegas, NV 89134

1 J. A. Canepa
Laboratory Lead for YMP
EES-13, Mail Stop J521
M&O/Los Alamos National Laboratory
P.O. Box 1663
Los Alamos, NM 87545

1 Repository Licensing & Quality
Assurance
Project Directorate
Division of Waste Management, MS T7J-9
US NRC
Washington, DC 20555

1 Senior Project Manager for Yucca
Mountain
Repository Project Branch
Division of Waste Management, MS T7J-9
US NRC
Washington, DC 20555

1 NRC Document Control Desk
Division of Waste Management, MS T7J-9
US NRC
Washington, DC 20555

1 Chad Glenn
NRC Site Representative
301 E Stewart Avenue, Room 203
Las Vegas, NV 89101

1 Center for Nuclear Waste
Regulatory Analyses
Southwest Research Institute
6220 Culebra Road
Drawer 28510
San Antonio, TX 78284

2 W. L. Clarke
Laboratory Lead for YMP
M&O/ Lawrence Livermore Nat'l Lab
P.O. Box 808 (L-51)
Livermore, CA 94550

1 Robert W. Craig
Acting Technical Project Officer/YMP
US Geological Survey
101 Convention Center Drive, Suite P-110
Las Vegas, NV 89109

1 J. S. Stuckless, Chief
Geologic Studies Program
MS 425
Yucca Mountain Project Branch
US Geological Survey
P.O. Box 25046
Denver, CO 80225

1 L. D. Foust
Technical Project Officer for YMP
TRW Environmental Safety Systems
101 Convention Center Drive
Suite P-110
Las Vegas, NV 89109

1 A. L. Flint
U. S. Geological Survey
MS 721
P. O. Box 327
Mercury, NV 89023

1 Robert L. Strickler
Vice President & General Manager
TRW Environmental Safety Systems, Inc.
2650 Park Tower Dr.
Vienna, VA 22180

1 Jim Krulik, Geology Manager
US Bureau of Reclamation
Code D-8322
P.O. Box 25007
Denver, CO 80225-0007

1 B. T. Brady
Records Specialist
US Geological Survey
MS 421
P.O. Box 25046
Denver, CO 80225

1 M. D. Voegele
Deputy of Technical Operations
M&O/SAIC
101 Convention Center Drive
Suite P-110
Las Vegas, NV 89109

2 A. T. Tamura
Science and Technology Division
OSTI
US Department of Energy
P.O. Box 62
Oak Ridge, TN 37831

1 P. J. Weeden, Acting Director
Nuclear Radiation Assessment Div.
US EPA
Environmental Monitoring Sys. Lab
P.O. Box 93478
Las Vegas, NV 89193-3478

1 John Fordham, Deputy Director
Water Resources Center
Desert Research Institute
P.O. Box 60220
Reno, NV 89506

1 The Honorable Jim Regan
Chairman
Churchill County Board of
Commissioners
10 W. Williams Avenue
Fallon, NV 89406

1 R. R. Loux
Executive Director
Agency for Nuclear Projects
State of Nevada
Evergreen Center, Suite 252
1802 N. Carson Street
Carson City, NV 89710

1 Brad R. Mettam
County Yucca Mountain
Repository Assessment Office
P. O. Drawer L
Independence, CA 93526

1 Vernon E. Poe
Office of Nuclear Projects
Mineral County
P.O. Box 1600
Hawthorne, NV 89415

1 Les W. Bradshaw
Program Manager
Nye County Nuclear Waste Repository
Project Office
P.O. Box 1767
Tonopah, NV 89049

1 Florindo Mariani
White Pine County Coordinator
P. O. Box 135
Ely, NV 89301

1 Tammy Manzini
Lander County Yucca Mountain
Information Officer
P.O. Box 10
Austin, NV 89310

1 Jason Pitts
Lincoln County Nuclear Waste
Program Manager
P. O. Box 158
Pioche, NV 89043

1 Dennis Bechtel, Coordinator
Nuclear Waste Division
Clark County Dept. of Comprehensive
Planning
P.O. Box 55171
Las Vegas, NV 89155-1751

1 Juanita D. Hoffman
Nuclear Waste Repository
Oversight Program
Esmeralda County
P.O. Box 490
Goldfield, NV 89013

1 Sandy Green
Yucca Mountain Information Office
Eureka County
P.O. Box 714
Eureka, NV 89316

1 Economic Development Dept.
City of Las Vegas
400 E. Stewart Avenue
Las Vegas, NV 89101

1 Community Planning & Development
City of North Las Vegas
P.O. Box 4086
North Las Vegas, NV 89030

2 Librarian
YMP Research & Study Center
101 Convention Center Drive, Suite P-110
Las Vegas, NV 89109

1 Library Acquisitions
Argonne National Laboratory
Building 203, Room CE-111
9700 S. Cass Avenue
Argonne, IL 60439

1 Glenn Van Roekel
Manager, City of Caliente
P.O. Box 158
Caliente, NV 89008

1 Gudmundur S. Bodvarsson
Head, Nuclear Waste Department
Lawrence Berkeley National Laboratory
1 Cyclotron Road, MS 50E
Berkeley, CA 94720

1 Steve Hanauer (RW-2)
OCRWM
U. S. Department of Energy
1000 Independence Ave.
Washington, DC 20585

Robert W. Clayton
M&O/WCFS
101 Convention Center Drive/MS423
Las Vegas, NV 89109

1 Richard C. Quitmeyer
M&O/WCFS
101 Convention Center Drive/MS423
Las Vegas, NV 89109

1 Mark C. Tynan
DOE/YMPSCO
101 Convention Center Drive/MS523/HL
Las Vegas, NV 89109

1 John Whitney
U.S. Geological Survey
P.O. Box 25046, MS 425
Denver, CO 80225

1 Ivan Wang
Woodward-Clyde Federal Services
500 12th Street, Suite 100
Oakland, CA 94607

1 Tim Sullivan
U.S. Department of Energy
Yucca Mountain Site Characterization
Office
101 Convention Center Drive, Suite P200
Las Vegas, NV 89109

2	1330	B. Pierson, 6811
	100/1.2.3.2.8.3.3/SAND95-1938/QA	
20	1330	WMT Library, 6752
1	9018	Central Technical Files, 8523-2
5	0899	Technical Library, 4414
2	0619	Review and Approval Desk, 12630, For DOE/OSTI
15	0750	M. C. Walck, 6116
1	0750	G. J. Elbring, 6116
1	0750	C. J. Young, 6115
1	0750	D. J. Borns, 6116
1	1160	H. D. Garbin, 9312